COLLOIDAL STABILITY IN BUTANOL

by

ROBERT STUART MARSDEN, B.Sc.

A Thesis submitted for the Degree of

Doctor of Philosophy

University of Edinburgh

January, 1977

To my parents

I declare that the work described in this thesis has not been submitted for any other degree and is the original work of the author except where acknowledgement is made by reference. The work was carried out in the Chemistry Department of the University of Edinburgh between October 1973 and September 1976 under the supervision of Dr. W.D. Cooper. Some time was also spent at Unilever Laboratories, Port Sunlight.

Post-graduate courses attended include: Computing (1 week Fortran programming course and 1 week introduction to Edinburgh Multi-Access System); High Speed Liquid Chromatography (5 lectures - Prof.J.H. Knox and Dr. J.N. Done); Chemical Aspects of Oil Products Research (5 lectures - Staff of Shell Research Ltd.); Chemistry of the Upper Atmosphere (5 lectures - Dr. R.J. Donovan and Dr. M.F. Golde); Biomimetic Organic Chemistry (5 lectures - Dr. R.M. Paton); Industrial Research and Development - the Management Systems (5 lectures - Prof. R.B. Gravenor); Recent Developments in the Theory of Concerted Processes (5 lectures - Dr. A.J. Bellamy).

Acknowledgements

The author is indebted to his supervisor, Dr. W.D. Cooper, for his constant encouragement and interest throughout the work.

He thanks Unilever Ltd. and the S.R.C. for the provision of a C.A.S.E. grant, and Dr. A.L. Smith for his interest in the project. He is grateful to the many personnel at Unilever Ltd. who gave assistance and in particular would like to thank Dr. G.C. Peterson for his help and for many useful discussions.

The assistance of the technical staff of the Chemistry Department is appreciated and the author is grateful to Mrs. J. Gorrie for undertaking the typing.

Abstract

Previous studies of colloidal stability in non-aqueous media have been reviewed and the relevant theories of electrostatic and electrodynamic interactions discussed. Colloidal dispersions of polytetrafluoroethylene (PTFE) and polystyrene latices and of carbon blacks in butanol have been described. Although the effect of water has been discussed and quantified the majority of the results are for dispersions in which the water content is minimal (< 5 ppm). It was possible to exclude atmospheric contaminants, such as water, from the dispersions by using a special combined electrophoresis/particle-counting cell and vacuum apparatus developed for this work.

Electrophoresis results indicated that proton transfer was the fundamental charging mechanism for the dispersions studied. Water has been shown to have no major effects on the systems other than those resulting from its relative acidity with respect to butanol.

Stability has been related to the magnitude of the zeta potential and to the electrolyte concentration. Predicted stabilities using DLVO theory agreed with those observed experimentally for Graphon dispersions but differed significantly from those for dispersions of polystyrene.

Qualitative agreement between theoretical predictions and experimental results was observed for mutually flocculating systems. The results indicated that although particle size and zeta potential may affect the rate constant of mutual flocculation, the primary controlling factor was the thickness of the electrical double layer. Results and calculations which infer that the electrodynamic interaction between PTFE and Graphon is one of repulsion have been presented.

CONTENTS

CHAPTER ONE

1.1 Introduction

By definition, a lyophobic colloidal dispersion is thermodynamically unstable. The total free energy of such a system can always be lowered by a reduction in the particle/medium interfacial area such as that incurred during flocculation. Despite this, colloidal systems often show coagulation rates that are virtually zero. It would therefore seem evident that for any study of colloidal systems the kinetics of flocculation are of paramount importance.

As a result of Brownian motion the colloidal particles have a finite probability of colliding with one another and if they remain in contact the number of dispersed primary particles decreases. In the absence of any forces between the particles the rate of flocculation is entirely controlled by diffusion. However the presence of either an attractive or repulsive force will modify the collision frequency and affect the flocculation rate. Attractive forces of the London - van der Waals type are generally responsible for the particles adhering to one another. Since the forces are effective before particle contact they cause a slight increase in the flocculation rate. The magnitude of this interaction is related to the nature of the particles, the medium and to the interparticle separation.

Colloidal particles are often found to be electrically charged. Using a simple electrostatic model to consider the interaction of two similarly charged colloidal particles, a repulsive interaction dependent on the magnitude of the charges and interparticle distance is predicted. This simple coulombic model is not applicable to a system where there is a significant ion concentration. Gouy[1] and Chapman[2] have given equations describing the diffuse electrical double layer at a charged interface in the presence of electrolyte. A number of authors[3,4,5] have suggested

that the repulsive interaction is due to the overlap of double layers and not to a direct particle-particle coulombic interaction.

Derjaguin and Landau[6] and Verwey and Overbeek[7] have independently developed a theory in which the potential energy resulting from the summation of the van der Waals and the double layer overlap interactions, is related to stability. The validity of DLVO theory for systems where the ion concentrations are too low to screen the charged particle efficiently has been questioned.[8] It has been suggested that for these systems the repulsive term is more accurately expressed as a coulombic interaction.

1.2 Choice of System

The generally accepted criterion for the applicability of DLVO theory to any system is the "thickness" of the double layer in relation to the particle radius. By definition, double layer thickness ($^{1}/_{\kappa}$) is proportional to $(^{\varepsilon}/_{c})^{\frac{1}{2}}$ where ε is the static permittivity and c is the ion concentration. Although this relationship suggests that, at a given electrolyte concentration, the double layer thickness would be less for media of low permittivity, this is generally not the case. It must be emphasised that c corresponds to the free ion concentration, which, because of ion association, is not necessarily the overall electrolyte concentration. Ideally, to obtain minimum values of $^{1}/_{\kappa}$, a liquid of low permittivity in which little ion association occurs is required. Butanol, having a relative static permittivity of 17.1 and being a good ionising solvent for lithium chloride (LiCl), is such a liquid. For any LiCl concentration less than 10^{-3} mol dm^{-3} the calculated double layer thickness is less in butanol than in water. Dispersions of butanol should therefore prove ideal systems to test the predictions of DLVO theory when $^{1}/_{\kappa}$ is small and c is low.

London - van der Waals interactions are present between all materials and generally give rise to attractive forces. The magnitude of the interaction is related to the nature of the materials involved and to the dielectric properties of the intervening medium. For two different materials, A and B, the A-B interaction will always be less attractive than either the A-A or the B-B interaction. It is possible for certain unlike types of material, in the appropriate medium, to show mutual repulsion. Recently, a number of authors[9,10,11] have revived the early work of Lifshitz[12] in which expressions describing London - van der Waals interactions were derived. Using this approach, it is predicted from the limited data available that in butanol the London - van der Waals force between polytetrafluoroethylene (PTFE) and carbon is repulsive. It may be possible to utilise such a system to demonstrate, at least qualitatively, a repulsive van der Waals force.

In addition to PTFE and carbon black, dispersions of polystyrene latices were also used. Their inclusion was merited by their high degree of sphericity and monodispersity which has led them to be commonly referred to as "model colloids".

1.3 Previous Work

1.3.1 Aqueous Systems

The colloidal state has long been recognised, but it is only recently that a deeper understanding of its physical properties has been attained. As early as 1857 Faraday,[13] in a lecture entitled "The Experimental Relations of Gold to Light", gave a detailed description of aqueous gold sols. Following this, Graham[14] distinguished between two groups of substances according to their rate of diffusion through parchment, defining those which diffused slowly, or not at all, as colloids.

At about the same time Quincke[15] reported the movement of particulate material in solution between two electrodes on the application of an electrical potential. He noted that the speed and direction of flow were independent of the state of aggregation but were dependent on the nature of the particles and of the dispersion medium. Helmholtz[16] presented a theory of electrokinetic phenomena and emphasised that the electrophoretic velocity was proportional to the zeta potential and not to the charge on the particle. Although these early workers believed that all colloids consisted of tiny solid particles dispersed throughout the aqueous phase it was not until the invention of the ultramicroscope[17] in 1903 that this could be verified. Ostwald[18] extended the definition of a colloid to the currently accepted model of two phases, one being dispersed uniformly throughout the other.

Around the beginning of this century colloidal stability was related to the presence of charge on the particles.[19] Powis[20] showed that the stability of an oil/water emulsion was related to the potential, calculated from electrophoretic velocity, at the oil/water interface and demonstrated that there was a critical potential below which, coalescence occurred.

Early attempts to explain the relationship between electrolyte concentration and stability were based on charge neutralisation models. Freundlich[21] initially believed that flocculation was due to the adsorption of counter-ions at the particle/medium interface but later, as a result of experimental observations,[22] rejected the idea.

Ostwald,[23] in his approach, chose to disregard entirely the properties of the particles and proposed that coagulation was induced by the nature of the dispersion medium alone. The ions in solution were considered to form a "statistical lattice", each ion being associated with counter-ions in a similar manner to the solid crystal. Increasing electrolyte concentration

led to interionic forces becoming so large that they forced the colloidal particles together. This theory was totally inadequate in that it ignored the nature of the particles and denied the existence of interparticle forces.

Hamaker[24] had already evaluated an attraction between particles in terms of London - van der Waals forces. The mathematical expression describing the electrical double layer around a particle, derived by Gouy[1] and Chapman,[2] had also been used[3,4,5] to evaluate the repulsion of two overlapping double layers. Derjaguin and Landau[6] and Verwey and Overbeek[7] independently presented a unified theory of colloid stability which considered the potential energy resulting from the summation of the attractive and repulsive terms. Although many minor modifications have been made to the basic theory it still provides the framework in the discussion of stability for many colloidal systems. Derjaguin[25] has commented that there are "no certain examples of inapplicability of the theory of stability of lyophobic colloids within the limits of its validity which follow logically from physical and mathematical foundations of this theory." For this reason he concludes that there is no reason to reject, or fundamentally revise the theory.

If theory is to be tested experimentally then systems closely resembling the theoretical models are desirable. Because of their highly spherical and monodisperse nature, polymer latices, particularly polystyrene have been extensively used in work attempting to verify DLVO theory.

Watillon and Joseph-Petit[26] studied the coagulation kinetics of polystyrene latex particles and from an experimentally determined value of the critical flocculation concentration (c.f.c.) estimated a Hamaker constant which was consistent with that predicted theoretically. Using a similar system Schenkel and Kitchener[27] have shown that DLVO theory adequately describes flocculation induced by 1:1 electrolyte.

Ottewill and Shaw[28] studied the kinetics of flocculation of a polystyrene latex dispersion by barium nitrate for a range of particle sizes. They found, contrary to the predictions of DLVO theory, that $d \log W / d \log c$ was independent of particle size. (W, the stability ratio = $\frac{\text{rapid rate constant}}{\text{reduced rate constant}}$.) Kotera, Furusawa and Kudo[29] also using a polystyrene dispersion obtained results which were at variance with the DLVO prediction that c.f.c. was independent of particle size. They showed that not only did the c.f.c. vary with particle size but also that the flocculation was reversible. However, Wiese and Healy[30] have resolved these apparent discrepancies in the theory by considering the possibility of secondary minimum flocculation. It was emphasised that the height of the energy barrier, V_{max}, was not necessarily a valid criterion for stability as it considers only flocculation into the primary minimum. They demonstrated that increasing particle size or increasing the ratio of the radii of one particle to the other (i.e. tending towards sphere/flat plate interaction) led to an increase in the depth of the secondary minimum.

The above evidence demonstrates that DLVO theory adequately describes idealised systems in which flocculation occurs between ideal particles. Real systems are usually more complex, containing different types and sizes of particle. In these polydisperse systems a knowledge of the hetero-flocculation (flocculation between unlike particles) kinetics is of great value. For practical and commercial systems the extension of DLVO theory to heteroflocculation was therefore important. More specifically, hetero-flocculation studies can be used to test the theoretical predictions that van der Waals forces between unlike substances can be repulsive.

The extension of DLVO theory to heterocoagulation by Derjaguin[31] and subsequently the treatment of Devereux and de Bruyn[32] proved very tedious mathematically. A simplified method, using a linear Debye-Hückel approximation, was presented by Hogg, Healy and Fuerstenau[33] and enabled

theoretical predictions for heterocoagulating systems to be compared with experimental results. A comparison[34] of the repulsive energies of interaction predicted by the simplified theory with those of Devereux and de Bruyn gave good agreement, especially when the surface potential was low.

Kitahara and Ushiyama[34] have studied heteroflocculation of mixed latices of polystyrene possessing different zeta potentials. Calculations of V_{max} for the various possible interactions were used to predict the most energetically favoured type of flocculation. The theoretical predictions were borne out by the experimental results. The extended DLVO theory has also been used to explain the marked reduction in overall stability observed when a small amount of an unstable component is present.[35] The system used consisted of dispersions of two types of carbon black, identical, except in size, the larger particles exhibiting secondary minimum flocculation.

Flocculation rates which are several times larger than diffusion controlled rates are generally interpreted in terms of mutual flocculation (flocculation between oppositely charged particles). Super-fast flocculation has been observed for citrate ion stabilised gold sols on the addition of $NaClO_4$.[36] It was believed that the addition of $NaClO_4$ caused charge reversal which was rapid with respect to the time of mixing, hence resulting in a mixture of positively and negatively charged particles. Lottermoser and May[37] have reported that the maximum mutual flocculation rate was observed when the charges on the two colloids were equal and opposite in sign. Princen and de Vena Peplinski[38] examined dispersions of ZnO and TiO_2 over a range of pH between the zero points of charge of each material. Under these conditions mutual flocculation would be expected. However, the mutual flocculation rates were found to be independent of pH but could be related to the relative particle sizes of the interacting pigments.

Hogg, Healy and Fuerstenau[33] have calculated that super-fast flocculation would be expected when double layer thickness was greater than particle radius i.e. $\kappa a < 1$. Although, for this situation their expression to calculate the double layer interaction term was not strictly valid it was however used to give an approximate indication of the effects of surface potential and double layer thickness on stability. Their results demonstrated that although surface potential had some effect on stability the main controlling factor was the magnitude of κa. It was shown that for $\kappa a < 1$ super-fast flocculation rates were anticipated but for $\kappa a > 1$ the rates tended towards the diffusion controlled rate.

1.3.2 Non-Aqueous Systems

It is evident that most of the early work was confined to aqueous systems. It has become accepted to classify systems as aqueous and non-aqueous, a distinction which is essentially artificial and has little theoretical significance. Water is a better ionising medium than most organic solvents, and for this reason, double layer thickness has generally, but mistakenly, been accepted to be less in water than in non-aqueous media for similar electrolyte concentrations. Because of this the use of double layer theory for many non-aqueous systems has been regarded with scepticism. If a division is required it would seem more reasonable that it should be one which takes account of double layer thickness, as this is the factor which decides the method to be adopted to calculate the repulsive interaction.

Some of the earliest recorded work on dispersions in non-aqueous media was due to Buckingham[39] who studied a number of dispersions in a series of liquids of various permittivities. Stability was related to the conductivity of the medium and consequently to its relative static permittivity and was attributed to charge on the particles in the higher permittivity media.

The flocculating effect of an indifferent electrolyte was also discussed and a "neutralisation of charge model", similar to that of Freundlich, was proposed.

During the 1930's Soyenkoff[40] demonstrated that dispersions were uncharged in benzene and concluded that electrical factors of stability were unimportant in low permittivity media. Following this, Damerell and co-workers studied dispersions of calcium carbonate[41] and silica[42] in xylene in the presence of surfactant. It was reported that increasing surfactant led to greater stability and that the particles were apparently charged. The presence of an electrical charge was found difficult to explain and although it was tentatively suggested that it may contribute to the stability, surfactant adsorption resulting in a "protective coating" was postulated as the primary stabilising factor. Van der Minne[43] studied peptisation and flocculation of dispersions in mineral oils, but was unable to explain the results in the light of contemporary Bjerrum theory[44] which suggested that free ion concentration was small in low permittivity media. Earlier work[45] which demonstrated that there was no observable electrophoresis in this system was confirmed. It was not until several years later that van der Minne and Hermanie,[45] having discovered the work of LaMer and Downes,[47] Fuoss,[48] and Strong and Krauss[49] demonstrating the existence of ions in low permittivity liquids were urged to develop an electrophoresis technique for non-polar media. It was shown that, contrary to popular opinion, dispersions in low permittivity media were often charged and, from results of carbon black dispersions[50] in benzene, that stability could be related to zeta potential.

Stable dispersions of rutile in n-butanol ($\varepsilon = 17.1$), n-butylamine ($\varepsilon = 7.8$), melamine and linseed oil thinned with xylene ($\varepsilon = 2.5$) have been reported by Romo.[51] Calculations, based on DLVO theory, led to the conclusion that the stability in the two media of higher permittivity was due

to the electrostatic repulsion whereas the stability of the other two dispersions was due to entropic repulsion of the interacting adsorbed molecules. The stabilities and zeta potentials of suspensions of alumina and aluminium hydroxide in the C_3, C_4 and C_5 alcohols have been shown to be markedly dependent on water concentration.[52] It was found that stability correlated with the net repulsive electrostatic potential predicted from the zeta potential.

McGown, Parfitt and Willis[53] have determined electrophoretic mobilities of a variety of dispersions in solutions of Aerosol OT (sodium di-2-ethylhexyl sulfosuccinate) in p-xylene over a range of surfactant concentrations. It was found that for particles of 1000-5000 Å diameter a zeta potential in excess of 50 mV produced long term stability, a result which was in general agreement with the predictions of DLVO theory. As traces of water were shown to affect the sign and magnitude of the zeta potential further work[54] was performed using a heptane system in which water had little effect. Although the experimentally determined stability ratios were of the same order of magnitude as theoretically predicted values it was necessary to assume a variation in Hamaker constant of over two orders of magnitude to obtain a close correlation with DLVO theory. A better agreement between experimental stability and that predicted by DLVO has been obtained for dispersions of pure rutile in Aerosol OT /p-xylene solutions.[55] Stability ratios have been related to measured zeta potentials, the signs and magnitudes of which were controlled by trace amounts of water in the system.
A criticism of this last piece of work was raised by Fowkes[56] who suggested that the value of the Hamaker constant used was unreasonably large and that about one third of the value used would be more acceptable. This would of course make the comparison of the results with DLVO theory less favourable.

Water has been shown to have marked effects on zeta potential[52,53,55] which were correspondingly reflected in dispersion stability. Further evidence for this was given by Meadus,Puddington,Sirianni and Sparks[57] who demonstrated that the stability of carbon blacks in toluene, m-xylene and nitrobenzene was increased by the addition of small amounts of water. It was found that water had a marked effect on the electrophoretic mobility and a strong correlation between maximum mobility and maximum stability was found.

The use of double layer theory to calculate repulsive interactions in low permittivity media has been criticised by Osmond[8] on the grounds that the "double layer" was too diffuse. In the example under discussion, for the interaction between rutile in p-xylene, it was calculated that the number of counter-ions between two "adjacent" particles (a volume of the order of hundreds of cubic microns) would seldom exceed ten, suggesting the inadvisability of ignoring their discrete nature. It was suggested that in low permittivity media, where ionisation is poor, that the repulsive forces should be calculated using a coulombic repulsion model. It has however been pointed out[58] that in the Parfitt work the expression used to calculate V_R,does in its dominant part,express the net coulombic repulsion and contains in addition a correction for the overlapping ionic atmospheres. Calculations have been made[59] to determine the influence of ionic molar volume and ionic polarisability on electrical double layer repulsion. The model chosen consisted of 1 μm particles in a solution of tetraisoamylammonium picrate in benzene. It was reported that in comparison with classical DLVO theory a large increase in repulsive energy was predicted due to the strong polarisability of the cation whereas a decrease would result from its finite molar volume. These effects were both predicted to increase with increasing surface potential and with increasing solute concentration.

Recently, copper phthalocyanine dispersions in n-heptane/Aerosol OT solutions have been used in an attempt to obtain a direct correlation between stability and theory. Previously, a correlation between zeta potential and stability for dispersions[61] of carbon black in the same media had been demonstrated, but it was hoped that this work could be more closely compared with a theoretical model. The models chosen were DLVO constant potential, DLVO constant charge, coulombic and an approach suggested by Parfitt, Wood and Ball.[62] This last method is a modification of the coulombic model using the imaging treatment of Maxwell[63] for conducting spheres of finite size in an inert dielectric medium. However, due to the low stabilities observed, only general qualitative trends were found and it was impossible to establish the validity of one theory in preference to another.

Much work has been done to elucidate charging mechanisms in non-aqueous media. In general, an estimate of the Stern potential is calculated from electrophoretic mobility. Surfactant adsorption has already been mentioned as a mechanism of particle charging. In the absence of adsorbable surfactants the dissociation of surface groups appears to be the most general mechanism and the ion which is almost exclusively responsible for the charge transfer between solvent and particle is the proton. Oxides, particularly those of titanium and aluminium have been extensively used to demonstrate this mechanism.

Rutile (TiO_2) has been reported as being positively charged in butanol,[51] pentanol,[64] heptanol[65] and acetic acid[66] but negatively charged in butylamine[51] and nitrobenzene.[65] These results have been explained[67] in terms of the relative acidity of the particle and the solvent. The alcohols and acetic acid, being more acidic solvents, tend to donate protons to the particle surface, so rendering it more

positive whereas more basic solvents are better proton acceptors. From this model, it is possible to explain the influence of trace amounts of water on the sign and magnitude of the surface charge in terms of increasing basicity of the particle surface. The mobility of TiO_2 in pentanol and in heptanol[65] has been shown to increase and pass through a maximum as a function of water concentration.

Romo[52] has determined the zeta potentials of alumina (Al_2O_3) and of aluminium hydroxide ($Al(OH)_3$) particles dispersed in propanol, butanol and pentanol as a function of water concentration. The $Al(OH)_3$ remained positively charged for all water contents whereas the Al_2O_3 was negatively charged at low water concentrations but became positively charged on the addition of more water. The isoelectric point for Al_2O_3 was estimated to occur at a concentration which would give monolayer coverage of water, assuming an equilibrium distribution between the alcohol and the interface. It was concluded that the water was adsorbed at the interface and being a more acidic solvent rendered the particle more basic. This prompted Fowkes[68] to comment "In the studies by Romo and by Micale et al on the effect of water on the electric charge of rutile or alumina particles in alcohol one needs to consider the mechanism of charging and how these studies fit in. As we have shown, the charging mechanism in non-aqueous media appears to be entirely a proton exchange phenomenon. The addition of water tends to make the rutile or alumina surface more basic and therefore to make it more positively charged; the aluminium hydroxide is basic and is uninfluenced by added water. Added water can also make the solution more basic but the main effect is on the oxide surfaces".

Many years earlier Verwey,[69] having studied dilute hydrochloric acid/alcohol solutions, had suggested that the charge at the oxide/alcohol interface was associated with the relative affinities of the proton and

the hydroxyl ion for the surface and the bulk liquid. More recently, it has been reported[66] that dispersions of TiO_2 in the lower alcohols exhibited a surface charge which was dependent upon surface treatment. It was found that the sign of charge reversed from negative to positive as the acidity of the surface decreased, i.e. the surface contained more basic groups. For an untreated rutile it was found that zeta was negative and decreased in magnitude with increasing alcohol chain length. This work has been extended by Jackson and Parfitt[70] who determined the zeta potentials of rutile dispersed in all the primary alcohols from methanol to decanol. The sign of the charge was shown to change from negative to positive with increasing alcohol chain length, the zero point of electrokinetic mobility lying between butanol and pentanol. Jackson and Parfitt suggest that two equilibria should be considered, that for proton exchange between surface and medium and that for the self ionisation of the alcohol, viz.

$$S\text{-}H_2^+ + M^- \overset{1}{\rightleftharpoons} S\text{-}H + M\text{-}H \overset{3}{\rightleftharpoons} S^- + M\text{-}H_2^+$$

$$\Big\Vert 2$$

$$M^- + H^+$$

where M = medium

S = surface

In the examples under discussion particle charge was determined solely by equilibria 1 and 3 and is independent of equilibrium 2.

All the above examples are of charge originating from either adsorption or desorption of ions from the particle surface. Apolar particles may become charged by the preferential adsorption of ions from solution. Various types of carbon black have been shown to be charged in a number of non-aqueous solvents due to the adsorption of Aerosol OT. Damerell and Urbanic[71] found three different carbon blacks to be negative in xylene. Sterling MTG has been shown to be negative in heptane[54] and Elftex-5[61] was negative in heptane, cyclohexane

and benzene. The absolute magnitude of the zeta potential was related[54,61] to the concentration of surfactant, passing through a maximum at between 10 and 20 mol m^{-3}. Water was shown[61] to reduce the absolute value of the zeta potential and to alter the position of the maximum. It was proposed that the formation of a water layer around the particle, into which the sodium ions from the surfactant migrated, produced a reduction in zeta potential.

The systems become more complex if proton transfer and surfactant adsorption occur simultaneously. Rutile and alumina have been shown to be positively[53] charged in solutions of Aerosol OT in xylene. In the case of rutile the magnitude of the zeta potential decreased with increasing surfactant concentration but for alumina it was independent of surfactant concentration. The addition of water to the rutile system led to an increase in zeta potential to a maximum at about 100 p.p.m. of water after which, it fell to values below the initial dry value. It would appear that neither the ionisation of surface groups nor surfactant adsorption is solely responsible for the charge in this system.

Although the stability of charged lyophobic colloids has satisfactorily been accounted for by DLVO theory there are still many unchanged systems which exhibit stability to which, quite obviously, DLVO theory cannot apply.

It has been shown[72] that colloidal dispersions of carbon black in a hydrocarbon medium can be stabilised by the adsorption of aromatic molecules with long aliphatic side chains. The degree of stability was observed to be directly related to chain length. This has been accounted for by Mackor[73], who assumed that the aliphatic chains were fixed to the surface by the aromatic nucleus but were otherwise free and were responsible for a repulsive force on the approach of one particle to another. It was suggested that the repulsion was due to the decrease in the number of possible configurations of the adsorbed molecule due to the steric

hindrance of the interpenetrating aliphatic side chains. This decrease led to an increase in configurational free energy corresponding to a repulsive force thus resulting in increased stability. This treatment, which assumes that surface coverage is low enough to justify ignoring mutual interactions, has been extended[74] to one which is valid for high surface coverage. An expression for the free energy of repulsion produced by the approach of two adsorbing planes was given and comparison with the above experimental data indicated the validity of this method.

It has also been demonstrated[75] that the presence of adsorbed molecules at the particle/medium interface leads to a reduction in the van der Waals interaction energy and so to an increase in stability. The magnitude of the effect was found to increase with increasing adsorbed film thickness and with decreasing particle radius.

Clayfield and Lumb[76] extended the earlier theory of Mackor,[73] specifically relating their model to terminally adsorbed macromolecules. They considered the change in configurational entropy produced on the compression of the adsorbed macromolecules by an inpenetrable barrier. Conversely an approach by Fischer[77] considered the change in the free energy of mixing of polymer and solvent produced by the interpenetration of the segments of the adsorbed macromolecules. Other authors[78] have suggested that these two effects are not independent but rather should be considered together. Hesselink et al[79,80,81] have calculated the total free energy change involved on the approach of two polymer-coated flat plates as a sum of three interactions. These are, a volume restriction repulsion due to the decrease of configurational entropy of adsorbed loops and tails, an osmotic repulsion due to the mixing of the adsorbed polymeric clouds and the van der Waals attraction between the particles. It was concluded that stabilisation was enhanced by high polymer adsorption, long polymer chains, small particles and low Hamaker constants. The solvent was also found to have an effect, the osmotic repulsion term

being reduced and even changing sign in the case of poor solvents. Extension of this theory to spherical particles is mathematically complex although a simplified expression for the osmotic term has been given by Ottewill and Walker.[82]

Direct measurements of the magnitude of steric repulsive forces have been made by studying the thickness of non-aqueous black films[83] formed from solutions of glycerol mono-oleate in hydrocarbon solvents of various chain lengths. The films, which were supported between bulk aqueous solutions of sodium chloride, were compressed by the application of a d.c. potential across the film. The adsorption of glycerol mono-oleate was calculated from surface tension measurements. Lower molecular weight hydrocarbons gave rise to films with greater equilibrium thickness which, as they contained a larger mole fraction of solvent, were found to be more compressible. Free energies were calculated from compression data and were found to change rapidly on compression.

Using a surface balance technique compression studies have been used to measure steric repulsion for polymer coated latex particles at a heptane/water interface. It was suggested that, in view of the solvent chosen, the osmotic term would dominate and that the volume restriction term could be neglected. The results obtained closely agreed with those calculated from the Ottewill and Walker theory.[82]

Experimental evidence in support of the Fischer solvency theory has been obtained[84] from stability measurements of sterically stabilised polymer particles in a variety of non-aqueous media. Flocculation was induced by decreasing the solvency of the dispersion medium for the stabiliser, either by non-solvent addition or by cooling.

Anomalies between the theory of Hesselink et al[81] and experimental results have been discussed by Evans and Napper.[85] Although a correlation between the θ point (the point at which the polymer configuration is

unaffected by the nature of the solvent), and the critical flocculation point (c.f.p.) has been extensively demonstrated experimentally,[85-88] it is not predicted theoretically. The theoretical prediction that stability is strongly dependent on stabiliser molecular weight is not borne out experimentally, for, although some dependence is noted,[85,86] it is of at least an order of magnitude less than that predicted. It has also been shown that, contrary to theoretical prediction, the c.f.c.s of sterically stabilised latices[85-88] are quite insensitive to particle radius. It has been suggested[85] that the discrepancy between theory and experimental results arises from a difficulty which appears in the calculation when entropy and solvency theories are combined.

In contrast to the results of Napper, Dunn and Vold[89] have reported strong dependence of the stability of Graphon in toluene on the chain length of a non-ionic stabiliser, polystyrene. It was shown that the logarithm of the stability ratio varies linearly as a function of the molecular weight of polystyrene and that there was a critical molecular weight, below which, no stability was exhibited.

The theory of Hesselink et al is limited to cases where each macromolecule is adsorbed on only one particle, this is not necessarily the case. It has been reported[90] that tetra-alkyl titanates show a dispersant action on TiO_2 dispersed in n-hexane at high surfactant concentrations but a marked flocculating action at low concentrations. The concentration at which the tetra-alkyl titanate showed the maximum flocculation rate decreased with increasing alkyl chain length. A bridging action of the surfactant when particle surface coverages were low has been suggested[91] as a possible explanation.

Stability found in the absence of charge need not be attributed to steric stabilisation. Effects of the surfactant on the medium and the possibility of solvent structuring at the particle/medium interface must also be considered.

Steric stabilisation was initially believed to be responsible for the observed stability of Graphon dispersed in alkylbenzene solutions in heptane.[92,93] However, further work[94] led to the conclusion that Graphon is not stabilised at all by the alkylbenzene and that the changes in flocculation rate with increasing alkylbenzene mole fraction were due entirely to bulk viscosity changes.

Carbon black dispersed in anhydrous aniline has been shown to be stable[57] but to be destabilised by the addition of small amounts of water. Stability was attributed to solvent structuring at the interface aided by hydrogen bonding between surface oxygen complexes on the carbon black and the amine groups on the aniline. The addition of water induced flocculation by reducing the number of available surface oxide sites on the particles. This is not the only mechanism by which water can destabilise uncharged lyophobic systems. Dry barium sulphate dispersions in benzene have been shown to be stable,[95] however, on the addition of small amounts of water, voluminous floccs were formed and, after further addition of water, spherical agglomerates became apparent. It was proposed that the hydrophilic nature of the particle surface led to the displacement of the organic solvent from the interface. Close approach of two particles, induced by mechanical agitation, allowed the formation of a water lens or bridge between them. At low water concentrations this gave rise to loose flocs ,whereas in the presence of excess water more linkages were possible and a tighter packed structure could be formed.

The thixotropy of suspensions of starch, quartz and glass beads dispersed in wet carbon tetrachloride has also been related to water content.[96] The increase in plasticity of the suspensions, occurring on addition of traces of water, was believed to be related to the work required to break the water linkages which were joining the particles. It was emphasised that it was not the non-polarity of the medium but its poor solubility for water which caused the formation of the third phase.

Structuring at the solid/liquid interface has been discussed for a number of organic molecules and related to their ability to form hydrogen bonds. Using a dilatometric technique Findenegg has measured the surface excess mass of a series of alkanes,[97] alcohols[98] and carboxylic acids[99] as a function of temperature. In all cases the surface excess was positive. For the alkanes surface excess increased steadily as the temperature was reduced until the freezing point was approached, whereupon the increase became more rapid. This indicated an ordering of molecules near the interface which would appear to be most pronounced at temperatures close to the freezing point. Alcohols were found to exhibit a similar ordering near the freezing point but, unlike the alkanes, showed a point of inflexion in the surface excess/temperature curves at a temperature about 50 K above the melting point of the alcohol. It was suggested that, below the critical temperature, the alcohol molecules are in ordered arrays arranged in such a manner that the hydroxyl groups form linear chains of hydrogen bonds. The sudden decrease in surface excess which occurred at the critical temperature was due to the "melting" of this layer. Although it might have been expected that carboxylic acids would have given a larger surface excess mass than the corresponding alkane or alcohol this was not observed. It was also noted that the acids did

not exhibit a sharp rise in surface excess mass close to the liquid freezing points nor did they show such a pronounced "step" as the alcohols. This indicated that, unlike the alcohols, the carboxylic acids did not form close-packed arrays of alkyl chains stabilised by hydrogen bonding. These results were readily explained in terms of thermodynamic and geometric considerations. Breschenko[100] and Groszek[101] had already attributed the tendency of paraffin chain molecules to form stable closely packed monolayers at the graphite surface to a geometrical fit between the hexagonal lattice of the graphite basal plane and the extended zig-zag hydrocarbon chains. It was proposed that each methylene group was positioned at the centre of a carbon hexagon with the methylene-methylene and surface carbon-carbon bonds "bisecting" one another. It was estimated that the heat of adsorption[99] for this configuration was about 3.8 $kJ\,mol^{-1}$ of $-CH_2-$ groups. Findenegg had demonstrated that alcohol molecules could be adsorbed in this manner to give a configuration in which the closest approach of two oxygen atoms was 0.255 nm which is within the range of strong hydrogen bonding in crystals. Carboxylic acids however, do not follow this behaviour because of their strong tendency to form cyclic dimers. In this configuration the preferred arrangement of the alkyl chains described above cannot be adopted. It was estimated that the energy involved in dimerisation is of the order of 42 $kJ\ mol^{-1}$ of molecules.

Although not strictly relevant in a discussion on non-aqueous media, the inclusion of some work on the adsorption of alcohols at Graphon and polystyrene interfaces from aqueous solution is perhaps merited. Ottewill and Vincent[102] have shown that the butanol surface excess at the Graphon/water interface initially increases steadily with butanol concentration. At a concentration of about 1 gram of butanol in 100 cms^3 of water a plateau region is reached. At this point the calculated values of the

area available to each adsorbed molecule were consistent with monolayer alcohol coverage, with the alkyl chain adsorbed and the hydroxyl in solution.

Unlike Graphon, polystyrene latex has hydrophilic areas on its surface due to presence of $-OH^-$, $-COO^-$ and $-SO_4^-$ groups resulting from the method of preparation. Consequently the adsorption isotherm of polystyrene is very different from that of Graphon. At small concentrations of butanol the adsorption is low, corresponding to an ion-dipole association with the ionised sites on the latex particle having their alkyl chains orientated towards the solution phase. As the butanol concentration is increased, adsorption is observed to rise suddenly to a point corresponding to a close-packed vertically orientated monolayer. Beyond this, the adsorption continues to increase more slowly, until by the time the solution phase saturation point is reached multilayer adsorption has occurred.

In conclusion it is evident that when dealing with the stability of non-aqueous dispersions consideration of the following factors is essential:-

1) The interaction between the dispersed particle and the medium.
2) The effect of trace water.
3) The effect of proton exchange between the surface and the medium.

For the systems discussed in this thesis some inference of the nature of the interaction at the interface will be derived from earlier work.[97-102] The effects of water and of proton exchange will be extensively studied and mechanisms proposed and discussed with some reference to earlier models.[68] The initial area of the stability work will be to attempt to demonstrate that the stability of these dispersions is not only related to the zeta potential but also to free ion concentration and particle size. The predictions of DLVO theory, using

standard thin double layer equations, will be compared with experimental results for homoflocculating systems. Experimentally determined super-rapid flocculation rates for mutually flocculating systems will be compared with rates predicted by the equations of Hogg, Healy and Fuerstenau.[33] Finally, the existence of a repulsive van der Waals force will be investigated by studying mutual flocculation between PTFE P.B. and carbon.

CHAPTER TWO

2. Theoretical Aspects of Colloidal Stability

According to DLVO[7,8] theory, the total interaction between colloidal particles is a superposition of the electrostatic double layer and the electrodynamic interactions. One of the main omissions of the theory is its failure to consider the possible effects of adsorbed polymeric molecules at the particle/medium interface. As no polymeric surfactants have been used in this work DLVO theory is expected to be applicable to the systems studied.

2.1 Potential Energy of Repulsion

Lyophobic colloids owe their stability against flocculation solely to mutual repulsion arising from electrical charges on the particles. There are several mechanisms by which electrical charge may be acquired.

a) Dissociation of surface groups. Typical examples are the oxides of titanium and aluminium discussed in Section 1.3.3.

b) Adsorption of ionised surfactants. Aerosol OT renders the apolar surface of Graphon negative in water.

c) Unequal adsorption or dissolution of "specific" ions from ionic solids. When the specific ions are adsorbed at the surface they constitute an integral part of the crystalline lattice. An excess of either anions or cations within the crystal gives rise to the surface charge. An example of this is the silver halide sol in which the silver ion is potential determining.

d) Isomorphic substitution. This is commonly observed for clay minerals where an ion in the solid lattice, e.g. Si^{4+}, is isomorphically replaced by another ion, e.g. Al^{3+}, resulting in a deficit of, in this case, positive charge on the particle.

e) Dipolar molecule adsorption and/or orientation at the particle surface. Although such dipoles do not directly contribute to the net charge on the particle they may have an important effect on the double layer. The dipoles may be the result of the deformation of polarisable molecules in the electric field at the interface.

In order to achieve overall electrical neutrality of the colloidal system the surface charge must be compensated by an equal but opposite charge. This countercharge is formed by an unequal distribution of anions and cations in solution around the particle. Together, the surface charge and its corresponding countercharge constitute the electrical double layer. The manner in which the countercharge is distributed is crucial to stability. If it extends far from the particle then the interpenetration of one double layer with another will lead to significant repulsion at large particle separations. Conversely, when the double layer is compressed the particles can approach one another very closely before a repulsive interaction occurs. In the latter case, at the interparticle separations involved, van der Waals attraction tends to dominate the overall interaction and flocculation occurs.

The distribution of the ions in the electrical double layer is governed by the balance between thermal and electrical forces. Gouy[1] and Chapman[2] have developed a theory of the electrical double layer on this basis, the following assumptions were made:-

i) the charge on the particle is uniformly smeared out,

ii) the ions in the double layer are dimensionless point charges,

iii) the electrolyte medium influences the double layer only through its static permittivity constant, which has a uniform value at all points throughout the dispersion medium.

The average concentration of ions in solution is given by the Boltzmann equation,

$$n_+ = n \exp(-z_+ e\psi/kT)$$

$$n_- = n \exp(+z_- e\psi/kT) \qquad (2.1.1)$$

where, n_+ and n_- are the respective numbers of positive and negative ions per unit volume at points where the potential is ψ,

z_+ and z_- are the respective valencies of the cation and anion species,

e is the charge on the proton,

k is the Boltzmann constant,

T is the absolute temperature,

n is the bulk concentration of each ionic species.

The space charge density, ρ, at points where the potential is ψ can be expressed as,

$$\rho = ze(n_+ - n_-) \qquad (2.1.2)$$

for a symmetrical electrolyte where $z = z_+ = -z_-$.

Combining equations (2.1.1) and (2.1.2),

$$\rho = zen \exp(-ze\psi/kt) - \exp(+ze\psi/kT) \qquad (2.1.3)$$

$$\rho = -2zen \sinh(ze\psi/kT) \qquad (2.1.4)$$

Poisson's equation describing the interaction between the charges in the double layer is given as,

$$\Delta\psi = -\rho/\varepsilon \qquad (2.1.5)$$

where, Δ is the Laplace operator = $(\partial^2/\partial x^2 + \partial^2/\partial y^2 + \partial^2/\partial z^2)$,

x,y and z representing cartesian co-ordinates.

ε is the permittivity in rationalised units and corresponds to $4\pi\varepsilon_o\varepsilon_r$, where ε_o is the permittivity of free space ($8.854 \times 10^{-12} kg^{-1} m^{-3} s^4 A^2$) and ε_r is the relative static permittivity of the material.

Combination of equations (2.1.4) and (2.1.5) gives

$$\Delta\psi = \frac{2zen}{\varepsilon} \sinh(ze\psi/kT) \qquad (2.1.6)$$

For a flat double layer the potential need only be evaluated in one direction, hence equation (2.1.6) becomes

$$\partial^2\psi/\partial x^2 = \frac{2zen}{\varepsilon} \sinh(ze\psi/kT) \qquad (2.1.7)$$

when $(ze\psi/kT) < 1$ the Debye-Hückel approximation that,

$$\exp(ze\psi/2kT) \simeq 1 + ze\psi/2kT \qquad (2.1.8)$$

may be used. Then

$$\partial^2\psi/\partial x^2 = 2ne^2z^2\psi/\varepsilon kT = \kappa^2\psi \qquad (2.1.9)$$

where $$\kappa = (2e^2nz^2/\varepsilon kT)^{\frac{1}{2}} \qquad (2.1.10)$$

One solution of equation (2.1.9) is

$$\psi = \psi_o \exp(-\kappa x) \qquad (2.1.11)$$

where ψ_o is the potential at the surface.

From this expression it is evident that the rate of decay of potential in the double layer is dependent upon the value of κ. At a distance $1/\kappa$ from the surface the potential will have decayed to 1/e of the surface potential, ψ_o. This distance, $1/\kappa$, is defined as the double layer thickness even though it does not extend to the point

where $n_+ = n_- = n$. From other approximations, further solutions to equation (2.1.7) may be obtained which do not exhibit the same simple relationship between κ and ψ. Despite this, the above definition of double layer thickness is still used even though it is not strictly accurate.

The influence of valency, and concentration, of the ions in the double layer must also be considered. The limiting expression for the applicability of the Debye-Hückel approximation is that $(ze\psi_o/kT) < 1$ which at 298 K is synonymous with $z\psi_o < 25$ mV. Consequently, increasing valency of the ions reduces the maximum magnitude of surface potential to which the approximation is applicable. Verwey and Overbeek[7] have shown that equation (2.1.11) is a good approximation for values of $(ze\psi_o/kT)$ less than 2.

From equation (2.1.10) it is seen that κ is directly proportional to the valency, z. Consequently the exponential tail decreases twice as rapidly with distance for bivalent ions as for monovalent ions. Similarly, since $\kappa \propto n^{\frac{1}{2}}$ an increase in ion concentration by a factor m results in the $\psi(x)$ curve being compressed more closely to the surface by a factor $m^{\frac{1}{2}}$.

According to Gouy-Chapman theory the potential decay is exponential from the surface to a point in solution where $\psi = 0$, at which point, $n_+ = n_- = n$ (for a symmetrical electrolyte). Although this would be feasible if the ions were dimensionless point charges, it is impossible for many real systems, as can be demonstrated by an example given by Verwey and Overbeek.[7] They considered a surface potential of 300 mV in 1 mol m^{-3}, 1.1 electrolyte. From equation (2.1.1) it was calculated that the concentration of counter-ions close to the surface was 1.6×10^5 mol m^{-3} which is unreasonably high in view of the finite dimensions of the ions. Although it may be permissible to ignore

the ionic dimensions for very dilute solutions, the theory will rapidly break down for situations where a considerable part of the space charge should, theoretically, be close to the surface.

Stern[103] proposed a modification to the model in which the double layer was divided into two parts, as illustrated schematically in Fig. 2.1.1. The inner layer, within the Stern plane, is composed of adsorbed ions and is of the order of a few Ångströms thick. Between the charged surface and the Stern plane the potential decays linearly as in a classical parallel plate condenser to a value defined as ψ_δ. Beyond this point the ions are mobile and the potential decay may be represented by Gouy-Chapman theory.

The Stern plane, located at a distance δ from the surface, represents the centres of any specifically adsorbed ions. This model has been refined by Grahame[104] who distinguished between the Stern plane, which he referred to as the outer Helmholtz plane and another plane, referred to as the inner Helmholtz plane. While the former was said to represent the closest approach of solvated ions in solution the latter was said to indicate the centres of specifically adsorbed ions. Such a distinction is usually necessary, for although the specifically adsorbed ions may be of the same type as those which dictate the position of the outer Helmholtz plane, they will almost certainly be desolvated, at least in the direction of the surface.

Interaction of Two Dissimilar Double Layers

According to the Gouy-Chapman model of the electrical double layer around a colloidal particle the potential at any point in the system is given by,

$$\Delta\psi = \frac{2zen}{\varepsilon} \sinh (ze\psi/kT) \qquad (2.1.6)$$

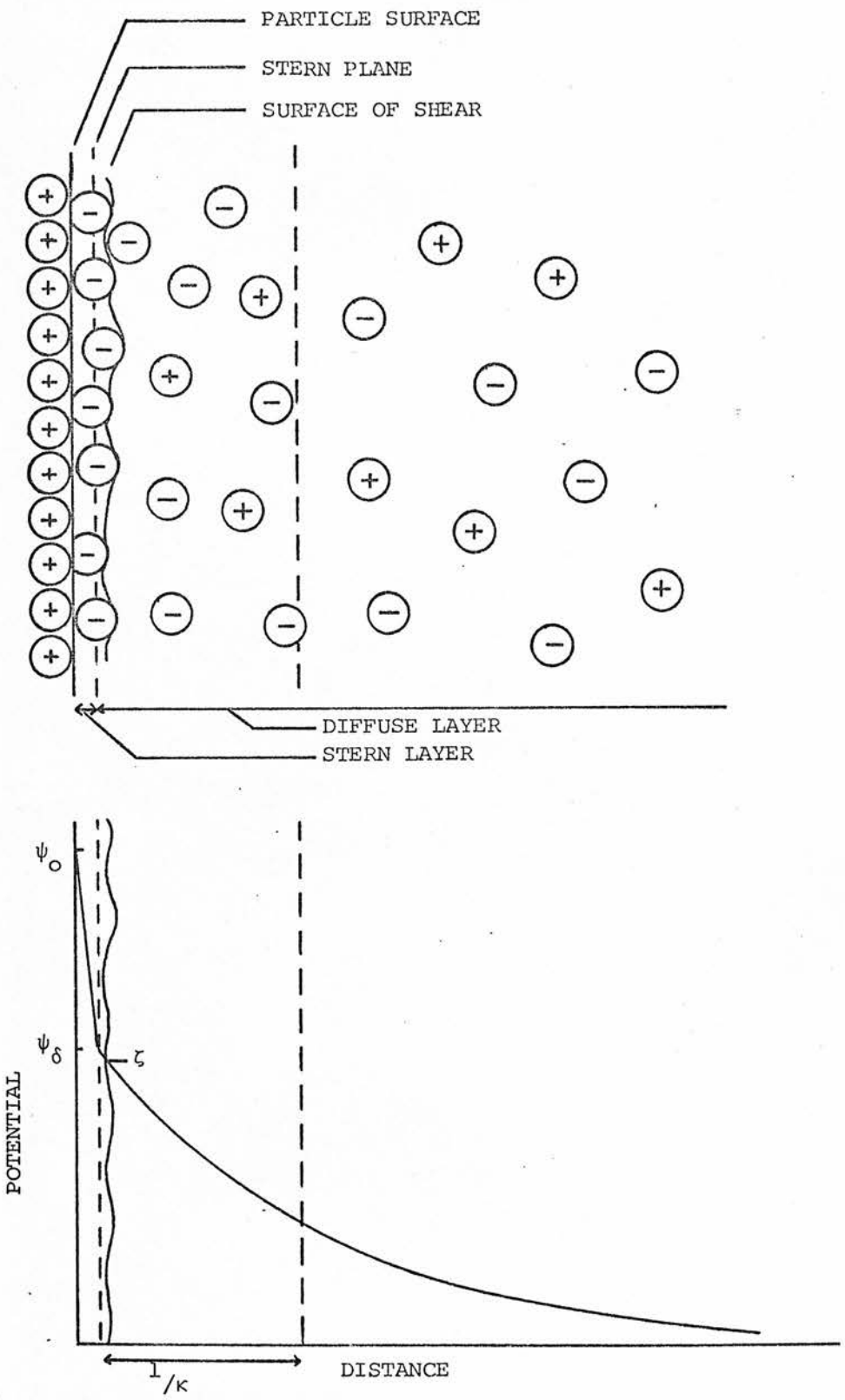

Fig 2.1.1

Schematic Representation of the Stern Model of the Electrical Double Layer

Applying the Debye-Hückel approximation allows this expression to be simplified to

$$\Delta\psi = \kappa^2\psi \qquad (2.1.12)$$

which for infinite flat plates can be expressed as

$$\partial^2\psi/\partial x^2 = \kappa^2\psi \qquad (2.1.13)$$

which may be solved directly to give equation (2.1.11). However the solution may also be expressed as

$$\psi = A_1 \cosh(\kappa x) + A_2 \sinh(\kappa x) \qquad (2.1.14)$$

where A_1 and A_2 are constants.
If $\psi = \psi_{O1}$ at $x = 0$ and $\psi = \psi_{O2}$ at $x = 2d$ then this represents the situation of two dissimilar plates of potentials ψ_{O1} and ψ_{O2} separated by a distance 2d. Hence from equation (2.1.14)

$$\psi = \psi_{O1} \cosh(\kappa x) + \left(\frac{\psi_{O2} - \psi_{O1} \cosh(2\kappa d)}{\sinh(2\kappa d)}\right) \sinh(\kappa x) \qquad (2.1.15)$$

Verwey and Overbeek[7] have shown that for small, constant surface potentials the total free energy is given by

$$G = -\tfrac{1}{2}\sigma\psi_o \qquad (2.1.16)$$

where σ is the surface charge density.

Hence for the above system of 2 plates having potentials ψ_{O1} and ψ_{O2} separated by a distance 2d, the free energy is given by

$$G_{2d} = -\tfrac{1}{2}(\sigma_1\psi_{O1} + \sigma_2\psi_{O2}) \qquad (2.1.17)$$

where σ_1 and σ_2 are the surface charge densities of the two double layers. From double layer theory,

$$\sigma = -\varepsilon(d\psi/dx)_{x=O} \qquad (2.1.18)$$

thus

$$\sigma_1 = -\varepsilon\kappa\left[\psi_{O2}\ \mathrm{cosech}(2\kappa d) - \psi_{O1}\ \coth(2\kappa d)\right] \qquad (2.1.19)$$

$$\sigma_2 = +\varepsilon\kappa\left[\psi_{O2}\ \coth(2\kappa d) - \psi_{o1}\ \mathrm{cosech}(2\kappa d)\right] \qquad (2.1.20)$$

which may be substituted into equation (2.1.17) to give

$$G_{2d} = \frac{\varepsilon\kappa}{2}\left(2\psi_{O1}\psi_{O2}\ \mathrm{cosech}(2\kappa d) - (\psi_{O1}^{\ 2} + \psi_{O2}^{\ 2})\ \coth(2\kappa d)\right) \qquad (2.1.21)$$

at large separations, $d \to \infty$

$$\therefore\ G_{\infty} = -\frac{\varepsilon\kappa}{2}(\psi_{O1}^{\ 2} + \psi_{O2}^{\ 2}) \qquad (2.1.22)$$

The difference between these last two expressions represents the resultant free energy change when two plates are brought to a separation of 2d from infinity. Hence, the potential energy of interaction, V_I, between two parallel, infinite, flat double layers is given by,

$$V_I = \Delta G = \frac{\varepsilon\kappa}{2}\left((\psi_{O1}^{\ 2} + \psi_{O2}^{\ 2})(1 - \coth(2\kappa d)) + 2\psi_{O1}\psi_{O2}\ \mathrm{cosech}(2\kappa d)\right) \qquad (2.1.23)$$

Derjaguin[31] has extended this to allow the interaction of two dissimilar spherical double layers to be considered. It is assumed that if the double layer thickness is small with respect to the particle size then the interaction may be equated to that of a collection of infinitesimally small parallel rings, each of which may be considered as a flat plate. Hence the energy of interaction is given by

$$V_R = \int_o^\infty 2\pi h V_I dh \qquad (2.1.24)$$

where V_I is as defined above,

h is the radius of the ring as shown in Fig. 2.1.2.

From Fig. 2.1.2 it is evident that

$$H-H_o = a_1 + a_2 - \sqrt{a_1^2 - h^2} - \sqrt{a_2^2 - h^2} \qquad (2.1.25)$$

which on differentiation gives

$$dH = \left(\frac{1}{(a_1^2 - h^2)^{\frac{1}{2}}} + \frac{1}{(a_2^2 - h^2)^{\frac{1}{2}}}\right) h dh \qquad (2.1.26)$$

When $h \ll a_1$ and $h \ll a_2$, then

$$h dh \simeq \left(\frac{a_1 a_2}{a_1 + a_2}\right) dH \qquad (2.1.27)$$

Equation (2.1.24) may now be written as

$$V_R = \frac{2\pi a_1 a_2}{a_1 + a_2} \int_{H_o}^\infty V_I(H) dH \qquad (2.1.28)$$

where $H = 2d$ in the flat plate model. Equation (2.1.28) may be evaluated analytically to give

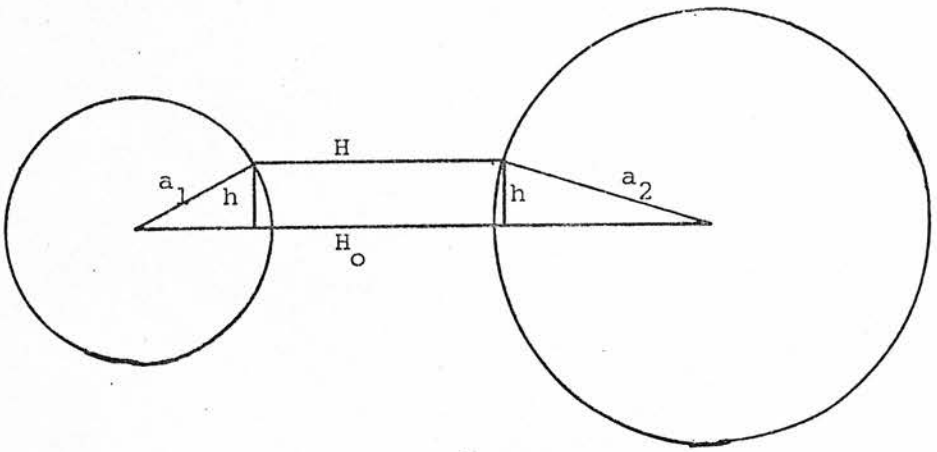

Fig 2.1.2

Geometry of the interaction between two dissimilar spherical particles

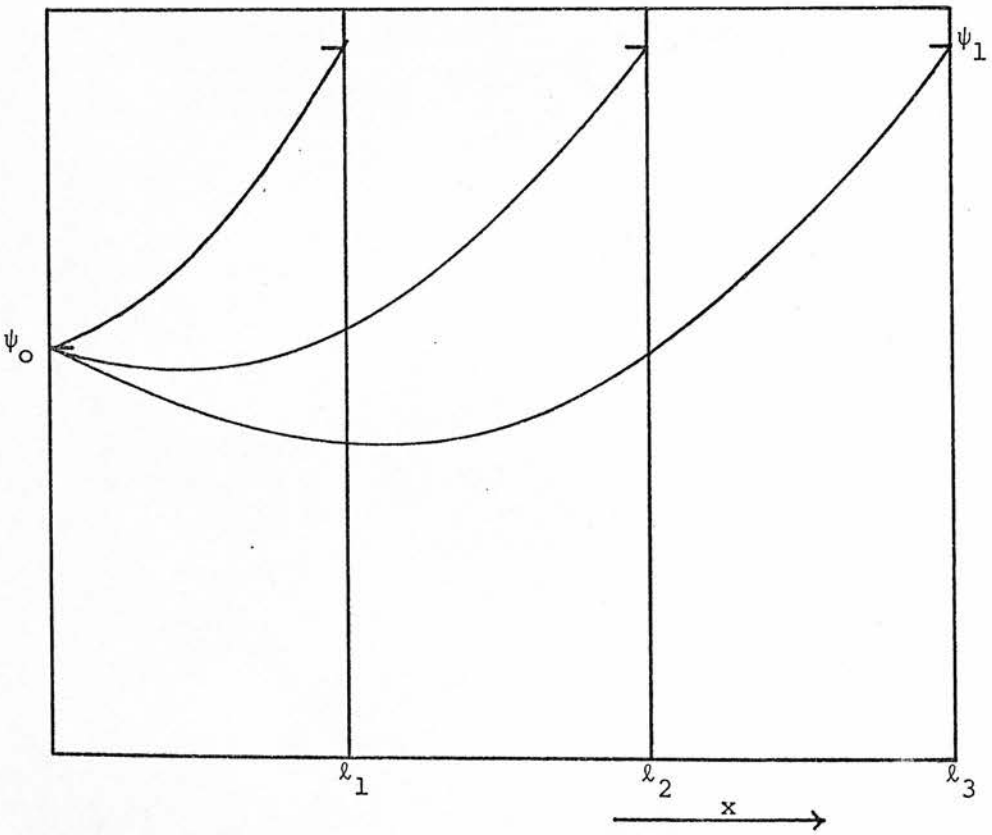

Fig 2.1.3

$\psi(x)$ curves, for various interparticle separations, for two dissimilar potentials

$$V_R = \frac{\varepsilon\pi a_1 a_2 (\psi_{01}^2 + \psi_{02}^2)}{(a_1 + a_2)} \left(\frac{2\psi_{01}\psi_{02}}{(\psi_{01}^2 + \psi_{02}^2)} \ln\left(\frac{1 + \exp(-\kappa H_o)}{1 - \exp(-\kappa H_o)}\right) + \ln(1-\exp(-2\kappa H_o))\right) \quad (2.1.29)$$

In the case of identical spherical particles, where $\psi_{01} = \psi_{02} = \psi_o$ and $a_1 = a_2 = a$ this reduces to

$$V_R = 2\varepsilon\pi a \psi_o^2 \ln(1 + \exp(-\kappa H_o)) \quad (2.1.30)$$

These expressions of the potential energy of interaction of two spherical double layers are only entirely valid for low potentials (< 25 mV) and for conditions such that the double layer thickness is small in comparison to the particle size. These two restrictions arise from the use of the Debye-Hückel and the Derjaguin approximations respectively. Verwey and Overbeek[7] have shown that Derjaguin's method gives a good approximation of the interaction provided $\kappa a > 10$. For $\kappa a = 10$ the error is about 5%, for $\kappa a = 5$, about 10% and for $\kappa a = 2$, about 30%.

Hogg, Healy and Fuerstenau[33] have given a tabulated comparison of electrostatic interaction energies predicted from the approximated equation (2.1.23) with those of the unsimplified expression.[32] They showed that, as expected, the agreement for potentials less than 25 mV was extremely good. Moreover, it was found that the divergence was not excessive even at potentials of 75-100 mV, except at very small interplate distances. In general, inaccuracies in the calculation of V_R at small separations are tolerable for practical systems since the van der Waals interaction is usually dominant at short range.

In conclusion it is apparent that the main criterion for the applicability of equations 2.1.29 and 2.1.30 is the value of κa, provided that the value of ψ_o is not unreasonably large.

Small κa

When κa is small it is no longer valid to approximate the interaction of two spheres to that of a series of flat plates. It is therefore necessary to solve the Poisson-Boltzmann equation (2.1.6) for all three co-ordinates x, y and z to calculate the electric field in the double layer around the particles. Mathematically this is a formidable problem unless some simplifications are made. Again it is assumed that the potential, ψ_o, is small, hence

$$\Delta\psi = \kappa^2\psi \tag{2.1.12}$$

The solution of this equation can be expressed in the form of an infinite series. Verwey and Overbeek[7] have taken the first three terms of this series and, having made use of Gauss's theorem expressing the charge on a particle (2.1.31),

$$Q = -\int \varepsilon\left(\frac{\partial\psi}{\partial r_1}\right) d\omega_1 \quad \begin{matrix}\theta_1 = \text{constant} \\ r_1 = a\end{matrix} \tag{2.1.31}$$

have derived an expression for ψ_o of the form

$$\psi_o = \frac{Q\left(1 + \frac{e^{-\kappa a(S-2)}}{2\kappa aS}\left(1 - e^{-2\kappa a}\right)\left\{1 + \lambda_1\left(1 + \frac{1}{\kappa aS}\right) + \lambda_2\left(1 + \frac{3}{\kappa aS} + \frac{3}{(\kappa aS)^2}\right)\right\}\right)}{4\pi a\varepsilon(1 + \kappa a)\{1 - \delta(1 + \alpha)\}} \tag{2.1.32}$$

where λ_1 and λ_2, α, and δ are parameters which may be calculated from the equations given by Verwey and Overbeek[7].

If it is assumed that the surface potential remains constant then the potential energy of interaction of the approaching particles is given by

$$V_R = \psi_o(Q_\infty - Q_R) \tag{2.1.33}$$

where Q_∞ and Q_R are the charges of one particle when the particles have an infinite separation and a separation distance R, respectively. Using equations (2.1.32) and (2.1.33)

$$V_R = \psi_o^2 \frac{4\pi \varepsilon a^2 e^{-\kappa H}}{(H + 2a)} \cdot \beta \qquad (2.1.34)$$

where ε, a, κ, H, and ψ_o are as defined earlier,

β is a variable which accounts for the distortion of the double layer on interaction.

Tables of β, given by Verwey and Overbeek[7] for several values of κa, illustrate that β varies between $\sim$0.6 and 1 as a function of inter-particle separation. Using equation (2.1.34) with values of β obtained from the tables, it is possible to calculate the repulsive interaction between two identical spheres in a system where κa is small. Unfortunately an extension to describe dissimilar spheres has not yet been published.

Verwey and Overbeek[7] have shown that they were justified in using only the first three terms of the series when $\kappa a < 3$ but that for κa values larger than this the contribution from the subsequent terms was too large to justify their exclusion.

When $\kappa a > 10$ the Derjaguin approximation is valid and equation (2.1.29) may be used to evaluate V_R whereas when $\kappa a < 3$ the above expression is applicable. In order to describe the intermediate region of κa values Verwey and Overbeek[7] have suggested the use of a graphical interpolation.

Recently a new method of solving the linearised Poisson-Boltzmann equation for the potential distribution in the vicinity of two spherical particles has been developed by McCartney and Levine.[105] The method, using a linear superposition approach (L.S.A.) was found to be most

suitable for $\kappa a > 5$. The L.S.A. and Derjaguin approach were found to give very similar results for small interparticle separations but it was shown that at large separations ($\kappa H > 3$) the Derjaguin approach overestimated V_R. The magnitude of this overestimate was shown to be insignificant for $\kappa a > 10$ but to increase with reducing κa values. It was concluded that by using the Derjaguin approach when $\kappa H < 3$ and L.S.A. for $\kappa H > 3$ the range of applicability of the DLVO equations could be extended further into the region of the intermediate κa values.

The above expressions of the electrostatic interactions are based on the Gouy-Chapman model which has already been shown to be inadequate in its description of the double layer in the close proximity of the particle. In this region, according to the Stern model, the potential, ψ_o, decays linearly to a value ψ_δ, from which point the potential decay is exponential. Equations (2.1.29) and (2.1.35) may be used to describe the repulsive interaction due to the overlap of the diffuse regions of two such double layers. If it is assumed that the repulsive interaction arises purely from a diffuse double layer interaction then ψ_δ must be substituted in place of ψ_o in these equations. It is generally assumed that the potential at the plane of shear (zeta potential, ζ), may be equated to, and hence substituted for, ψ_δ. The validity of this assumption will be discussed in a later section.

Equation (2.1.16) illustrates the interdependence of surface charge density (σ) and surface potential (ψ_o). Mathematically it is convenient to assume that, during double layer interaction, one is a variable and the other a constant. In the above derivations it was assumed that the particle surface potential remained constant for all interparticle separations. This need not be so, indeed, Bierman[106] has demonstrated that such a situation becomes unrealistic as the interparticle distance decreases. Fig. (2.1.3) illustrates that the $\psi(x)$ curve between two

dissimilar plates progressively steepens as the interplate separation decreases. Since charge density is proportional to $d\psi/dx$ this infers that the charge density tends to infinity as x tends to zero. Clearly, this is impossible. Furthermore, if the constant potential model is valid, it appears that, as the interplate separation decreases (Fig. 2.1.3), the sign of $d\psi/dx$ reverses at the plate of lower potential. This corresponds to reversal of the sign of the surface charge density at this plate. It is therefore possible to obtain an attractive double layer interaction between constant dissimilar potentials of the same sign.

For the system in which rapid exchange of ions at the particle surface is not possible the assumption that the surface charge density remains constant is more useful. An equation, calculated using the Derjaguin approximation, describing the constant charge situation has been given by Wiese and Healy[30] as

$$V_R^{\sigma} = V_R^{\psi} - \frac{2\pi\varepsilon a_1 a_2(\psi_{o1}^2 + \psi_{o2}^2)}{(a_1 + a_2)} \{\ln(1-\exp(-2\kappa H_o))\} \qquad (2.1.35)$$

This model may be criticised in a similar manner to the constant potential model, in this case the theory predicts that the surface potential tends to infinity at short distances of separation.

Consequently it appears that although the real system may tend to one or other of these models, it cannot be completely represented by either extreme.

Electrostatic interactions need not always give rise to potential energies of repulsion. The predominant driving force in mutual flocculation is often the presence of the attractive electrostatic interaction. The same expressions which have been used to describe the repulsive interactions may be used to evaluate the electrostatic attractive potential.

2.2 Potential Energy of Attraction

Following the recent revival of Lifshitz theory[12] there has been an upsurge of interest in the calculation of electrodynamic attractive interactions which has resulted in the publication of a number of useful review articles.[107-111]

Ever since the advent of atomic theory the idea of interatomic interactions has been postulated to explain why matter exists in a condensed state. In 1873 van der Waals[112] proposed a correction factor to the ideal gas law, to account for the non-ideality of real gases, based on the principle that non-ideality was a result of interatomic attraction. By 1920, the dipole-induced dipole interaction had been postulated by Debye,[113] the energy of attraction between a polar and a neutral atom being given by,

$$V_{DEBYE} = -(u_1^2\alpha_2 + u_2^2\alpha_1)/\ell^6 \qquad (2.2.1)$$

where α_1 and α_2 are the respective polarisabilities,

u_1 and u_2 are the respective dipole moments,

ℓ is the interatomic distance.

A year later Keesom[114] gave the following expressions to describe the dipole-dipole attraction,

$$V_{KEESOM} = -2u_1^2u_2^2/3kT\ell^6 \qquad (2.2.2)$$

for $kT >> u_1u_2/\ell^3$

$$= -2u_1u_2/\ell^3 \qquad (2.2.3)$$

for $kT << u_1u_2/\ell^3$

Following this, Wang[115] showed that even two non-polar atoms attract one another. Although the time average dipole moment of an atom may be zero it will still exhibit instantaneous finite dipole moments because

of the non-symmetrical distribution of the electrons around the nucleus. This instantaneous dipole moment generates an electric field which polarises a nearby neutral atom, inducing in it a dipole moment, the resultant interaction between the atoms being one of attraction. The expression for the potential energy of attraction between two identical non-polar atoms was given by London[116] as,

$$V_{LONDON} = 3h\nu\alpha^2/4\ell^6 \qquad (2.2.4)$$

where h is Planck's constant,

ν is the characteristic fluctuation frequency of the atom.

For macroscopic bodies, such as colloidal particles the overall energy of attraction is of more interest than the individual interatomic attractions. Although all three types of interaction contribute to the total van der Waals energy it is the London dispersion force which is generally responsible for the macroscopic interactions. Only in the case of the London-van der Waals forces are the separate interatomic interactions additive (at least to a first approximation) for macroscopic bodies. As a result of this, although London dispersion forces are weak and short range for atoms and molecules, they are relatively strong and long range for macroscopic bodies.

Hamaker[24] evaluated the London dispersion energy for two spherical particles as a function of diameter, interparticle separation and material involved. The expression given by Hamaker consisted of a geometrical factor multiplied by an interaction parameter

$$V_A = - A/12 \left[\frac{y}{(x^2+xy+x)} + \frac{y}{(x^2+xy+x+y)} + \frac{2\ln(x^2+xy+x)}{(x^2+xy+x+y)} \right] \qquad (2.2.5)$$

where V_A is the potential energy,

ℓ is the interparticle separation,

x is the ratio ℓ/D_1 and y the ratio D_2/D_1,

D_1 and D_2 are the respective particle diameters,

A is the interaction parameter.

Hence, for a given value of A, the value of V_A will depend entirely on the ratios x and y.

The interaction parameter, A, is known as the Hamaker constant and is related to the nature of the material of the particles. There are two fundamentally different methods of evaluating the Hamaker constant which are commonly known as the microscopic and macroscopic approaches.

Microscopic Approach (London-Hamaker Approach)

This is based on the assumption of additivity of intermolecular forces which requires that the interparticle separation is large enough to cause individual molecules in the two bodies to appear as one continuous medium. Hamaker defined

$$A_{12} = \pi^2 N_1 N_2 B_{12} \qquad (2.2.6)$$

where A_{12} is the Hamaker constant for the interaction between materials 1 and 2,

N_1 and N_2 are the numbers of molecules per unit volume of material,

B_{12} is the London constant.

For two hydrogen atoms,

$$B_{12} = B_{11} = 3\alpha_o^2 h\nu_o/4 \qquad (2.2.7)$$

where ν_o is the frequency of an electron in its ground state which is related to the static polarisability by the expression,

$$\nu_o^2 = e^2/4\pi^2 m_e \alpha_o \qquad (2.2.8)$$

where e is the charge on the electron,

m_e is the mass of the electron,

α_o is the static polarisability of the atom.

For more complex atoms Eisenschitz and London[117] derived the following expression which may be written for two different atoms as,

$$B_{12} = (3he^4/32\pi^4 m_e^2) \sum_1 \sum_2 \frac{f_1 f_2}{\nu_1 \nu_1 (\nu_1+\nu_2)} \qquad (2.2.9)$$

where f_1 and f_2 are the oscillator strengths corresponding to transition frequencies ν_1 and ν_2 in atoms 1 and 2.

In the case of only one important transition frequency for each material this becomes

$$B_{12} = (3he^4/32\pi^4 m_e^2)\{s_1 s_2/\nu_{1c}\nu_{2c}(\nu_{1c}+\nu_{2c})\} \qquad (2.2.10)$$

where s_1 and s_2 are $\sum_1 f_1$ and $\sum_2 f_2$ respectively and are regarded as the effective number of dispersion electrons,

ν_{1c} and ν_{2c} are defined as the "characteristic frequencies".

In terms of the static polarisability, for two similar molecules

$$B = 3h\nu_c \alpha_o^2/4 \qquad (2.2.11)$$

since

$$\alpha_o = e^2 s/4\pi^2 m_e \nu_c^2 \qquad (2.2.12)$$

Equations (2.2.11) and (2.2.7) differ only in the frequency term used, the expression for H atoms using ν_o and that for more complex atoms using ν_c. Equations (2.2.14) and (2.2.8) enable the following simple relationship to be obtained,

$$s = (\nu_c/\nu_o)^2 \qquad (2.2.13)$$

Hence

$$B = 3s^{\frac{1}{2}} h\nu_o \alpha_o^2/4 \qquad (2.2.14)$$

Similar expressions to this have been derived by other methods. Slater and Kirkwood,[118] using a variational method obtained

$$B = 3Z^{\frac{1}{2}} h \nu_o \alpha_o^2/4 \qquad (2.2.15)$$

where Z is the number of outer shell electrons.
Moelwyn-Hughes[119] arbitrarily modified equation (2.2.15) by replacing ν_o with ν_c,

$$B = 3Z^{\frac{1}{2}} h \nu_c \alpha_o^2/4 \qquad (2.2.16)$$

Experimentally determined values of B have been shown[108] to compare favourably with values predicted by the London and Slater-Kirkwood expressions but badly with the Moelwyn-Hughes expression.
Combination of equations (2.2.6) and (2.2.10) gives

$$A_{12} = \frac{N_1 N_2 \, 3he^4 \, s_1 s_2}{32\pi^2 m_e^2 \nu_{1c} \nu_{2c} (\nu_{1c}+\nu_{2c})} \qquad (2.2.17)$$

From a combination of the expression for the polarisability of an atom at frequency ν,

$$\alpha_1(\nu) = \frac{e^2}{4\pi^2 m_e} \sum_1 \frac{f_1}{\nu_1^2 - \nu^2} \qquad (2.2.18)$$

with the Lorentz-Lorentz equation for molar refraction,

$$R_1 = \frac{(n_1^2 - 1)}{(n_1^2 + 2)} \qquad \frac{M_1}{\rho_1} = 4\pi N_A \alpha_1(\nu)/3 \qquad (2.2.19)$$

Gregory[108] has obtained a relationship between refractive index and frequency of the form,

$$\frac{(n_1^2 - 1) M_1}{(n_1^2 + 2)\rho_1} = \frac{e^2 N_A s_1}{3\pi m_e (\nu_{1c}^2 - \nu^2)} \qquad (2.2.20)$$

where s_1 is given as Σf_1 (as defined above),

n_1 is the refractive index of 1 at frequency ν,

M_1 is the molecular weight,

ρ_1 is the density,

N_A is Avogadro's number.

This expression is only approximate for many substances in that it assumes that the variation of refractive index with frequency can be represented by a dispersion equation with only one term. From equation (2.2.20) when $\nu = 0$ and by making use of the relationships,

$$\varepsilon = n^2 \qquad (2.2.21)$$

$$N_1 = N_A \rho_1 / M_1 \qquad (2.2.22)$$

Gregory[108] has given an expression for the Hamaker constant,

$$A_{12} = (27/32) \frac{h\nu_{1c} h\nu_{2c}}{(\nu_{1c} + \nu_{2c})} \left(\frac{\varepsilon_{1o}^2 - 1}{\varepsilon_{1o}^2 + 2}\right)\left(\frac{\varepsilon_{2o}^2 - 1}{\varepsilon_{2o}^2 + 2}\right) \qquad (2.2.23)$$

The values of ε_{io} used are given directly as the squares of the limiting refractive indices and the values of ν_{ic} are the corresponding dispersion frequencies. These two parameters are most conveniently obtained from dispersion plots. Consideration of equation (2.2.20) shows that a plot of $(n_1^2+2)/(n_1^2-1)$ against ν^2 will theoretically be linear with a slope of K/s and an intercept of $K\nu_{1c}^2/s$ where $K = (3m_1\pi m_e)/(\rho_1 e^2 N_A)$

Fig. 2.2.1 shows a dispersion plot for butanol (Data: H. Voellmy[120]), for which

$$\nu_{1c} = 3.36 \times 10^{15} \ s^{-1}$$

$$s = 15.0$$

$$n_o = 1.39$$

$$\varepsilon_o = n_o^2 = 1.92$$

where n_o is the limiting refractive index.

Therefore A_{11} for butanol is given by

$$A_{11(but)} = (27/64)\ h\ 3.36 \times 10^{15} \left(\frac{1.92-1}{1.92+2}\right)^2$$

$$= 5.2 \times 10^{-20} \ J$$

From similar data for polystyrene[108]

$$A_{11(ps)} = 7.7 \times 10^{-20} \ J$$

Also

$$A_{12(but/ps)} = 6.3 \times 10^{-20} \ J$$

These Hamaker constants refer to the 1-1 or 1-2 interaction across a vacuum and are therefore meaningless in practical terms. Hamaker[24] proposed a modification to account for any intervening material, 3, such that,

$$A_{132} = A_{12} + A_{33} - A_{13} - A_{23} \qquad (2.2.24)$$

and

$$A_{131} = A_{11} + A_{33} - 2A_{12} \qquad (2.2.25)$$

Fig 2.2.1

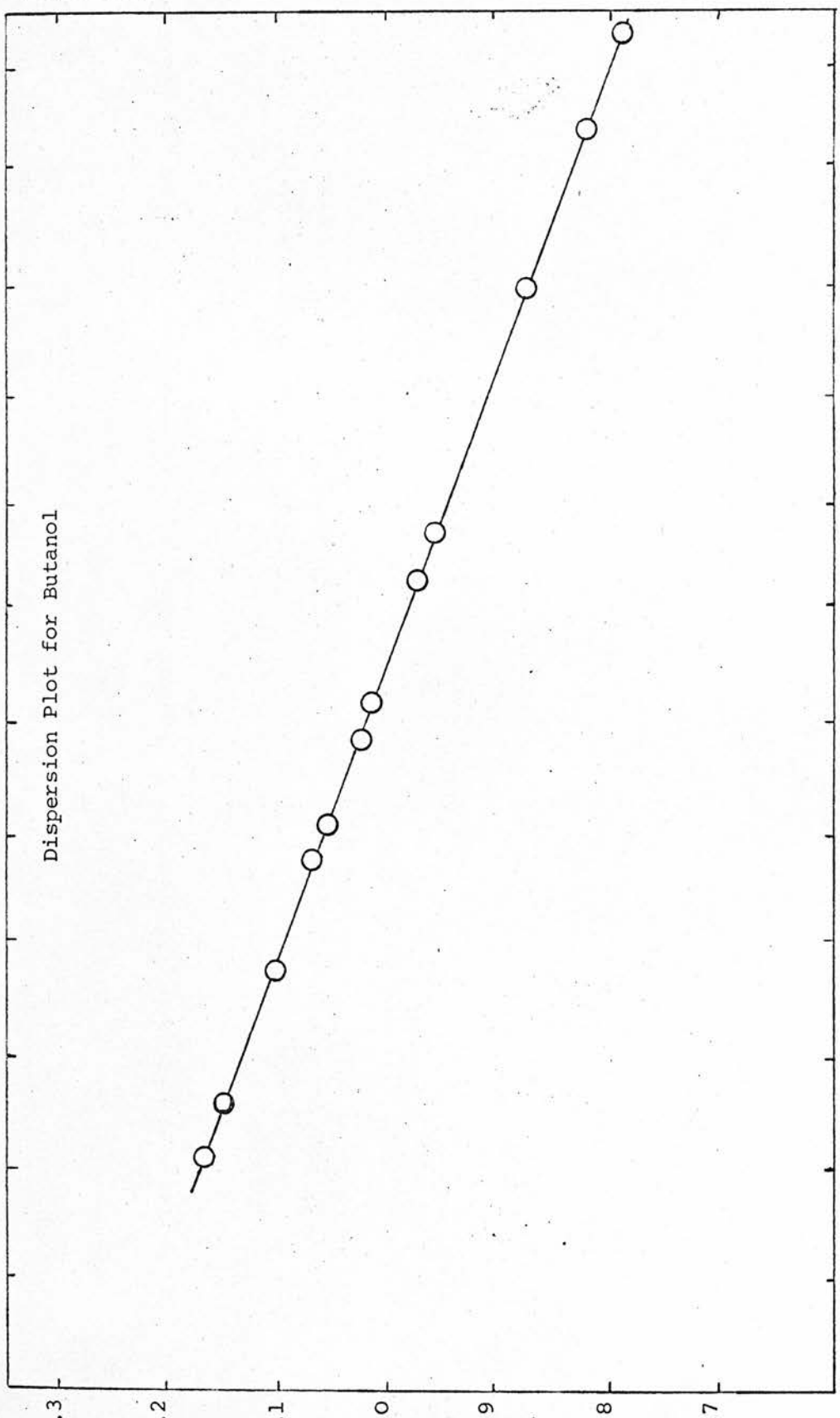
Dispersion Plot for Butanol
$\frac{n^2+2}{n^2-1}$
4.3
4.2
4.1
4.0
3.9
3.8
3.7
10
20
30
40
50
60
70
80
90
100
110
120
$10^{-28} \times \nu^2/s^{-2}$

Substituting the above values of A_{11}, A_{12} etc gives

$$A_{131(ps/but/ps)} = 0.3 \times 10^{-20} \text{ J}$$

Retardation

Since dispersion forces are caused by the production and collapse of electromagnetic fields and the propagation time for such a process is finite, the interparticle separation must also be considered. At large separations there will exist a phase difference between the oscillating electrons of the interacting molecules which will result in a reduction or retardation of the force. Casimir and Polder,[121] using quantum electrodynamics, showed that at very large separations the distance dependence term in the London equation changed from the sixth to the seventh power, so considerably reducing the magnitude of the interaction. Schenkel and Kitchener[27] have derived useful approximate formulae for the retarded interaction between two identical spherical particles. For the close approach of particles, when $\ell << a$ they give

$$V_A \simeq -A\, a/12\ell \qquad (2.2.26)$$

When $\ell > 2\lambda$, where λ is the characteristic wavelength, then the force is fully retarded and V_A is given as

$$V_A \simeq 2.45\, A\, a\lambda/120\pi\ell^2 \qquad (2.2.27)$$

At intermediate distances, when $\ell >> \lambda/6$, the expression for partial retardation is,

$$V_A \simeq \frac{Aa}{\pi}\left(\frac{2.45\lambda}{120\ell^2} - \frac{\lambda^2}{1045\ell^3} + \frac{\lambda^3}{5.62 \times 10^4 \ell^4}\right) \qquad (2.2.28)$$

The Macroscopic Approach

Despite its relative simplicity, the London-Hamaker calculation of the electrodynamic interaction gives results which are compatible with experimental observations. Recently however, the validity of some of the inherent assumptions has been questioned. The theory depends on the assumption that the overall interaction may be derived from the summation of the separate interactions between unit segments of the constituent materials. It seems unreasonable to assume that individual interactions will be independent of one another. It is also assumed that all the electronic dipole fluctuations which contribute, occur about one characteristic frequency, yet for many substances this will not be the case. Finally, the theory proposes that the problem of dealing with any intermediary substance can be solved merely by the insertion of an arbitrary dielectric constant correction at a single frequency.

These inadequacies have been resolved in a theory developed by Lifshitz et al[12] which calculates the interaction between materials from their bulk properties. For a condensed medium, where the range of strong interaction exceeds the distance between atomic centres, the macroscopic theory considers all the individual spontaneous electric field fluctuations as one electromagnetic field which extends over the whole system. Furthermore, unlike the London-Hamaker approach which assumes that the interaction arises from only one characteristic frequency, the Lifshitz approach considers contributions from all frequencies. It also exploits the relationship between the strength of the electromagnetic field at any frequency with the response of the material to an applied field at that frequency (i.e. the permittivity at that frequency) and considers the effects that boundary surfaces between unlike materials have on these fields.

It was long considered that Lifshitz calculations were not possible in the absence of complete spectral information. Although such information is desirable, a knowledge of the single average absorption frequencies in the microwave, IR and UV regions and the corresponding permittivities at these frequencies is generally adequate.

Gingell, Ninham, Parsegian and Richmond have revived[9,10,11] the ideas of Lifshitz[12] to produce several similar equations for "A" of the general form,

$$A_{132} = \frac{3kT}{2} x^2 \sum_{n=0}^{\infty}{}' \int_1^{\infty} p\,dp\{\ln(1-\bar{\Delta}_1\bar{\Delta}_2 e^{-px})(1-\Delta_1\Delta_2 e^{-px})\} \qquad (2.2.29)$$

where

$$\bar{\Delta}_1 = \frac{s_1\varepsilon_3 - p\varepsilon_1}{s_1\varepsilon_3 + p\varepsilon_1} \qquad \bar{\Delta}_2 = \frac{s_2\varepsilon_3 - p\varepsilon_2}{s_2\varepsilon_3 + p\varepsilon_2}$$

$$\Delta_1 = \frac{s_1 - p}{s_1 + p} \qquad \Delta_2 = \frac{s_2 - p}{s_2 + p}$$

$$s_1 = \sqrt{(\varepsilon_1/\varepsilon_3) - 1 + p^2} \qquad s_2 = \sqrt{(\varepsilon_2/\varepsilon_3) - 1 + p^2}$$

$$x = 2\xi_n \ell\, \varepsilon_3^{\frac{1}{2}}/c \qquad \xi_n = (2\pi kT/\hbar).n$$

where

ℓ is the distance between materials 1 and 2,

n is the integer,

k is the Boltzmann constant,

$2\pi\hbar$ is Planck's constant,

T is the absolute temperature

c is the velocity of light in vacuo,

ξ is the frequency on the imaginary axis,

p is the dummy variable of integration,

ε is the permittivity evaluated on the imaginary frequency axis, i.e.

$$\varepsilon_1 = \varepsilon_1(i\,\xi_n);\quad \varepsilon_2 = \varepsilon_2(i\,\xi_n);\quad \varepsilon_3 = \varepsilon_3(i\,\xi_n)$$

Note that, as only the ratios of permittivities, or of their sums appear in these expressions, then it is irrelevant whether absolute or relative permittivities are used so long as the usage is consistent. The prime on the summation indicates that the n = 0 term is to be multiplied by ½.

From this expression it is immediately evident that "A" is not a constant for any given system but rather it is a function of separation and temperature. Consequently Hamaker coefficients defined via energy and force will differ. All Hamaker functions discussed in this thesis are defined in terms of energy.

It is usual to calculate the n = 0 term separately, hence,

$$A = A_{n=0} + A_{n>0} \tag{2.2.30}$$

$A_{n=0}$ is obtained from

$$A_{n=0} = \frac{3kT}{4} \sum_{j=1}^{\infty} \frac{(\Delta_{01}\Delta_{02})^j}{j^3} \tag{2.2.31}$$

where

$$\Delta_{01} = \left(\frac{\varepsilon_3(0) - \varepsilon_1(0)}{\varepsilon_3(0) + \varepsilon_1(0)} \right)$$

and

$$\Delta_{02} = \left(\frac{\varepsilon_3(0) - \varepsilon_2(0)}{\varepsilon_3(0) + \varepsilon_2(0)} \right)$$

where $\varepsilon_i(0)$ are the zero frequency permittivities.

The terms in n > 0 are calculated from a modified form of equation (2.2.29),

$$A_{\substack{132 \\ n>0}} = \frac{3kT}{2} x^2 \sum_{n=1}^{\infty} \int_1^{\infty} pdp \left(\ln(1-\overline{\Delta}_1\overline{\Delta}_2 e^{-px}) (1-\Delta_1\Delta_2 e^{-px}) \right) \tag{2.2.32}$$

One important modification to the n=0 term is necessary when any, or all of the materials are ionic solutions. The electrodynamic interaction is produced by oscillating dipoles of one material inducing dipoles within another. It is evident that the insertion of a charged species (ions) will lead to screening of the dipoles and result in a reduction in the magnitude of the interaction. Since ionic diffusion is a relatively slow process in comparison to dipolar oscillations only the low frequency oscillations need be considered to be screened. The zero frequency term is modified[111] to

$$A_{132}^{n=0} = \frac{3kT}{4} \kappa^2 \ell^2 \int_1^\infty p\,dp\, \ln\left[1-\nabla_1\nabla_2 e^{-2p\kappa\ell}\right] \qquad (2.2.33)$$

where

$$\nabla_1 = \left(\frac{\varepsilon_1\sqrt{p^2-1} - \varepsilon_3 p}{\varepsilon_1\sqrt{p^2-1} + \varepsilon_3 p}\right)$$

$$\nabla_2 = \left(\frac{\varepsilon_2\sqrt{p^2-1} - \varepsilon_3 p}{\varepsilon_2\sqrt{p^2-1} + \varepsilon_3 p}\right)$$

and κ is the reciprocal double layer thickness as defined by equation (2.1.10).

The $A_{n>0}$ term is unchanged and is given by equation (2.2.32).

In order to make quantitative calculations it is necessary to construct a representation of the permittivity as a function of frequency. The permittivity is required only on the imaginary axis, where it is real and decreases monotonically. Either of two expressions relating permittivity to frequency have been employed depending on the format of the available data. Table 2.2.1 shows the dispersion data for graphite[122] from which $\varepsilon(i\xi)$ is obtained by use of the Kramers-Kronig relation,

$$\varepsilon(i\xi) = 1 + \frac{2}{\pi}\int_0^\infty \frac{\varepsilon''(\omega).\omega}{(\xi^2 + \omega^2)}\, d\omega \qquad (2.2.34)$$

where $\varepsilon''(\omega)$ is the imaginary part of the complex permittivity at frequency ω.

Table (2.2.1) ε as a Function of Frequency for Graphite

ε"	16.0	8.0	6.8	8.0	10.3	4.0	1.2	0.3
ω/electron volts	0.85	1.85	3.0	4.0	4.5	5.25	6.25	8.5
ε"	0.7	2.0	7.0	7.0	2.7	1.5	0.8	0.0
ω/electron volts	10.0	11.25	13.5	14.5	15.5	17.0	20.0	28.0

Table (2.2.2). Spectroscopic and Material Data for Plastics and Butanol

	n-Butanol	Polystyrene	PTFE
$C_{mw}(1)$	12.95		
$C_{mw}(2)$	1.69		
$C_{mw}(3)$	0.79		
$C_j(1)$	0.31	.36	1
$C_j(2)$	0.96	.49	
$C_j(3)$		.37	
$C_j(4)$		.34	
$\omega_{mw}(1)$ rad s^{-1}	1.49×10^{9}		
$\omega_{mw}(2)$ " "	4.05×10^{10}		
$\omega_{mw}(3)$ " "	4.2×10^{11}		
$\omega_j(1)$ " "	4.1×10^{14}	1.03×10^{16}	1.54×10^{16}
$\omega_j(2)$ " "	1.6×10^{16}	2.26×10^{16}	
$\omega_j(3)$ " "		1.78×10^{16}	
$\omega_j(4)$ " "		3.25×10^{16}	

The data are inadequate in that they do not include low frequency contributions and so cannot be used to calculate the low frequency permittivities.

Graphite exists in layers of two dimensional giant crystals, each of which comprises an infinitely extended array of carbon hexagons. Since graphite exhibits appreciable conductivity along these sheets the low frequency values of permittivity will be very large and it becomes unreasonable to consider a static permittivity constant. Graphon, however, does not exist in such a form and although it may exhibit localised graphitised areas it is not a bulk conductor. Although its high frequency permittivities may resemble those of graphite, its value of static permittivity will be finite.

To the author's knowledge there are no published dispersion data for Graphon and so for the purposes of calculation of Hamaker functions the data for Graphite are used. A range of estimated static permittivities are used and it is generally found that the Hamaker function obtained is relatively insensitive to the value chosen.

For real frequencies, $\varepsilon(\omega)$ may be expressed as

$$\varepsilon(\omega) = 1 + \sum_{mw} \frac{C_{mw}}{1-i\omega/\omega_{mw}} + \sum_{j} \frac{C_j}{1-(\omega/\omega_j)^2+i\gamma_j\omega} \qquad (2.2.35)$$

where C_{mw} are microwave constants,

C_j are IR and UV constants,

ω_{mw} are characteristic frequencies corresponding to C_{mw},

ω_j are characteristic frequencies corresponding to C_j,

γ_j are the bandwidths.

The first summation describes the Debye relaxation and the second the Lorentz oscillator dispersion. The constants and their corresponding frequencies are derived from spectroscopic data, an example of the method used is given for n-butanol in Appendix 1. Table 2.2.2 shows the constants

used for polystyrene,[110] PTFE[123] and butanol. The bandwidths, γ_j, are usually unknown which makes calculation of $\varepsilon(\omega)$ on the real axis very difficult, however, if $\omega = i\xi$ then

$$\varepsilon(i\xi) = 1 + \sum_{mw} \frac{C_{mw}}{1+\xi/\omega_{mw}} + \sum_{j} \frac{C_j}{1+(\xi/\omega_j)^2+\gamma_j.\xi/\omega_j} \qquad (2.2.36)$$

Since γ_j is always small in comparison with ω_j the term in γ_j in equation (2.2.36) is usually omitted.

Equations (2.2.34) and (2.2.36) are both applicable for frequencies ranging from the microwave to the far UV. If contributions from frequencies beyond this are to be considered then the following limiting form of $\varepsilon(\omega)$ is required,

$$\varepsilon(\omega) = 1 - \omega_p^2/\omega^2 \qquad (2.2.37)$$

or

$$\varepsilon(i\xi) = 1 + \omega_p^2/\xi^2 \qquad (2.2.38)$$

where ω_p is the plasma frequency = $(4\pi Ne^2/m_e)^{\frac{1}{2}}$

where e is the electronic charge,

N is the number density of electrons,

m_e is the mass of the electron.

The limiting expression is used to calculate $\varepsilon(i\xi)$ at frequencies above the plasma frequency.

On the imaginary axis the Kramers-Kronig expression, the Debye-Lorentz expression and the limiting expression all decrease monotonically. However the limiting expression does not coincide with the Debye-Lorentz or Kramers-Kronig expressions at frequencies where each are valid. It is therefore often necessary to construct an interpolation to describe this intermediate region. For butanol, the plasma frequency, ω_p, is 3.3×10^{16} rad s^{-1} which corresponds to n = 135 in equation(2.2.29).

It is therefore unnecessary to introduce any form of interpolation until frequencies corresponding to n = 100 are exceeded. However, to reduce computer time on what is already a lengthy calculation, the summation was, in this work, usually terminated at n = 100. High frequency contributions to the electrodynamic interaction are strongly damped by retardation when the thickness of the intervening material is large. Figure 2.2.3 shows that even at 5×10^{-9}m the high frequency contributions to the interaction are very small and that the error introduced by restricting the summation to n = 100 is, in this case, less than 10%. For larger separations ($> 1 \times 10^{-8}$m) the error involved becomes negligible whereas for small separations ($< 1 \times 10^{-9}$m) the error becomes large and the limitation of n is no longer valid. For most colloidal systems this will not be important since at such small separations the attractive interaction constitutes such a dominant part of the overall interaction that the fate of the colloid is relatively independent of its absolute magnitude.

Graphon dispersions were studied experimentally but the only available dispersion data were for graphite. It is impossible to estimate the error involved in the assumption that both have identical dielectric behaviour. As previously mentioned the value of ε_o(Graphon) has been estimated to allow the calculation of the zero term in "A". The error involved in this will naturally depend on the magnitude of the $A_{n>0}$ contributions in comparison to the estimated $A_{n=0}$ term. Table 2.2.3 illustrates, that whilst the Hamaker functions for the graphite/butanol/graphite and graphite/butanol/polystyrene interactions are relatively insensitive to the size of the $A_{n=0}$ term, that of the graphite/butanol/PTFE interaction is not.

Table 2.2.3

The Contribution of the $A_{n=0}$ Term in Comparison to that of the $A_{n>0}$ Term. ($l = 5 \times 10^{-8}$ m, T = 298 K)

System	Graphite/Butanol/Graphite				Graphite/Butanol/Polystyrene				Graphite/Butanol/PTFE			
ε_o (Graphite)	22	100	250	1000	22	100	250	1000	22	100	250	1000
$10^{21} \times A_{n=0}$ Joules	0.036	1.6	2.6	3.4	-0.25	-1.5	-1.9	-2.0	-0.26	-1.6	-1.97	-2.16
$10^{21} \times A_{n>0}$ Joules	106	106	106	106	27.2	27.2	27.2	27.2	0.68	0.68	0.68	0.68
$\frac{A_{n=0}}{A_{n>0}}$	0.0003	0.01	0.025	0.032	0.01	0.06	0.07	0.07	0.38	2.3	2.9	3.2

Fig. 2.2.2/2.2.3 and 2.2.4/2.2.5 qualitatively illustrate the relationship that

$$A(i\xi) \propto (\varepsilon_3(i\xi) - \varepsilon_1(i\xi))(\varepsilon_3(i\xi) - \varepsilon_2(i\xi)) \qquad (2.2.39)$$

where $\varepsilon_3(i\xi)$ is the relative permittivity of the medium at frequency $(i\xi)$

$\varepsilon_1(i\xi)$ and $\varepsilon_2(i\xi)$ are the relative permittivities of the interacting materials at frequency $(i\xi)$.

Moreover, they illustrate that at frequencies where the permittivity of the medium lies between that of the two interacting materials the contribution to "A" from that frequency is negative.

It has already been shown, for the graphite/butanol/PTFE system, that the zero term dominates at separations of about 5×10^{-9}m. Because it is opposite in sign to the $\sum_{1}^{n} A_{n>0}$ term it will not only control the magnitude of the Hamaker function but also the sign. Fig. 2.2.6, showing Hamaker coefficients for the graphite/butanol/PTFE interaction plotted as a function of separation, illustrates the effect of using different values of the static permittivity of graphite.

Conversely figures 2.2.7 and 2.2.8 show that the Hamaker functions of the graphite/butanol/polystyrene and graphite/butanol/graphite systems are virtually independent of the value of ε_o(graphite) chosen. Screening of the zero frequency contribution by ions in solution will have little effect on the Hamaker functions of these two systems but its effect on the graphite/butanol/PTFE Hamaker function will be profound. This is shown in figures 2.2.9-11. (Hamaker functions were calculated using computer program "SALTHAM". They were stored as series of polynomial functions which are tabulated in Appendix 2).

In conclusion, if the dielectric behaviour of Graphon may be approximated to that of graphite, then the Hamaker function for all systems used in this work, except Graphon/butanol/PTFE may be accurately evaluated

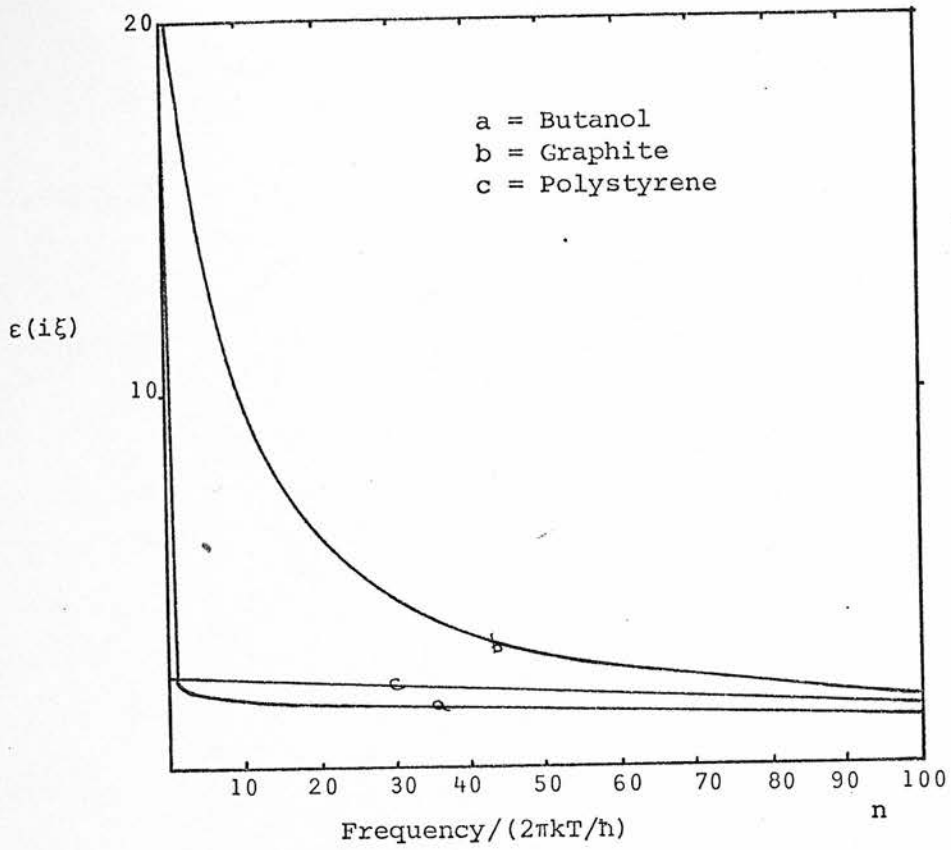

Fig 2.2.2

Dielectric Constant as a Function of Frequency

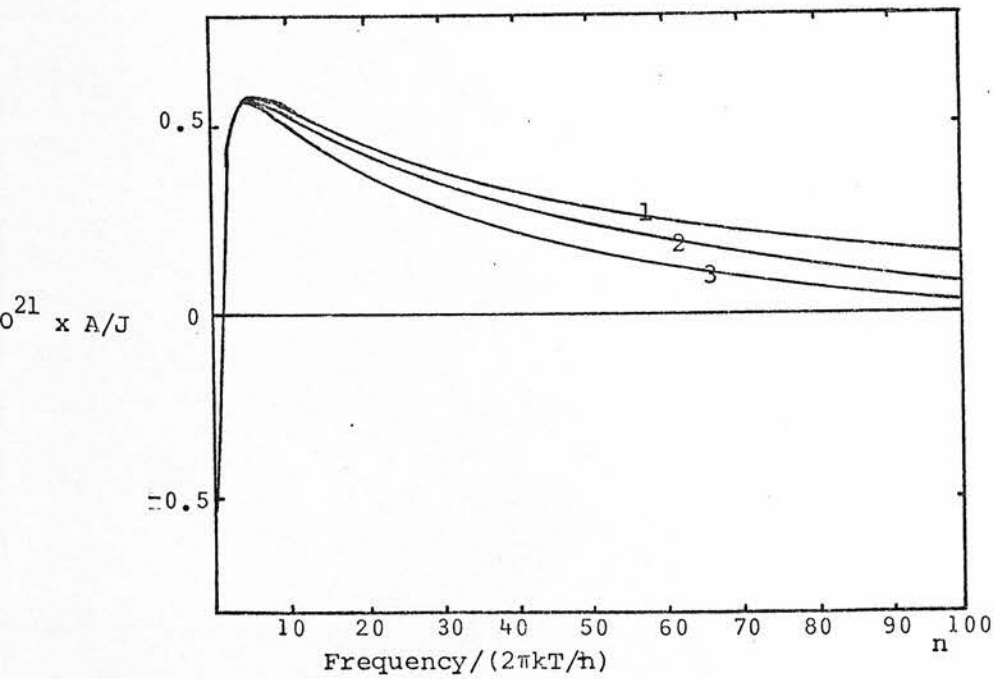

Fig 2.2.3 Contribution of Each Term (A) in the Summation to the Overall Value of the Hamaker Function for the Polystyrene/Butanol/Graphite at 298 K at Separations of

1) 1×10^{-9} m
2) 5×10^{-9} m
3) 1×10^{-8} m

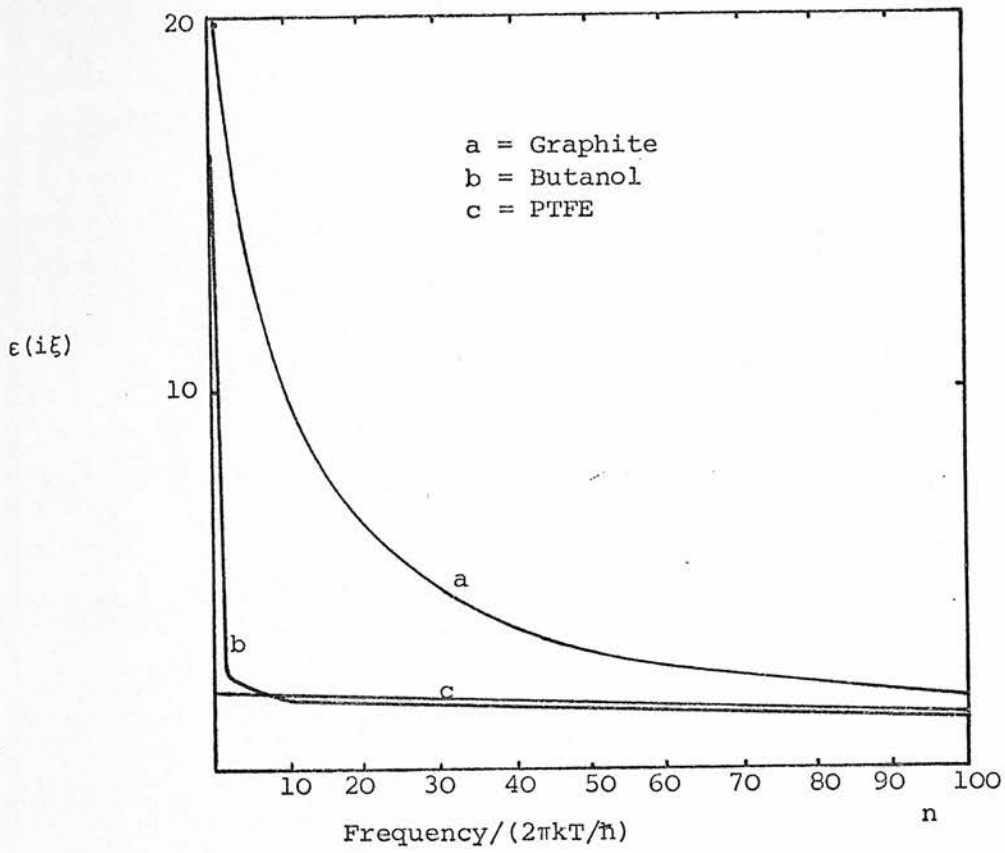

Fig 2.2.4 Dielectric Constant as a Function of Frequency

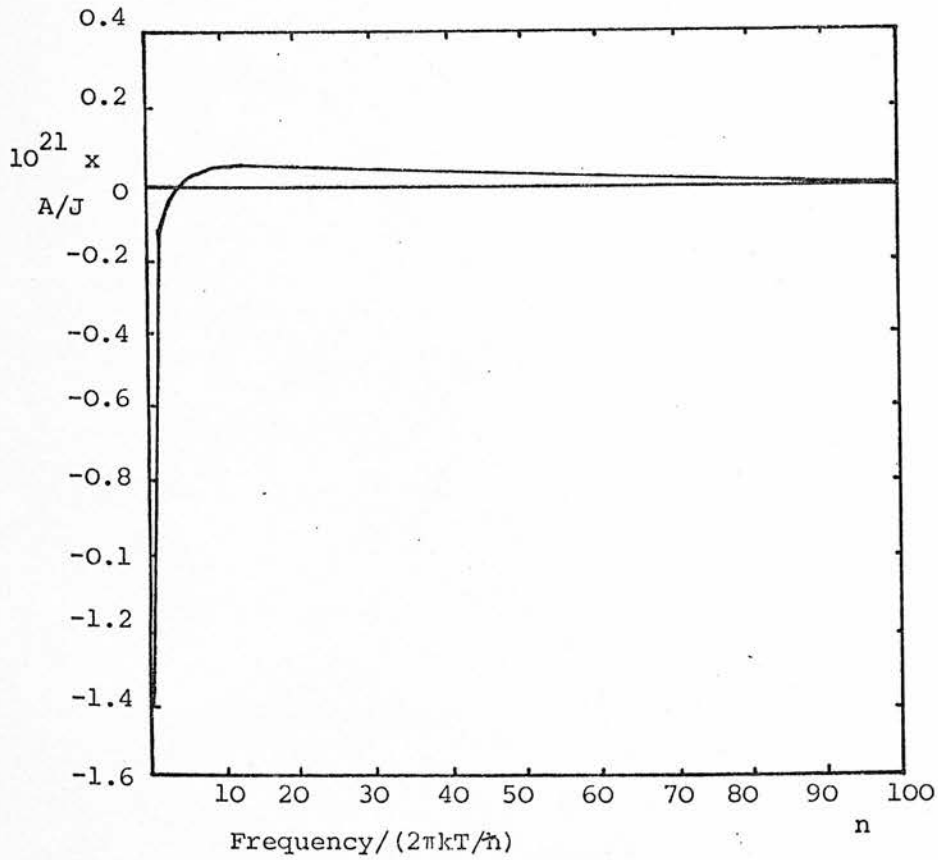

Fig 2.2.5

Contribution of Each Term (A) in the Summation to the Overall Value of the Hamaker Function for the PTFE/Butanol/Graphite at 298 K at a separation of 1×10^{-9} m

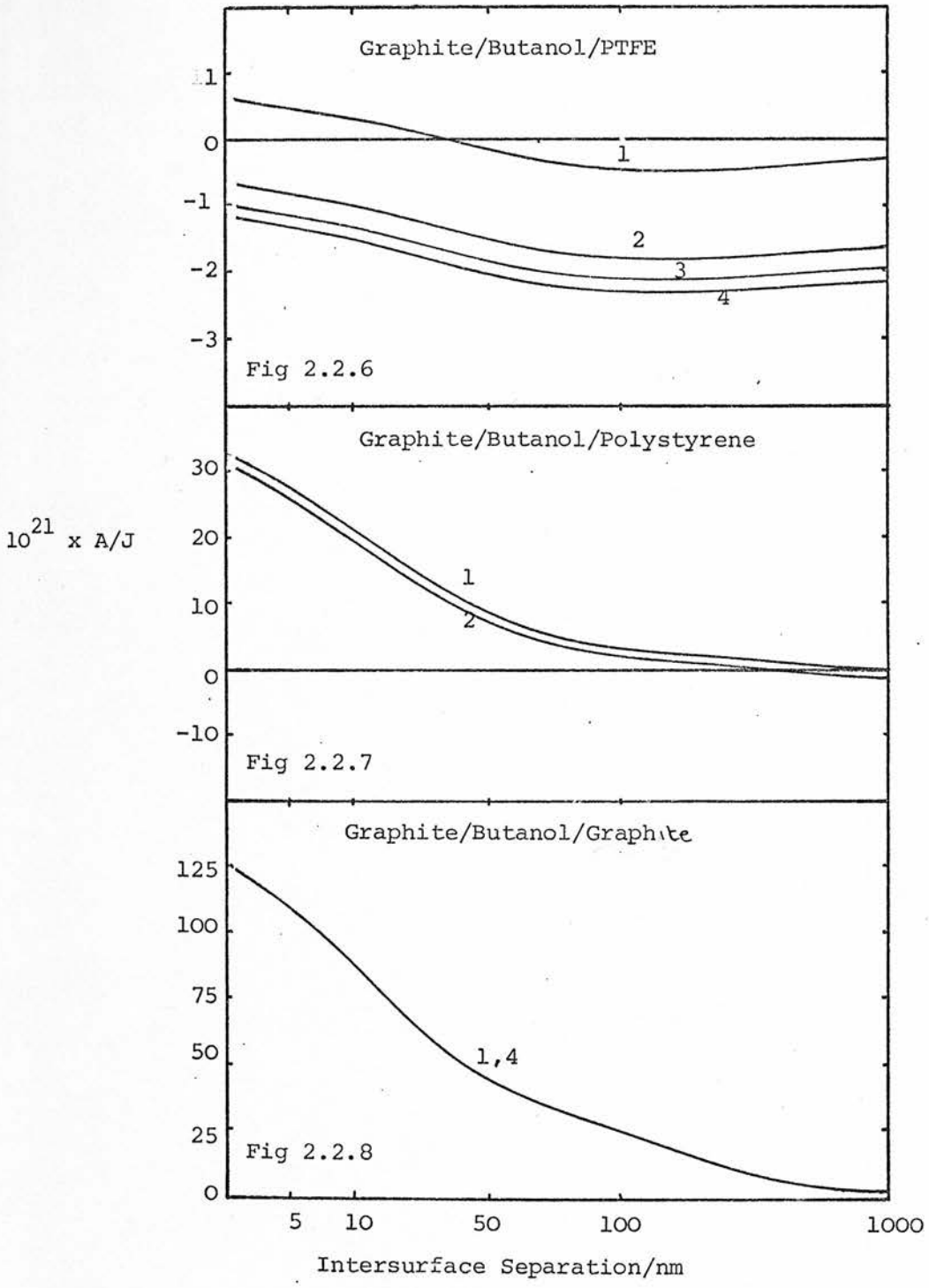

Figs 2.2.6 - 8

Hamaker Coefficients as a Function of Distance Illustrating the Effect of Using Different Values of ε_o (Graphite)

1) ε_o (Graphite) = 22
2) ε_o (Graphite) = 100
3) ε_o (Graphite) = 250
4) ε_o (Graphite) = 1000

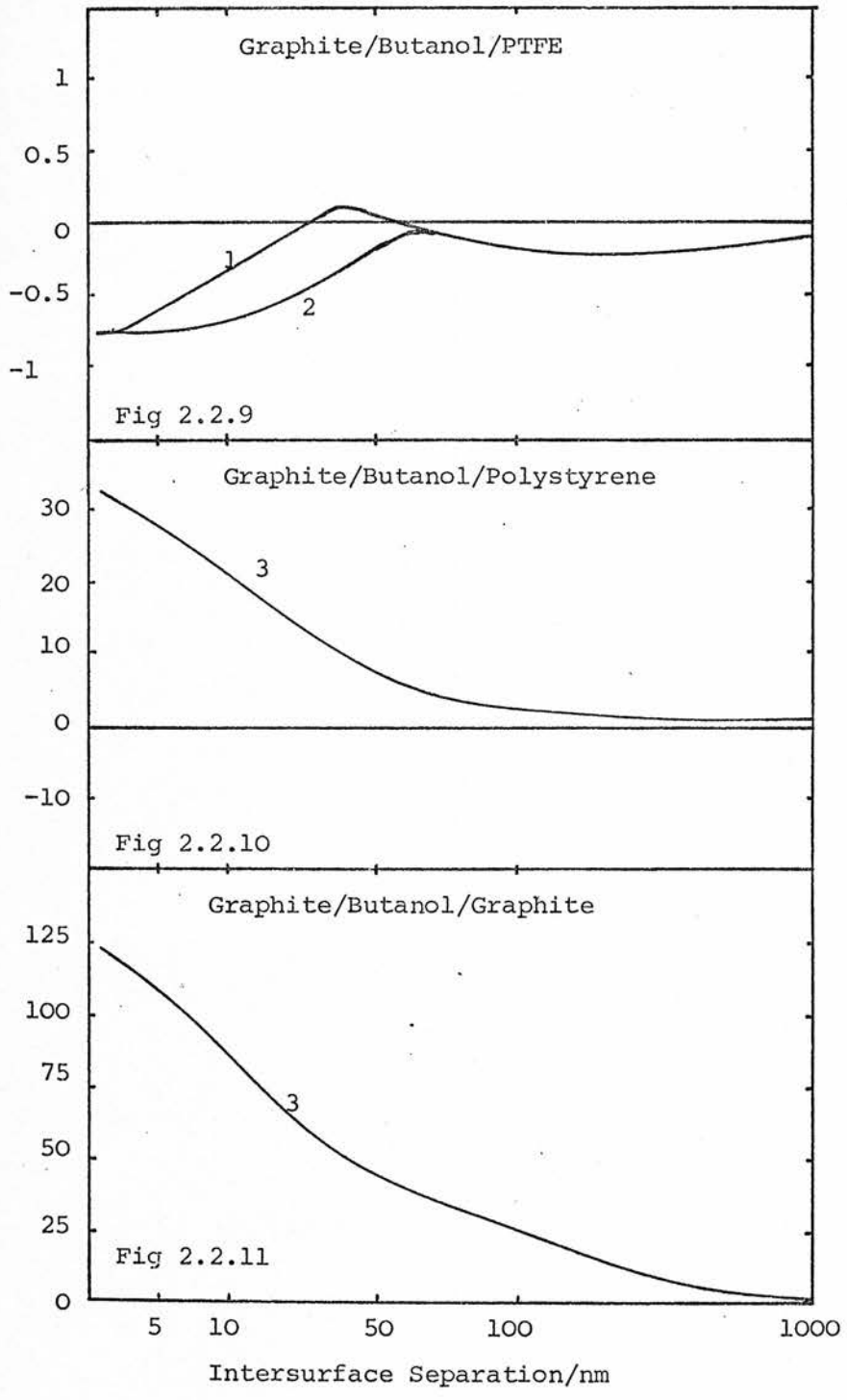

Figs 2.2.9-11

Salt Corrected Hamaker Coefficients as a Function of Distance at Various Electrolyte Concentrations (ε_o (Graphite) = 100) 1) 2×10^{-5} mol dm^{-3} LiCl
2) 10^{-4} mol dm^{-3} LiCl
3) 10^{-3} mol dm^{-3} LiCl

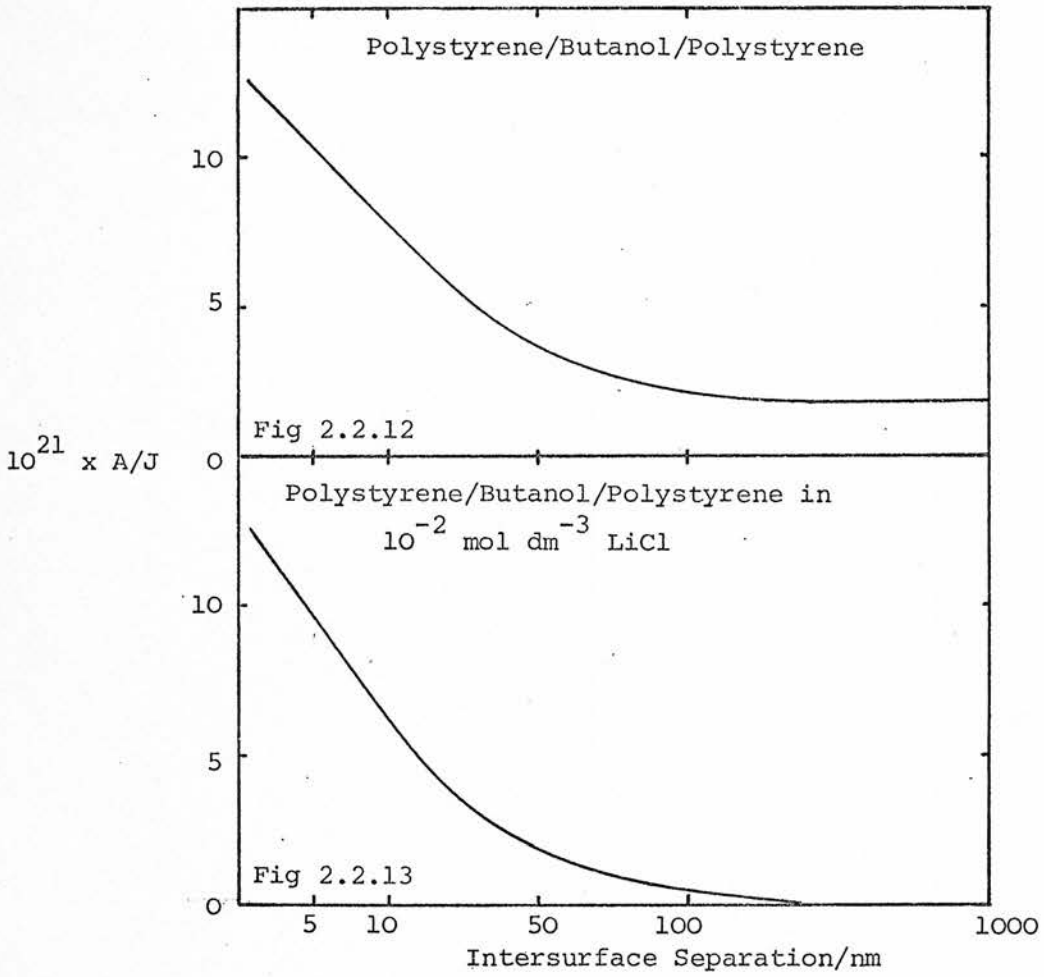

Figs 2.2.12 and 13

Hamaker Coefficients as a Function of Distance for Polystyrene in Butanol

and used to calculate the magnitude of the attractive interactions. These, when combined with a knowledge of the repulsive interactions, will permit quantitative discussion of stability (see Section 2.2.3). This is not possible for the Graphon/butanol/PTFE system and it will be necessary to restrict the discussion to the comparison of quantitative theoretical predictions with experimental results.

2.3 Total Potential Energy of Interaction

The potential energies of attraction and repulsion are both scalar quantities expressed in the same units and may therefore be directly summed to give the total potential energy of interaction. The form of the resultant potential energy curve is therefore dependent on the small difference between two comparatively large potential energy curves, both of which are difficult to evaluate accurately. Van der Waals attraction exhibits an approximately inverse relationship with interparticle distance whereas the electrostatic double layer repulsion decays approximately exponentially with distance. Attraction predominates at short distances, until the separation is of the order of interatomic distances, when Born repulsion, due to electron cloud overlap occurs. Fig. 2.3.1 shows a typical plot of potential energy as a function of distance for colloidal particles in a dilute electrolyte solution. Three important features are shown in Fig. 2.3.1, the depth of the primary minimum, the depth of the secondary minimum and the size of the potential energy barrier, $V_{max.}$ In general the primary minimum is very deep and particles once flocculated into it become very difficult to redisperse. If $V_{max.}$ is large in comparison to the thermal energy of the particles the system will be stable with respect to flocculation into the primary minimum. However, if the secondary minimum is sufficiently deep, loose aggregates of

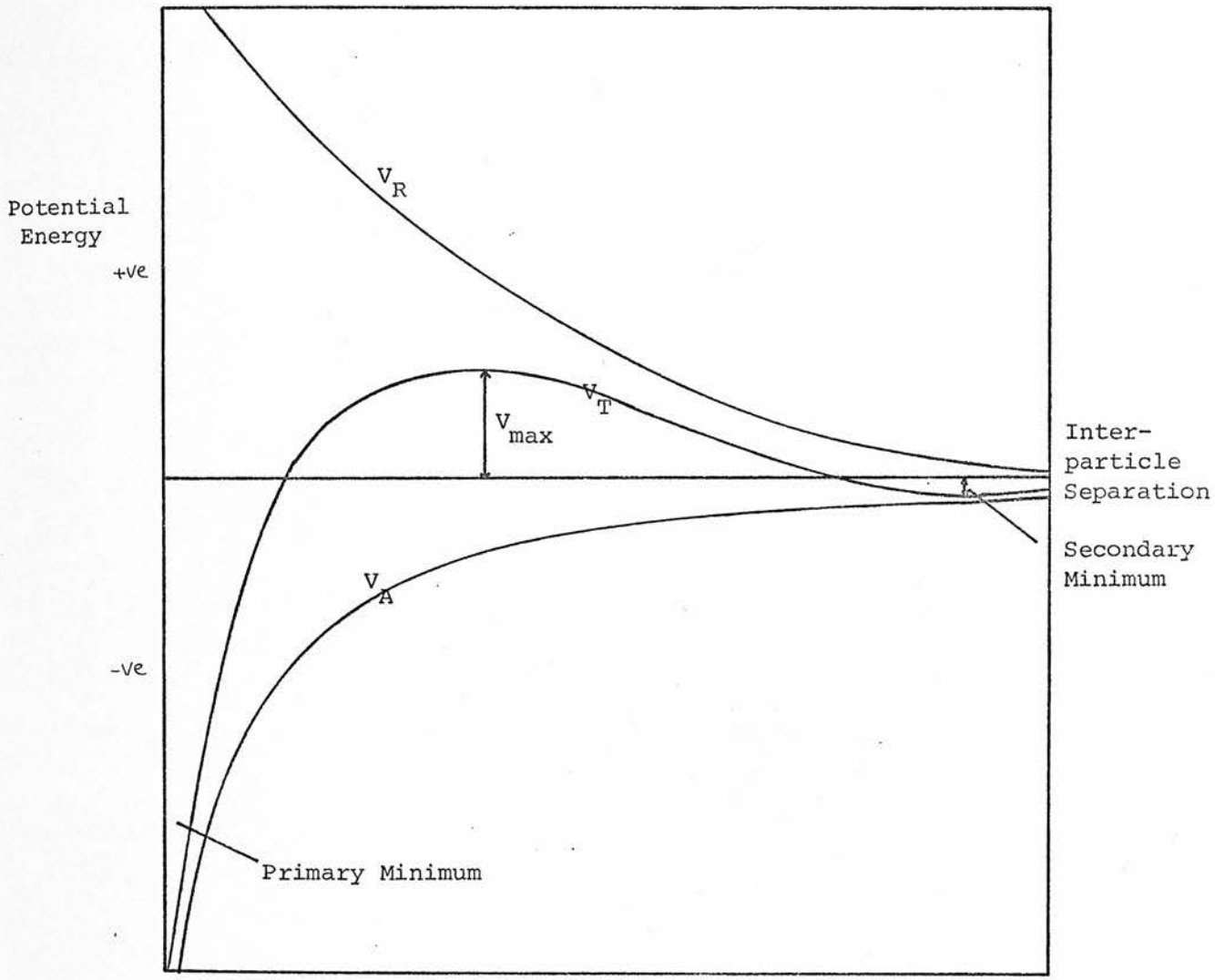

Fig 2.3.1

Potential Energies of Attraction and Repulsion and the Total Potential Energy of Interaction as a Function of Interparticle Separation

particles which are readily redispersed will be formed. Since both the attractive and repulsive forces are approximately proportional to the particle radius, the secondary minimum becomes increasingly more important with increasing particle size.

The form of the total potential energy curve is dependent on a number of parameters including particle size, Stern potential (ψ_δ) and double layer thickness ($1/\kappa$). Verwey and Overbeek[7] have demonstrated that, at constant ψ_δ and $1/\kappa$, small particles are less stable with respect to primary minimum flocculation than large ones. The low stability of small particles is said to be due to the low maximum value of repulsive potential energy. Fig. 2.3.2 illustrates the effect of particle size on $V_{max.}$

Fig. 2.3.3 shows, that as predicted by equation (2.1.29), V_R is directly dependent on the electrical potential (ψ_δ) i.e. ($V_R \propto \psi_\delta^2$). Since V_A is entirely independent of ψ_δ the resultant effect of increasing ψ_δ is an increase in $V_{max.}$ which leads to an increase in stability against primary minimum flocculation.

Compression of the double layer leads to a reduction in the distance over which the repulsive forces are operative (Fig. 2.3.4). In the absence of any effect on V_A, a reduction in $V_{max.}$ occurs which promotes primary minimum flocculation. However it has already been shown that, due to screening of the zero frequency contribution, the Hamaker function becomes smaller as the double layer becomes thinner. Consequently, increasing κ reduces V_A by an amount which is dependent upon the contribution of the zero frequency term in the Hamaker function for that particular system. Since both V_A and V_R are related to κ and for V_A the relationship is a system variable, it is impossible to give a universal definition of the effect on V_T of increasing κ. In general however, since the effect on V_R is usually more pronounced than that on V_A, an increase in primary minimum flocculation is expected.

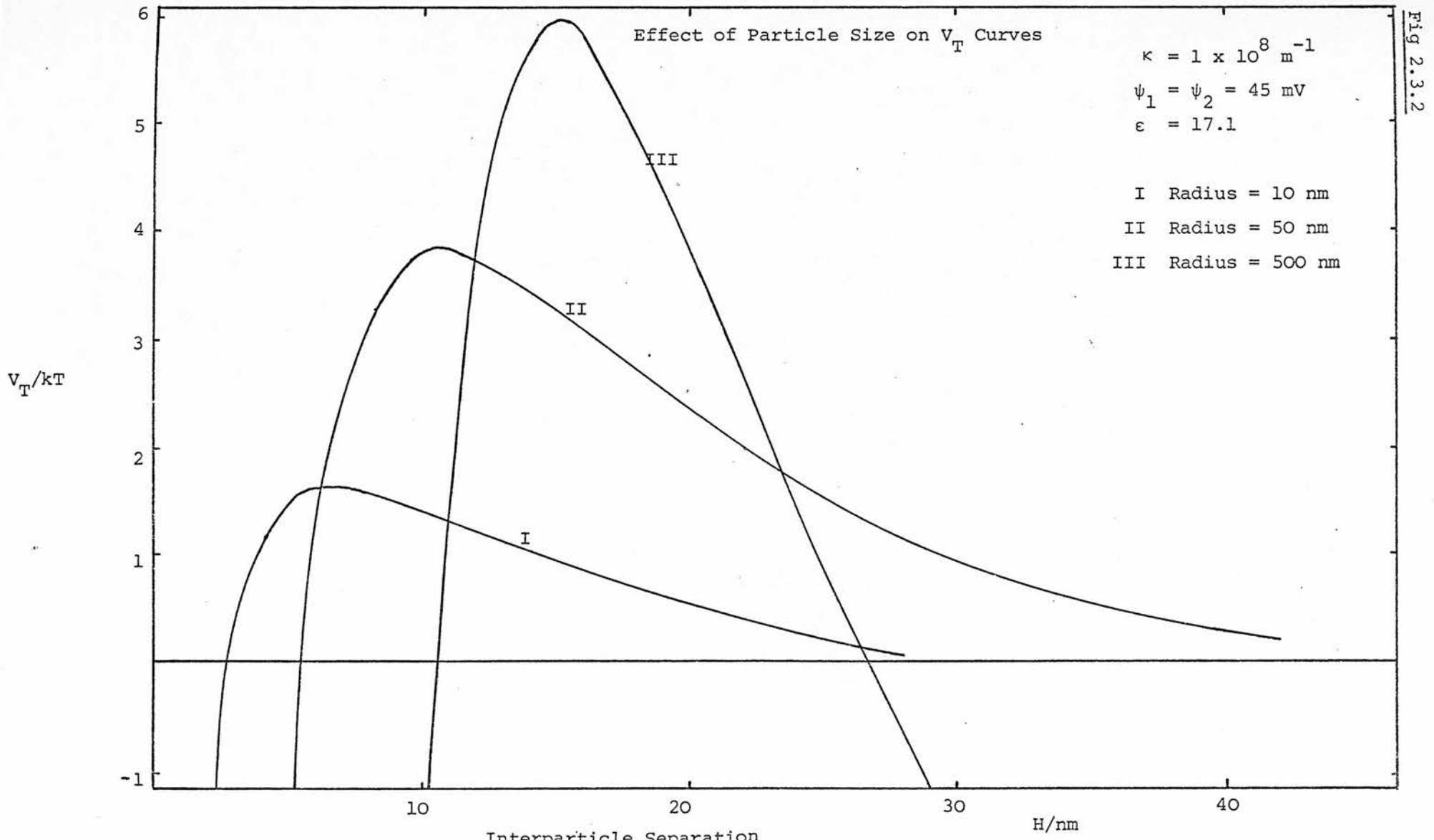
Effect of Particle Size on V_T Curves
$\kappa = 1 \times 10^8\ m^{-1}$
$\psi_1 = \psi_2 = 45$ mV
$\varepsilon = 17.1$
I Radius = 10 nm
II Radius = 50 nm
III Radius = 500 nm
III
II
I
V_T/kT
6
5
4
3
2
1
-1
10
20
30
40
H/nm
Interparticle Separation

Fig 2.3.2

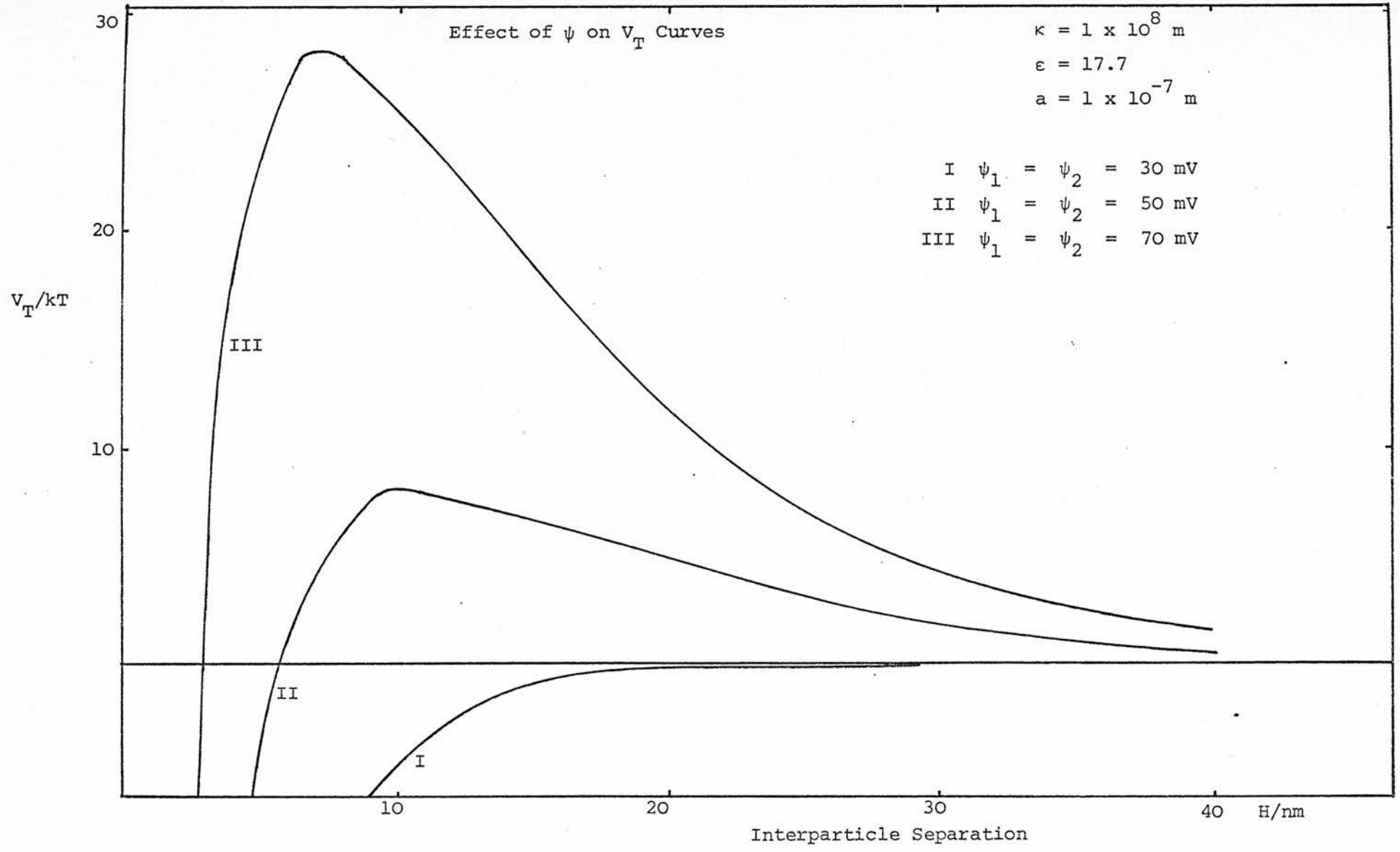
Effect of ψ on V_T Curves
κ = 1 x 10^8 m
ε = 17.7
a = 1 x 10^-7 m
I ψ1 = ψ2 = 30 mV
II ψ1 = ψ2 = 50 mV
III ψ1 = ψ2 = 70 mV
30
20
10
V_T/kT
III
II
I
10
20
30
40
H/nm
Interparticle Separation

Fig 2.3.3

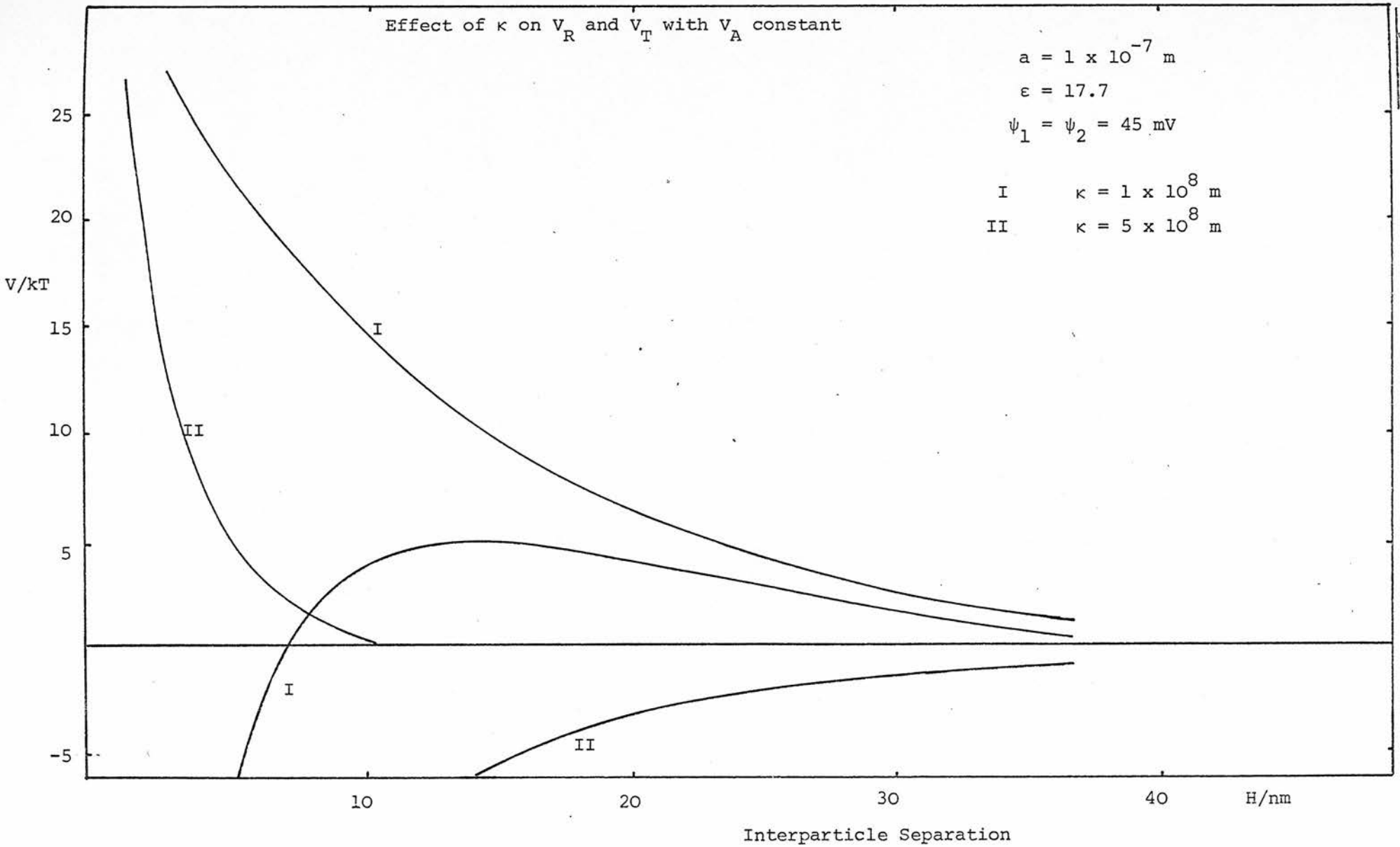
Effect of κ on V_R and V_T with V_A constant
$a = 1 \times 10^{-7}$ m
ε = 17.7
$\psi_1 = \psi_2 = 45$ mV
I κ = 1×10^{8} m
II κ = 5×10^{8} m
V/kT
25
20
15
10
5
-5
I
II
I
II
10
20
30
40
H/nm
Interparticle Separation

Fig 2.3.4

If adsorbed macromolecules are present at the particle/medium interface it may also be necessary to consider a steric repulsion term, V_S. Fig. 2.3.5 illustrates the effect such a term has on an already electrostatically stabilised system.

These energy relationships indicate whether or not a dispersion may be expected to be stable but give no indication of the rate of flocculation. To obtain such information a study of the kinetics of flocculation is required.

2.4 Kinetics of Flocculation

2.4.1 Rapid Flocculation

In considering the kinetics of flocculation of two particles Smoluchowski[124] adopted the idealised model where $V_R = 0$ and there is no interparticle attraction until particle contact. Flocculation under such conditions is entirely diffusion controlled and is defined as rapid flocculation. The rate of collision of particles is obtained by considering the steady state when the number of particles, J, diffusing through any closed spherical surface in the direction of a central fixed particle is constant and equal to the number of particles colliding with the central one. From Fick's first law

$$J = 4\pi Dr^2 \frac{\partial N}{\partial r} \qquad (2.4.1)$$

where D is the diffusion coefficient of the particles

r is the distance from the centre of the fixed particle

N is the number of particles per unit volume.

Using the conditions that $N = N_o$ when $r = \infty$; and $N = 0$ when $r = R$ the number of collisions with a central particle is,

$$J = 4\pi DRN_o \qquad (2.4.2)$$

where R is the sum of the particle radii; N_o is the total particle number.

Fig 2.3.5

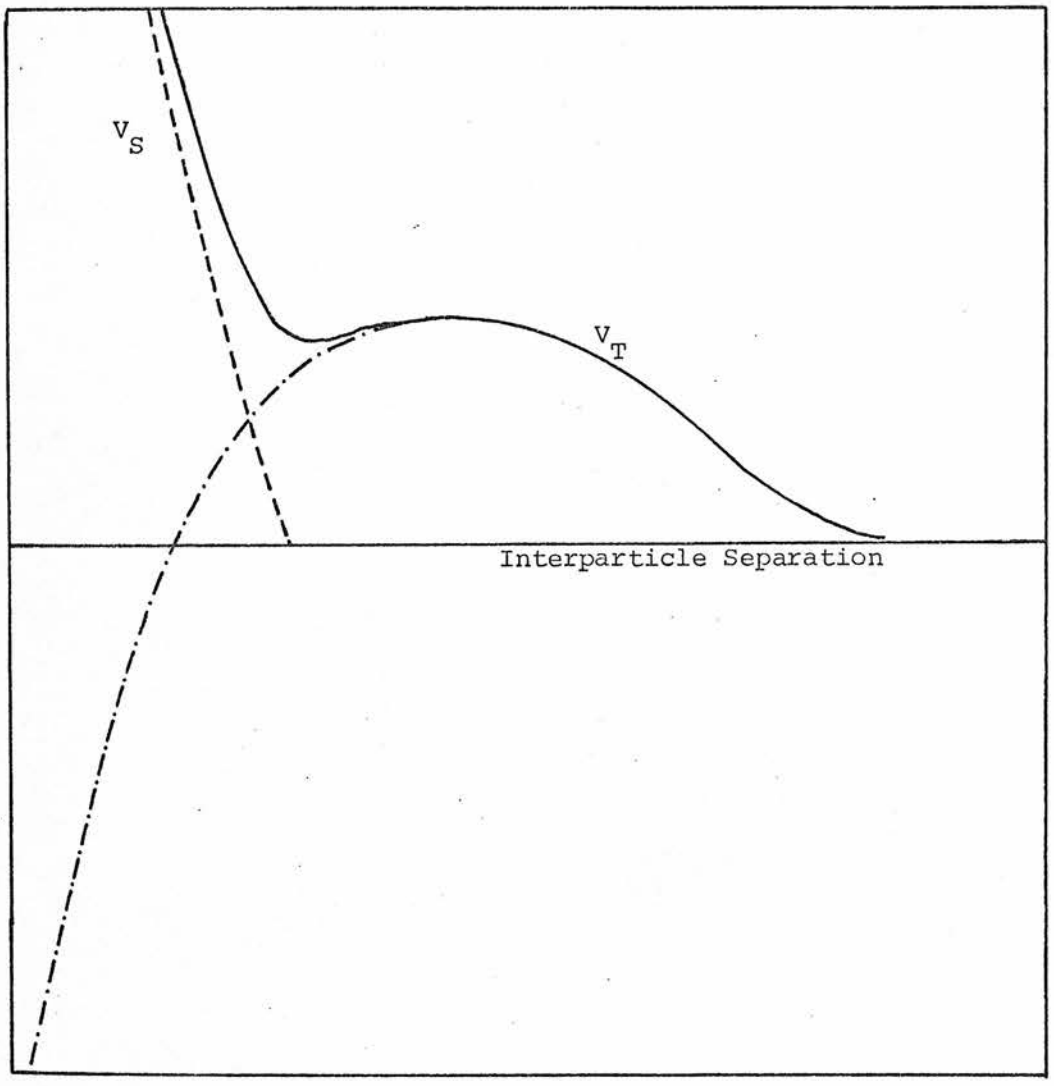

The effect of a Steric Stabilisation Term (V_S) on the Potential Energy Curve V_T

V_S = ----------

V_{T_1} = —·—·—·—·—·—

V_T = $V_T + V_S$ = ———

If the central particle is also subject to Brownian motion then the diffusion coefficient in equation (2.4.2) must be modified to describe the relative motion of the two particles. Since the motions of the two particles are independent of one another

$$D_{12} = D_1 + D_2 \tag{2.4.3}$$

which for two identically sized particles becomes,

$$D_{11} = 2D_1 \tag{2.4.4}$$

therefore

$$J = 8\pi D_1 R N_o \tag{2.4.5}$$

where J is now the number of particles colliding with one individual particle. The rate of disappearance of primary particles is therefore given by

$$-\frac{dN}{dt} = 8\pi D_1 R N_1^2 \tag{2.4.6}$$

where N_1 is the number of primary particles at time t. Equation (2.4.6) only describes the flocculation process at the very beginning when all collisions are between two primary particles. In order to describe the disappearance of all particles it must be modified to

$$-\frac{dN}{dt} = 4\pi D R N^2 \tag{2.4.7}$$

where N is the number of particles of all types.

The diffusion constant, D, for Brownian motion is given by

$$D = kT/6\pi\eta a \tag{2.4.8}$$

where k is the Boltzmann constant; T is the absolute temperature, η is the viscosity of the medium; a is the particle radius.

Since R = 2a equation 2.4.7 may be written as

$$-\frac{dN}{dt} = \frac{4kT}{3\eta} N^2 \qquad (2.4.9)$$

$$= k_o N^2 \qquad (2.4.10)$$

$$\text{where } k_o = \frac{4kT}{3\eta} \qquad (2.4.11)$$

Flocculation therefore proceeds as a second order reaction where k_o is the rate constant. This expression is only strictly applicable for dispersions of spherical particles. Consequently it is most accurately applied to the initial part of the flocculation before the concentration of multiple particles becomes significant.

2.4.2 Slow Flocculation and Stability

The rate of flocculation of a system for which there is an energy barrier, $V_{max.}$, is a function of the probability of particle encounters having sufficient energy to overcome this barrier. In this situation only a fraction, 1/W, of the encounters between particles leads to permanent contact. W is defined as the stability ratio,

$$W = \frac{k_o}{k} \qquad (2.4.12)$$

where k is the flocculation rate constant,

k_o is the rapid rate constant.

Fuchs[125] has given the expression for slow flocculation as

$$-\frac{dN}{dt} = \frac{4\pi D N^2}{\int_{2a}^{\infty} (\exp(V_T/kT)/R^2)\, dR} \qquad (2.4.13)$$

where R = 2a+H, where H is the minimum distance between particle surfaces.

Combination of equations 2.4.7 and 2.4.13 gives

$$W = 2a \int_{2a}^{\infty} (\exp(V_T/kT)/R^2)\,dR \qquad (2.4.14)$$

$$= 2 \int_{2}^{\infty} (\exp(V_T/kT)/s^2)\,ds \qquad (2.4.15)$$

where $s = R/a$

McGown and Parfitt[126] have suggested a modification to account for van der Waals forces being significantly attractive before particle contact. For rapid rate flocculation the number of collisions with one particle is given by,

$$J = \frac{8\pi D N_1}{\int_{2a}^{\infty} (\exp(V_A/kT)/R^2)\,dR} \qquad (2.4.16)$$

Hence the rate of disappearance of primary particles is given by

$$-\frac{dN_1}{dt} = \frac{8\pi D N_1^2}{\int_{2a}^{\infty} (\exp(V_A/kT)/R^2)\,dR} \qquad (2.4.17)$$

and the rate of disappearance of all particles by

$$-\frac{dN}{dt} = \frac{4\pi D N^2}{\int_{2a}^{\infty} (\exp(V_A/kT)/R^2)\,dR} \qquad (2.4.18)$$

Combination of equations 2.4.18 and 2.4.13 gives

$$W = \frac{\int_{2a}^{\infty} (\exp(V_T/kT)/R^2)\,dR}{\int_{2a}^{\infty} (\exp(V_A/kT)/R^2)\,dR} \qquad (2.4.20)$$

$$= \frac{\int_{2}^{\infty} (\exp(V_T/kT)/s^2)\,ds}{\int_{2}^{\infty} (\exp(V_A/kT)/s^2)\,ds} \qquad (2.4.21)$$

From a knowledge of the relevant potential energy curves it is therefore possible to evaluate a theoretical value of W by numerical integration.

Spielman[127] has criticised the assumption of additivity of single particle Brownian diffusion coefficients (equation 2.4.3) to describe the relative diffusion of two particles during collision. It is known that the viscous motion of two neighbouring particles is quite different from that of a single particle.[128,129] Equation (2.4.3) will only be valid when the particles are separated by a distance which is large in comparison to the particle size. Generally however, the dominant region of colloidal interaction is at much smaller distances. Spielman has proposed a modified Brownian relative diffusion coefficient, D_{12}, such that

$$D_{12} = kT/f \qquad (2.4.22)$$

where f is a function of parameters describing the fluid viscosity, the dimensions and the separation of the spheres.

Equation (2.4.21) is modified to

$$W = \frac{\int_2^{\infty} (D_{12}^{\infty}/D_{12}) \exp(V_T/kT)\, ds/s^2}{\int_2^{\infty} (D_{12}^{\infty}/D_{12}) \exp(V_A/kT)\, ds/s^2} \qquad (2.4.23)$$

where $D_{12}^{\infty} = D_1 + D_2$ i.e. the relative diffusion coefficient as defined by Smoluchowski.

For a dispersion containing two types of particles there are three possible interactions between particles each of which has its own value of W. If the particles are defined to be of types 1 and 2 these are written as W_{11}, W_{22} and W_{12} corresponding to the 1-1, 2-2 and 1-2 interactions respectively. The probabilities of these encounters are given as

$$P_{11} = n^2$$

$$P_{22} = (1-n)^2$$

$$P_{12} = 2n(1-n)$$

where n is the fraction of particles of type 1 present in the system. Hogg, Healy and Fuerstenau[33] have given the expression for the total stability ratio, W_T, as

$$\frac{1}{W_T} = \frac{n^2}{W_{11}} + \frac{(1-n)^2}{W_{22}} + \frac{2n(1-n)}{W_{12}} \qquad (2.4.24)$$

CHAPTER THREE

3. EXPERIMENTAL

3.1 Equipment and Materials

The presence of very small concentrations of water has been shown to produce profound effects on both zeta potential and dispersion stability.[52,53,55] The hygroscopic nature of dry butanol necessitates its isolation from the atmosphere. This was most easily accomplished by using a vacuum line system incorporating greaseless taps and joints.

Similarly, since small concentrations of ions have significant effects on butanol systems, thorough cleaning of the apparatus is essential. Ultrasonic irradiation of the glassware, occasionally filled with surfactant solution, was used to remove particles from the walls of equipment which had previously contained a dispersion. If surfactant was used the glassware was soaked in water overnight. Superficial cleaning with water was followed by careful washing with permanganic acid (H_2SO_4 + $KMnO_4$ crystals) and subsequent rinsing with dilute hydrochloric acid to remove permanganate residues. Copious rinsing with doubly distilled de-ionised water (conductivity < 1 μmho) was followed by overnight drying in an oven at 383 K. In the case of vacuum equipment a period of several hours of outgassing then followed. Using this method it was possible to prepare, reproducibly, dispersions in which butanol had an approximately measured conductivity of less than 10^{-8} mho (cf. 9×10^{-9} mho[130]).

3.1.1. Preparation of Polystyrene Latices

For this work the requirements of a model colloid are that it is monodisperse and that the particles are spherical. Although polystyrene dispersions which fit these criteria can be readily prepared in aqueous solution, styrene polymerisation in alcohols has not yet been reported. The latex dispersions were therefore made in water and the

medium then exchanged for butanol by dialysis. In order that the particles should exhibit maximum stability in the non-aqueous medium, maximum ionisation of the acidic groups on the particle surface is essential. For this reason it is preferable to produce dispersions which are stabilised by $-SO_4^-$ groups rather than $-COO^-$ groups.

a) Aqueous Dispersions

Materials:- 780 cm^3 water, (2 x distilled de-ionised)

0.5 g $K_2S_2O_8$, (2 x recrystallised)

80 cm^3 styrene, (distilled to remove inhibitor).

Argon was bubbled through a mixture of styrene and water in a flange-flask to remove dissolved oxygen (Plate 3.1.1). The mixture was stirred vigorously and the temperature raised to 343 K, a cold aqueous solution of the initiator ($K_2S_2O_8$) was then added carefully. The argon bubbling and the stirring were continued and the temperature was maintained at 343 K for a further 16 hours. Since H_2SO_4 is a by-product of the reaction and acid conditions favour the reaction,

$$RCH_2SO_4^- \longrightarrow RCH_2OH \longrightarrow RCOOH$$

it was necessary to maintain the pH at about 7 by the addition of NaOH as required.

The surface of the particles produced by this method has a preponderance of $-SO_4^-$ groups with some $-COO^-$ and -OH groups. Other dispersions, with almost solely $-COO^-$ groups on the particle surface were prepared by using $\alpha\alpha'$ azobisisobutyronitrile (A.Z.B.N.) as an initiator.

b) Dialysis

For maximum dispersion stability it was also necessary to minimise the electrolyte concentration. This was achieved by extensive dialysis through treated cellulose dialysis tubing against doubly distilled

Plate 3.1.1

Polymerisation Equipment

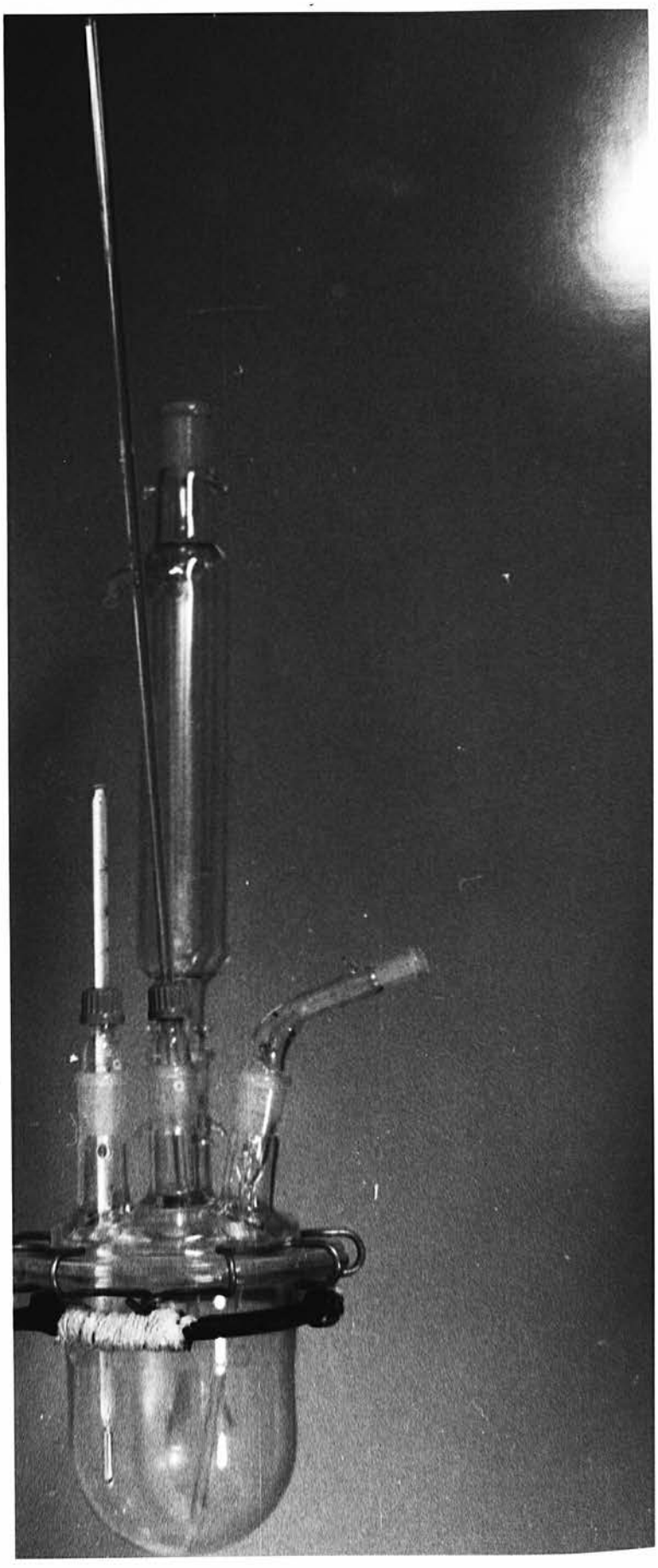

de-ionised water. The pretreatment of the dialysis tubing involved repeated washing with water, using a Soxhlet extractor, in order to remove plasticiser.

Direct exchange of the dispersion medium for butanol by dialysis is not possible since this results in flocculation. Hiltner et al[131] have, however, shown that for certain aqueous polystyrene sols it is possible to exchange the dispersion medium for methanol and then for butanol. This technique was found to work well for $-SO_4^-$ stabilised sols but flocculated those stabilised by $-COO^-$ groups. Carboxyl ion stabilised sols were therefore rejected.

The aqueous polystyrene sol was dialysed ten times against AnalaR methanol, a ten-fold excess of methanol being used each time. This was repeated for dialysis against AnalaR butanol and then five times against distilled butanol with a ten-fold excess of butanol. Karl Fischer[132] titration showed that the water content of the final dispersion medium was about 250 p.p.m. This technique produced a particle number density in the dispersion of approximately 10^{17} particles m^{-3} which is of the order of a thousand times greater than would be used experimentally.

c) Particle Size

Plate 3.1.2. is an electron micrograph of the polystyrene latex and shows that the particles are spherical and approximately uniform in size. The size distribution histogram (Fig. 3.1.1) is approximately Gaussian about a peak value of 0.32 μm diameter. The mean diameter was calculated to be $0.320 \pm .017$ μm. This value was used in the calculation of zeta potentials and potential energy curves. However this value describes the dry, desolvated particle, these being the conditions under which the micrographs were obtained and it does not take into account any swelling which may occur in butanol.

Plate 3.1.2

Electron Micrograph

of

Polystyrene

Plate 3.1.3

Electron Micrograph

of

PTFE

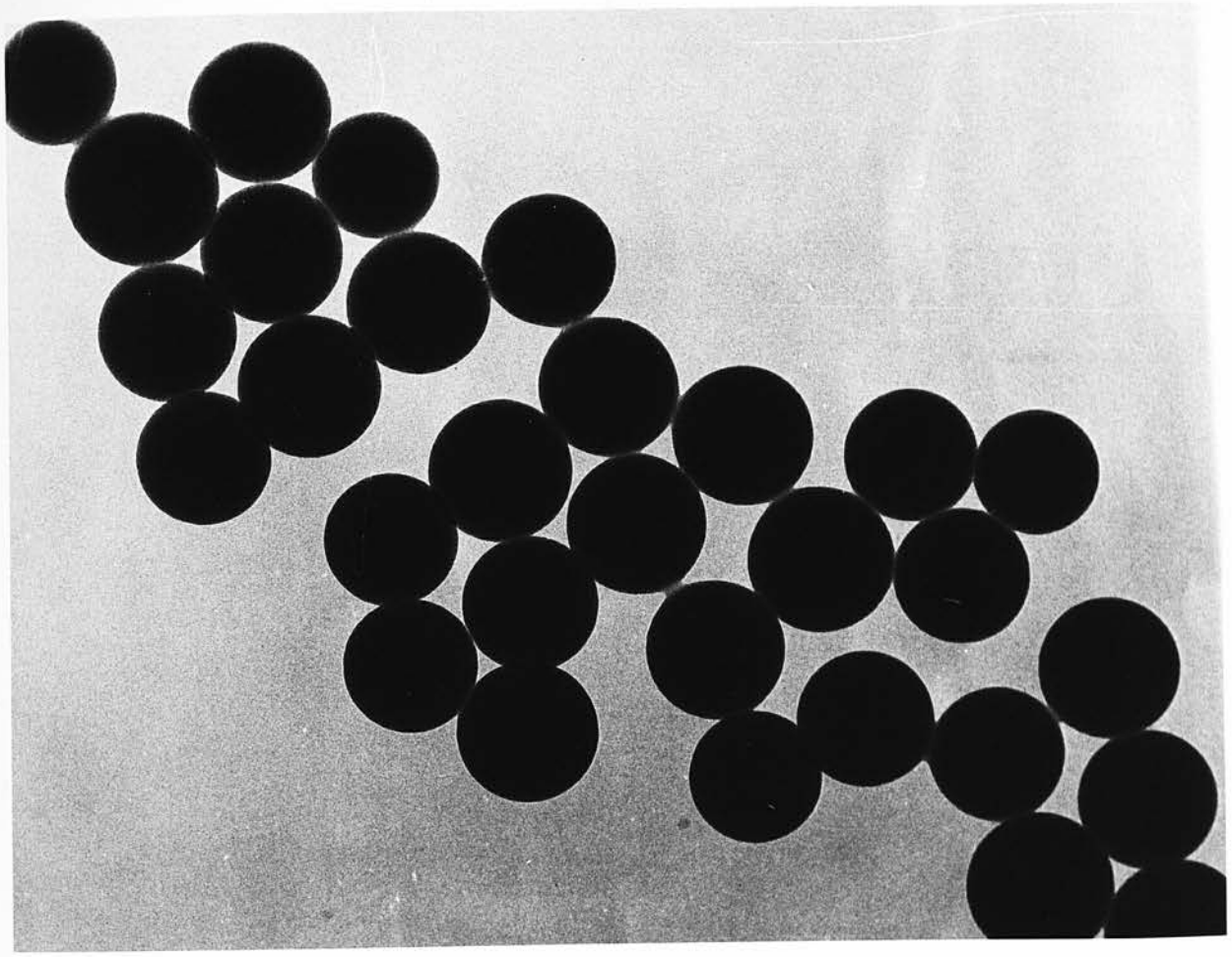

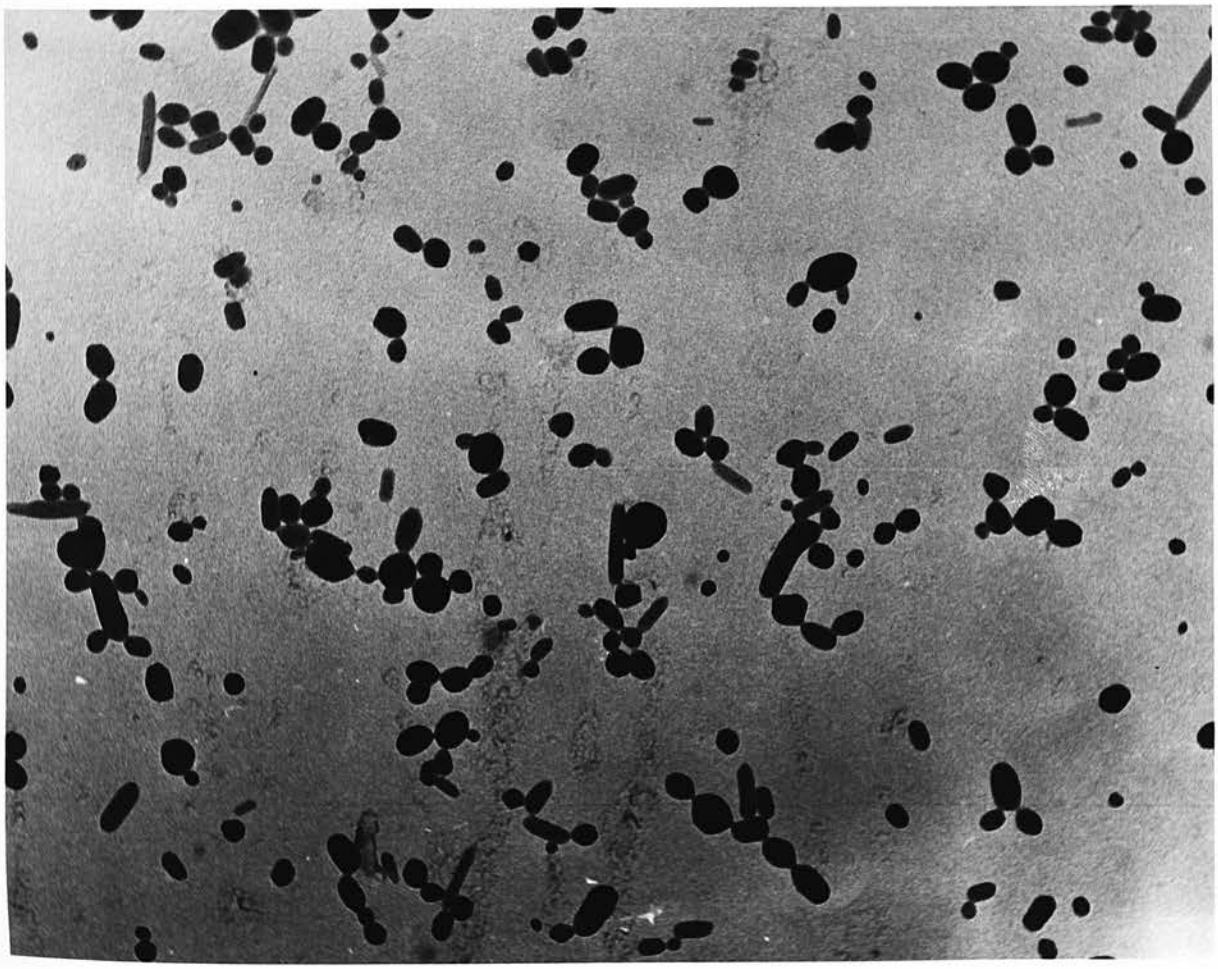

Fig 3.1.1

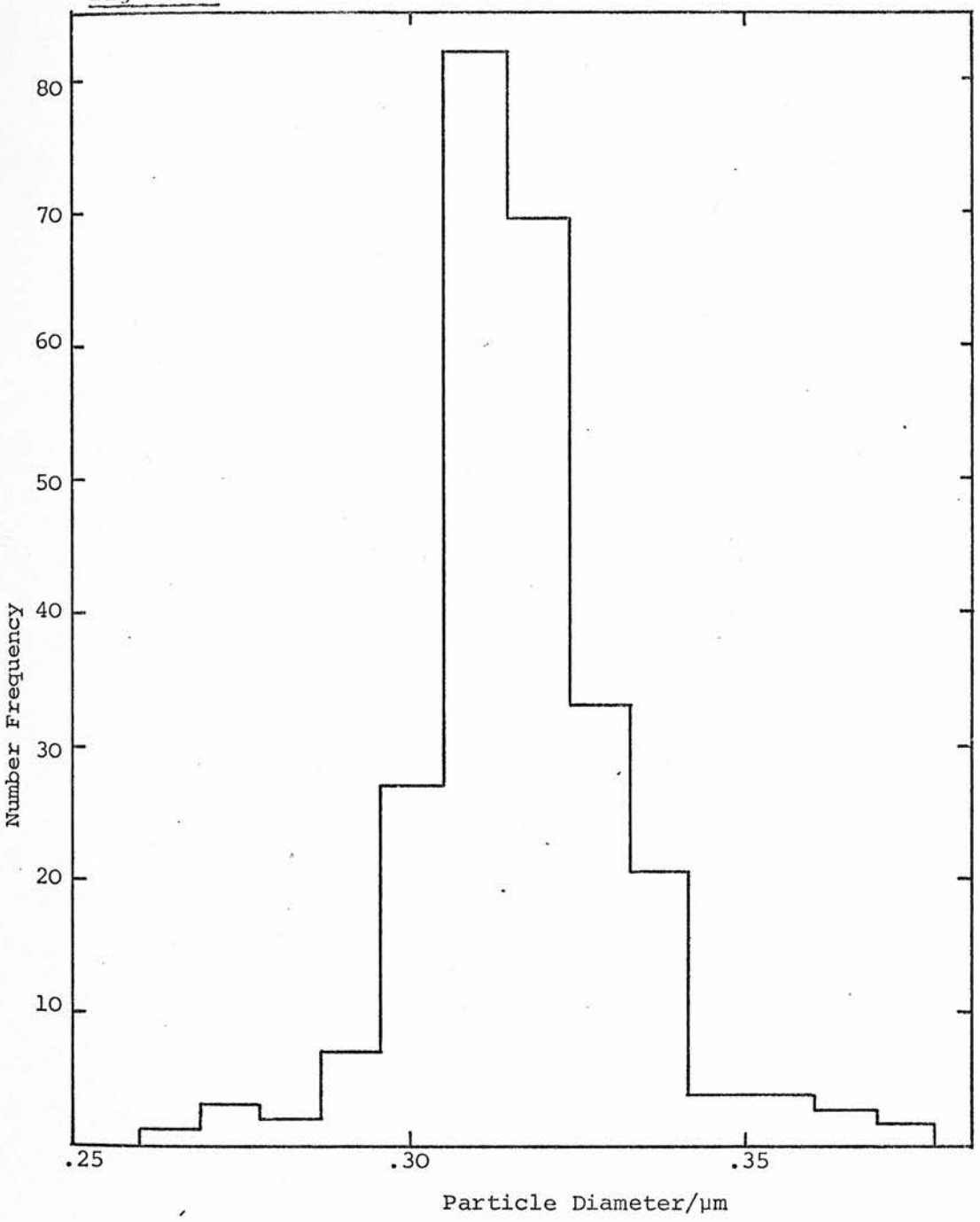

Histogram Illustrating Polystyrene Size Distribution

3.1.2 Polytetrafluoroethylene (PTFE) Latices

An aqueous dispersion of a PTFE latex (I.C.I. Fluon GP 2) was obtained from Dr. D. Rance of Bristol University. The sample had been dialysed fifteen times at pH 10 to remove $C_7F_{15}COONH_4$ and then a further fifteen times to return the pH to about 7. In each case the dialysis involved daily exchanges with about a ten-fold excess of dialysing solution.

One modification was required in the technique used to exchange the aqueous medium for butanol from that used for the polystyrene dispersions. In order to prevent flocculation during the first dialysis with methanol it was necessary to dilute the aqueous dispersion by a factor of ten with methanol. The final particle number of the PTFE dispersion in butanol was approximately 10^{16} particles m^{-3}.

Plate 3.1.3 is an electron micrograph of the PTFE particles which shows that they are irregular in shape and size. The particles approximate to ellipsoids and have therefore been sized in terms of their major and minor axes. Histograms (Figs. 3.1.2 and 3.1.3) show that the size distributions are non-Gaussian, the average and the most probable dimensions being given by:

Major Axis	Mean size = .163 $\pm$ .058 μm	
	Most probable size $\simeq$ .13 μm	
Minor Axis	Mean size = .104 $\pm$ .042 μm	
	Most probable size $\simeq$ .08 μm.	

For the interpretation of electrophoresis data and the calculation of potential energy curves the particles were approximated to spheres having a diameter of 0.1 μm.

The potential determining ion for this sample of PTFE is also the proton, the surface groups being $-CF_2COOH$ and $-CF_2(CH_2)_2COOH$. Karl Fischer water determination showed that the PTFE dispersion contained about 250 p.p.m. of water.

Fig 3.1.2

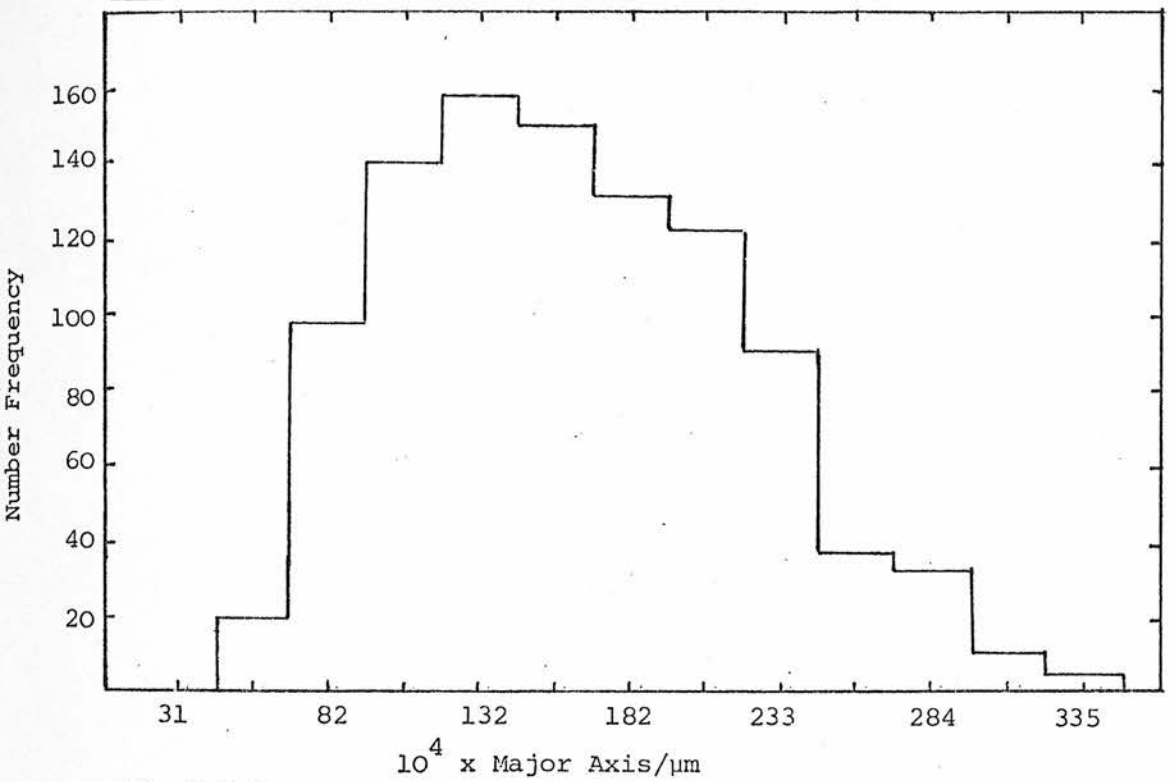

Fig 3.1.3

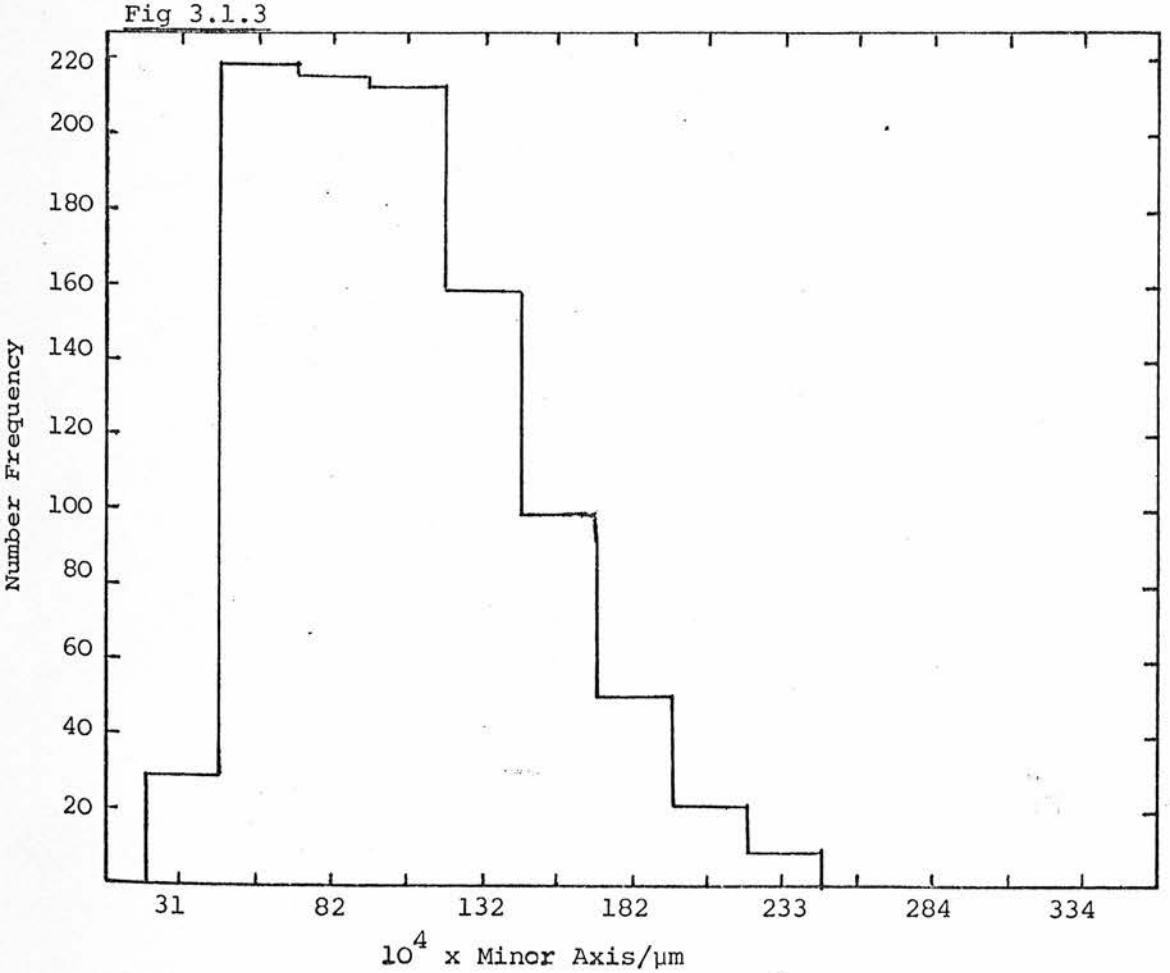

Histograms Illustrating PTFE Size Distribution

Both polystyrene and PTFE dispersions were kept in airtight containers to minimise absorption of atmospheric water.

3.1.3 Carbon Blacks

Two types of carbon blacks, Graphon and Black Pearls A, were used in this work. The samples were supplied by the Cabot Corporation and apart from outgassing directly before use they were used as received.

Graphon has an apolar surface and consists of aggregates of small particles with an overall diameter of about 0.25 μm. Black Pearls A consist of individual particles which are approximate spheres of diameter 0.028 μm. An analysis of the surface[133] oxygen groups of Black Pearls is as follows,

	%
-OH	32
CO	56
O ‖ -C-OH	13
O ‖ -C-OR	

Plates 3.1.4 and 3.1.5 are electron micrographs of Graphon and Black Pearls respectively.

3.1.4 Butanol

Using a round bottomed flask of the type shown in Fig. 3.1.4a AnalaR-n-butanol (B.D.H.) was dried over a freshly prepared molecular sieve (Linde 4A, BDH). Preparation involved outgassing at 673 K for 3 days. After several weeks drying the butanol was transferred to a test-tube, Fig. 3.1.4b, containing molecular sieve where it was stored. When required dry butanol was obtained by vacuum distillation, as shown in Fig. 3.1.4c, the first and last 10% of the distillate being discarded.

Plate 3.1.4

Electron Micrograph

of

Graphon

Plate 3.1.5

Electron Micrograph

of

Black Pearls

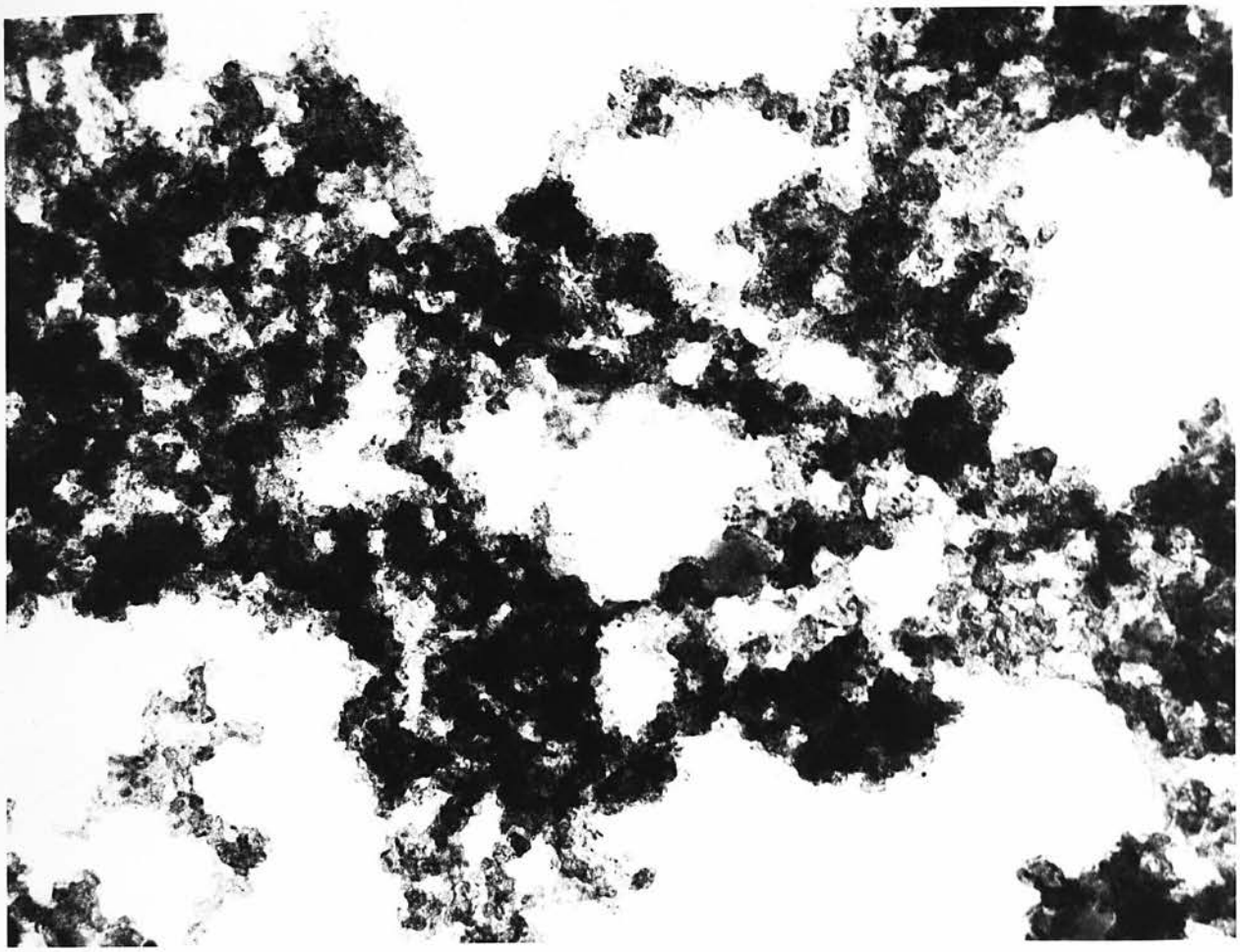

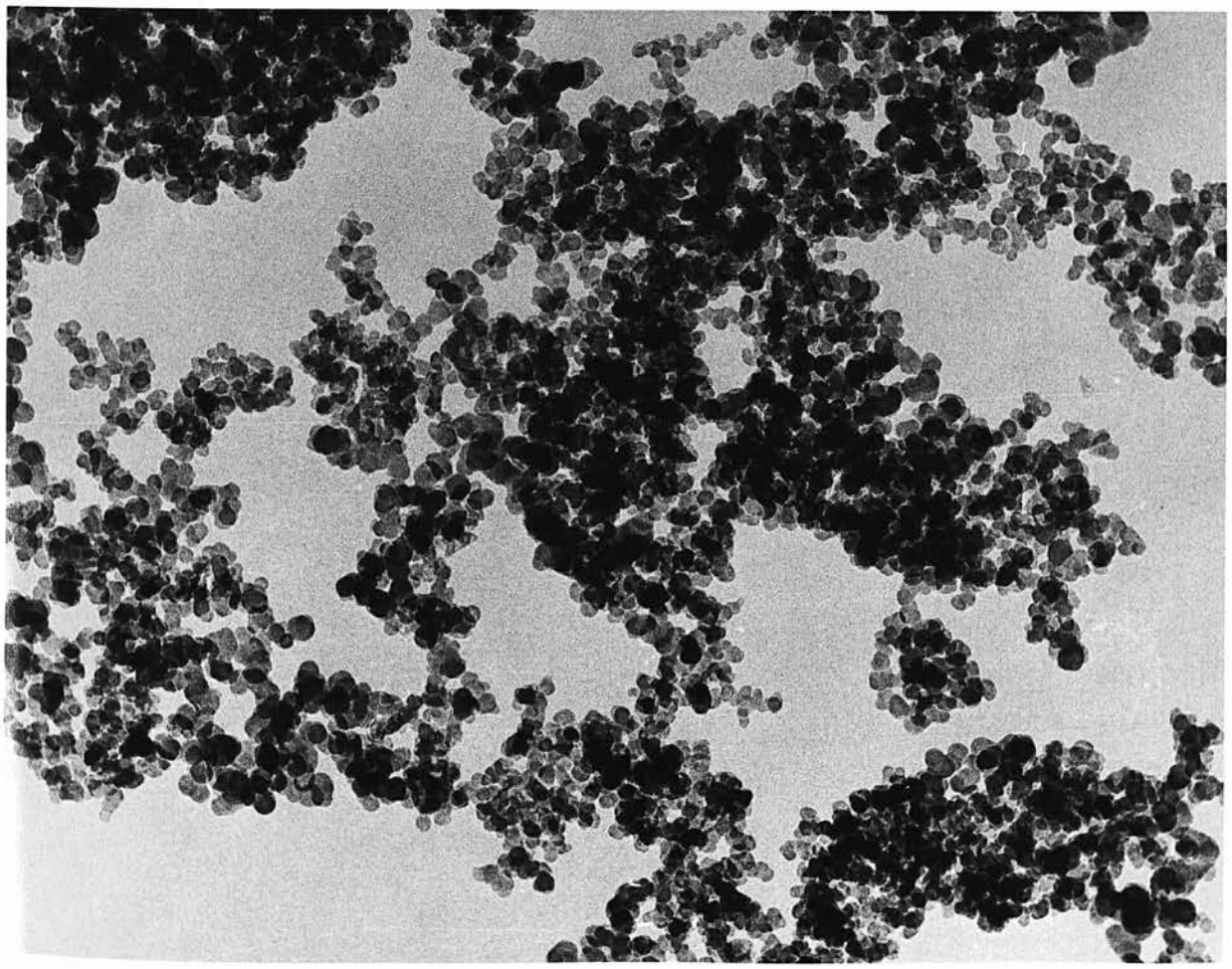

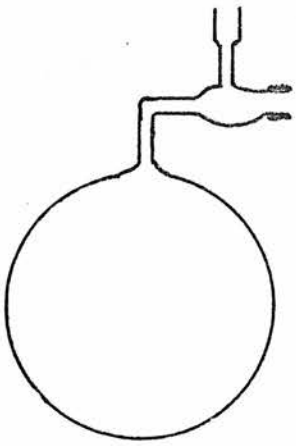

a) Round-bottomed flask

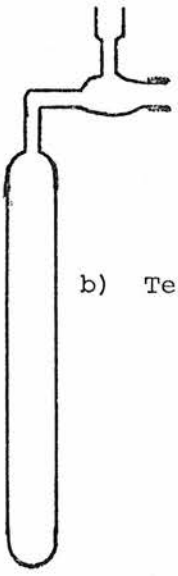

b) Test-tube

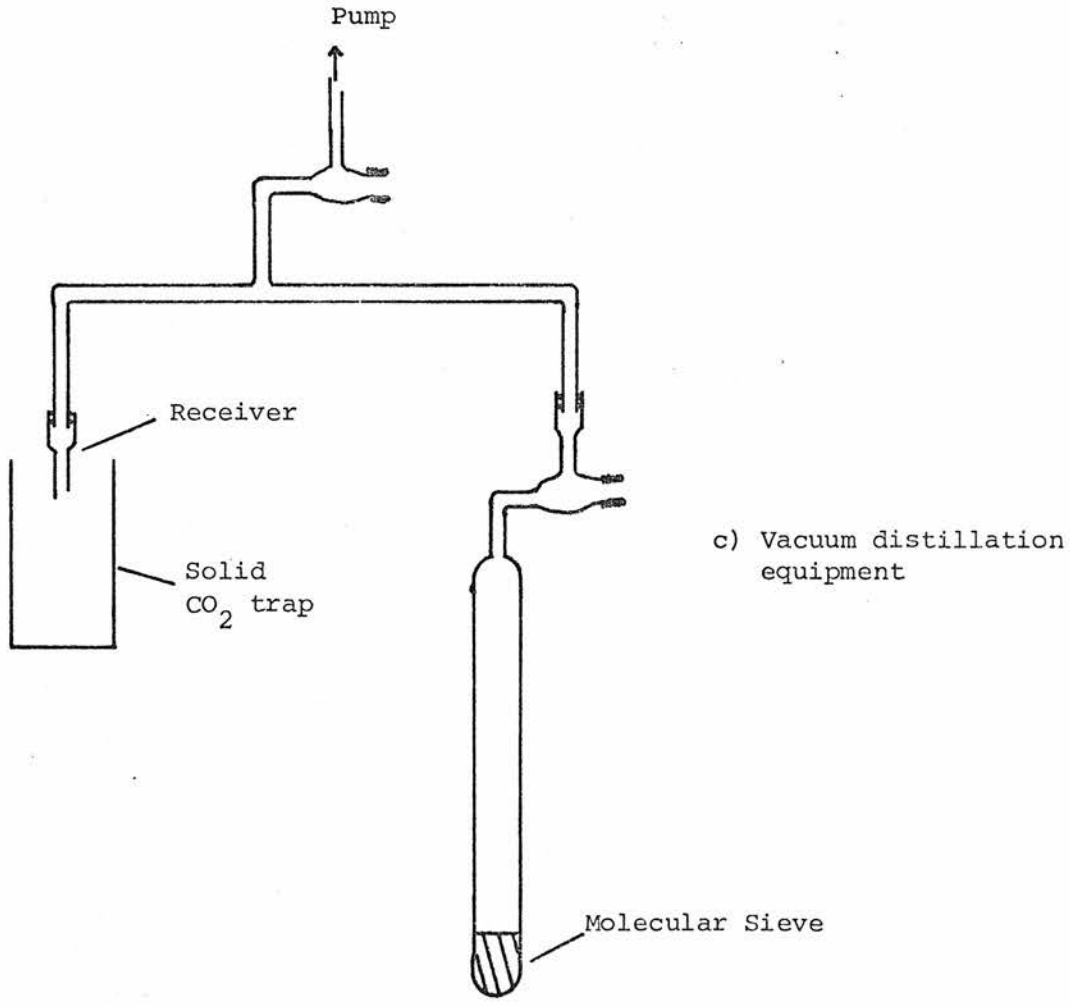

c) Vacuum distillation equipment

Fig 3.1.4

Vacuum Equipment

Karl Fischer water determination indicated that, within the sensitivity of the technique, the butanol was completely dry. This corresponds to a water content of less than 5 p.p.m.

3.1.5 Electrolyte Solutions (LiCl and HCl)

Dry butanol was distilled under vacuum into a test-tube containing a known weight of vacuum dried LiCl (B.D.H. Anhydrous) to give an approximately 1 mol dm^{-3} solution. A small volume of this solution was extracted with a syringe via a "Suba-seal stopper" and pipetted into a number of similar test-tubes. Dry butanol was introduced to produce standard solutions of approximately 10^{-1}, 10^{-2} and 10^{-3} mol dm^{-3} LiCl. These were kept sealed under partial vacuum until required when a few cm^3 of solution was transferred using a syringe and "Suba-seal stopper" to a small airtight bottle from which it could be easily pipetted. Karl Fischer titration indicated that the water content of the solutions handled in this way was between 100 and 200 p.p.m.

The preparation of an HCl solution in butanol is more complex. Ideally an anhydrous solution would be preferable but due to the reactivity of the alcohol with the acid this was not possible. Bubbling HCl gas through butanol leads to the reaction,

$$CH_3(CH_2)_3 - OH \longrightarrow CH_2(CH_2)_3 - Cl$$

The addition of hot concentrated aqueous HCl to butanol will, in the presence of a catalyst ($ZnCl_2$), also induce this reaction. In order to minimise the possibility of the formation of butyl chloride it was decided to use a cold 1 mol dm^{-3} aqueous solution of HCl. An accurately pipetted volume of this solution was dissolved in a known volume of butanol to produce a standard HCl/butanol solution of approximately 10^{-3} mol dm^{-3}. The water content was verified by Karl Fischer titration to be about 1000 p.p.m. The solution was kept in a sealed container in a cool dark place.

3.1.6 The Electrophoresis and Particle Counting Cell

Plate 3.1.6 shows one of the five cells used in this work. The cell consists of a calibrated Pyrex burette and test-tube arrangement attached via graded seals to a 1 mm x 10 mm silica rectangular cross-section optical cell. It incorporates a greaseless joint for attachment to the vacuum frame. The platinum electrodes are fused in soda-glass cones which in turn are sealed into the cell with Apiezon W (Picien Black Wax). The wax was applied only at the external junction of the cone and socket and care was taken to ensure that these were pressed tightly together before its application to prevent contamination by the wax. With this arrangement it was possible to prepare and observe a dispersion while maintaining its isolation from the atmosphere.

3.2 Techniques

3.2.1 Preparation of Dispersions

a) Carbon Blacks

A small sample (< 1 mg) of carbon black was introduced into the test-tube part of the cell through the lower tap socket. The tap barrel was replaced and the apparatus evacuated. The carbon was dried at approximately 500 K, under vacuum, for 10-12 hours and allowed to cool without exposure to the air. Using the arrangement shown in Fig. 3.1.4c, butanol was distilled into the burette part of the cell which was cooled with solid CO_2. When sufficient had been distilled the tap was closed and any surplus butanol which had condensed around it was pumped away. The required volume of butanol could now be introduced into the lower part of the cell and the carbon black dispersed. Dispersion was facilitated by immersing the test-tube part of the cell in an ultrasonic irradiation bath (Dawe Soniclean 500W Generator, 40 k Hz) for a few minutes.

Plate 3.1.6

The Electrophoresis and

Particle Counting Cell

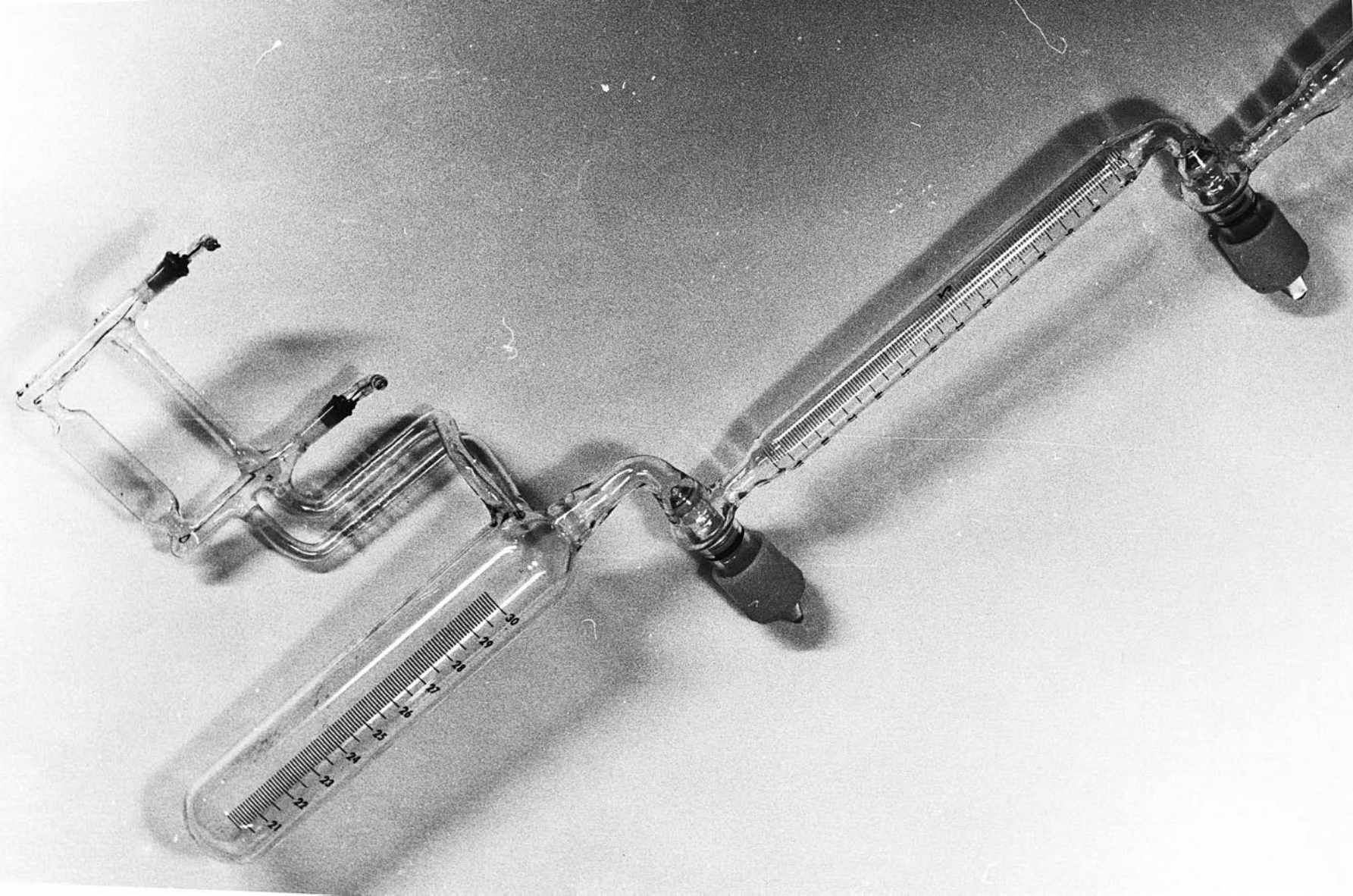

A volume (between 0.01 and 0.1 cm^3) of a standard electrolyte solution was pipetted into the joint section of the cell and, after the insertion of a stopper, mixed with the butanol. It was necessary to add such a small volume of electrolyte in order that, after dilution, the water concentration would be as low as possible. LiCl solutions in which the water content was negligible were produced. Due to the high water content of the standard solution, this was not possible for HCl solutions, for example a 10^{-5} mol dm^{-3} solution of HCl contained 10 p.p.m. of water. Attempting to accurately pipette such small volumes of solution constitutes the largest error in the determination of the electrolyte concentration. It is estimated that the error does not exceed 10% and in most cases is considerably less.

Similarly, by the addition of a drop of water, standard solutions of "damp butanol" could be prepared in the burette section of the cell.

b) Polymer Latices

A small volume (between 0.01 and 0.05 cm^3) of concentrate was injected through the lower tap socket into the cell. After replacing the tap, the burette section of the cell was evacuated and the pressure in the test-tube section rapidly reduced to about 10 torr (approximately the vapour pressure of butanol at 293 K). This pressure reduction was necessary to permit the introduction of butanol from the burette. The distillation and preparation of the medium was as described above for carbon blacks. Sufficient butanol was added from the burette to produce dispersions of the required particle number concentration. Because of the large dilution factor involved the volume of water in the final dispersion, contributed by the "wetness" of the concentrate, was insignificant, assuming uniform distribution.

c) Mixed Dispersions

The two types of particles were prepared as described above in the test-tube parts of two cells. Dispersion medium, prepared in the burette

part of one of the cells was transferred via an evacuated T-piece to the other cell. In this manner two dispersions with identical dispersion media were prepared. Having been studied separately the dispersions were mixed in known proportions in one cell.

3.2.2 Electrophoresis

Theory

There are four electrokinetic phenomena, electrophoresis, electro-osmosis, streaming potential and sedimentation potential, each of which involves a relative tangential motion between charged phases. Under the application of an electric field a particle in a dispersion moves with an electrophoretic velocity proportional to the sign and magnitude of the potential at the surface of shear between the phases in relative motion. This potential is called the zeta potential (ζ) and bears no direct relationship to ψ_o or ψ_δ although it is often assumed to be approximately equal to ψ_δ.

The application of an electric field not only causes electrophoretic migration of the particles but also, due to the surface charge generally present on the cell walls, an electro-osmotic flow of the medium in the vicinity of the walls. Since the cell is closed and there is no net transport of liquid there is a compensating return flow of liquid down the centre of the cell. For a rectangular cross-section flat cell, observed as shown in Fig. 3.2.1, there are two depths, known as "stationary levels", at which the opposing liquid flows just balance. Only at these points can the electrophoretic mobility be observed directly.

Komagata[134] showed that for a flat cell the liquid flow velocity (V_L) was given by

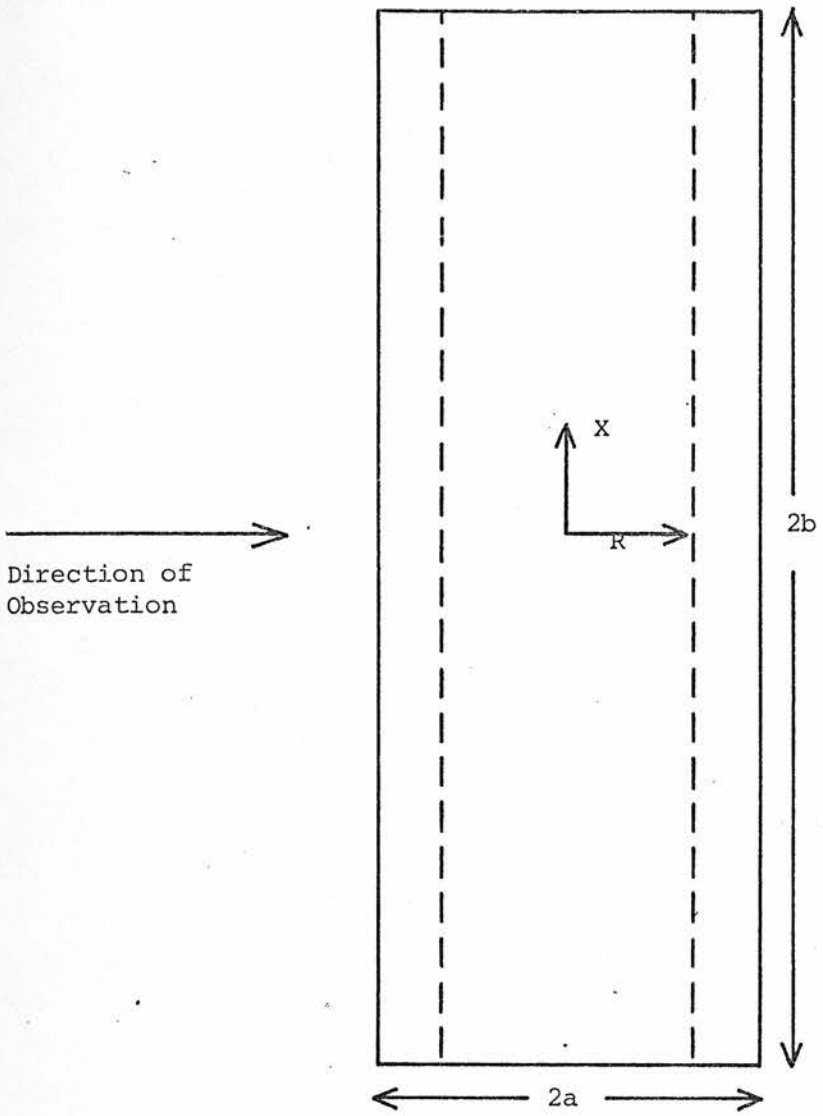

Fig 3.2.1

Cross-sectional View of the Electrophoresis Cell
Showing the Positions of the Stationary Levels

$$V_L(x = 0) = V_{E.O.} \left(1 - {}^{3}/_{2}\left(1 - \frac{R^2}{a^2}\right)\left(1 - \frac{192a}{\pi^5 b}\right)^{-1}\right) \qquad (3.2.1)$$

where $V_{E.O.}$ is the electro-osmotic velocity

and a, b and R are as defined in Fig. 2.2.1.

If the geometry of the cell is such that b/a = 10 (e.g. a 1 mm x 10 mm cross-section cell) then, since $V_L = 0$, $R^2/a^2 = 0.375$ at the stationary levels which corresponds to a distance of 0.194 of the cell thickness (2a) from the wall.

The observed velocity (V_{OBS}) corresponds to the combination of the electrophoretic (V_E) and liquid flow (V_L) velocities i.e.

$$V_{OBS} = V_E + V_{E.O.} \left(1.6004(R^2/a^2) - 0.6004 \right) \qquad (3.2.3)$$

From a plot of V_{OBS} against R^2/a^2

$$V_{E.O.} = \text{Slope}/1.6004 \qquad (3.2.4)$$

$$V_E = \text{Intercept } (R^2/a^2 = 0) + .6004\ V_{E.O.} \qquad (3.2.5)$$

The electrophoretic velocity may also be determined directly as the observed velocity at $R^2/a^2 = 0.375$.

Several equations have been proposed to calculate zeta potentials from electrophoretic velocity data.

Conversion of Electrophoretic Velocities to Zeta Potentials.

By considering electrophoresis to be the converse of electro-osmosis Smoluchowski[135] derived the expression,

$$V_E = E\ \zeta\ \varepsilon/\eta \qquad (3.2.6)$$

where E is the field strength,

ε is the relative static permittivity as defined previously,

η is the viscosity.

If the electrophoretic mobility, μ_E, is defined

$$\mu_E = V_E/E \qquad (3.2.7)$$

then

$$\mu_E = \zeta\varepsilon/\eta \qquad (3.2.8)$$

This expression is limited to cases where the double layer is thin, in relation to the particle size (i.e. $\kappa a >> 1$). It is assumed that the particle is non-conducting and that the permittivity and viscosity are constant at all points in the medium.

If electrophoresis is considered to be caused by the force exerted on the charge of the particle by the applied field then, for a spherical particle of radius a and charge q,

$$\mu_E = q/6\pi\eta a \qquad (3.2.9)$$

By modifying this equation to account for the "electrophoretic retardation" caused by the action of the electric field on the double layer and assuming $\kappa a << 1$ Hückel[136] derived the expression,

$$\mu_E = \frac{\zeta\varepsilon}{1.5\eta} \qquad (3.2.10)$$

Henry[137] derived a general expression for the electrophoretic mobility of non-conducting spheres,

$$\mu_E = (\zeta\varepsilon/1.5\eta)\, f(\kappa a) \qquad (3.2.11)$$

where $f(\kappa a)$ is a function of κa and varies between 1.0 for small κa and 1.5 for large κa. The Smoluchowski and Hückel equations are therefore limiting forms of the Henry equation.

The movement of the particle relative to the mobile part of the double layer results in the deformation of the otherwise symmetric double layer around the particle. Symmetry is restored by diffusion but this takes a finite time, known as the relaxation time. The asymmetric distribution of the ionic atmosphere leads to an additional retarding force on the particle, known as the relaxation effect. The relaxation effect is not considered by the Henry treatment.

Overbeek[138] and Booth[139] both derived equations for spherical particles which take into account relaxation and retardation, expressing the electrophoretic mobility as a power series in $e\zeta/kT$. However, mathematical difficulties forced them to develop the series for a limited number of terms only. Wiersema[140] Loeb and Overbeek were able, with the aid of a computer, to solve the relevant differential equations numerically. They provided tables of results relating zeta potentials to electrophoretic mobility and κa values. The parameters E, q_o and y_o were defined,

$$E = 1.5\eta e\mu_E/\varepsilon kT$$

$$y_o = e\zeta/kT$$

$$q_o = \kappa a/\lambda$$

where $\lambda^2 = (z_+ + z_-)2z_-$

z = charge on each ion

e = charge on a proton.

Values of E were tabulated as a function of y_o and q_o enabling plots of the type shown in Fig. 3.2.2 to be constructed.

A number of assumptions have been made in this treatment, these are listed below.

1) Only a single particle is considered, interparticle interactions being neglected.

Fig 3.2.2

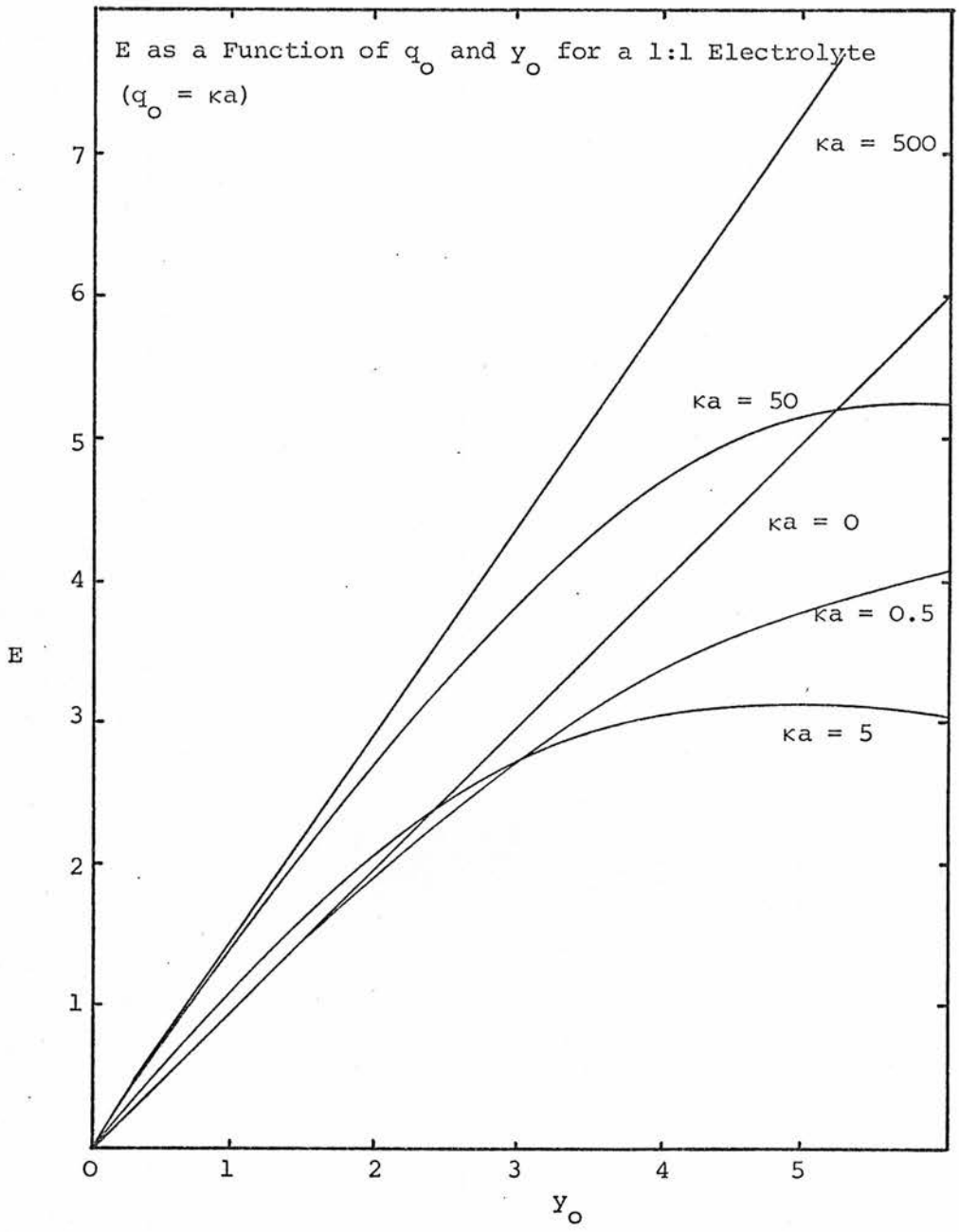
E as a Function of q_o and y_o for a 1:1 Electrolyte
(q_o = κa)
κa = 500
κa = 50
κa = 0
κa = 0.5
κa = 5
E
y_o
0
1
2
3
4
5
6
7

2) The particle, plus its adhering liquid layer, is treated as a sphere throughout which the permittivity is uniform.

3) The particle is non-conducting.

4) The charge is uniformly distributed over the surface.

5) The mobile part of the double layer is described by Gouy-Chapman theory.

6) The permittivity and viscosity are constant throughout the double layer.

7) Brownian motion is neglected.

8) Only terms which are linear in the field are taken into account in the calculation.

Dipolar orientation, induced by the high field strengths in the double layer, may result in a non-uniformity of permittivity and viscosity throughout the double layer. Lyklema and Overbeek[141] have investigated this effect and although they concluded that the effect of field strength on E was insignificant (until ζ > 200 mV) at electrolyte concentrations used in electrophoresis, it was suggested that the effect on η could be large. More recently however, this suggestion has been criticised by Hunter,[142] who has shown that the viscoelectric constant of water estimated by Lyklema and Overbeek was of the order of 100 times too large. This supports the work of Stigter[143] who has shown that the shift in the position of the shear plane produced by a viscoelectric effect was experimentally very much less than theoretically predicted by Lyklema and Overbeek.

Technique

Of the two experimental techniques associated with electrophoresis, namely the moving boundary method and microelectrophoresis, the latter was chosen as being most suitable for the study of systems used in this thesis. It has the following advantages:

a) The isolation of the system from the atmosphere is easier.

b) The particles are observed in their normal environment.

c) Since very dilute dispersions are studied particle interactions are minimal and flocculation rates are very slow.

d) Due to the high magnification of the ultramicroscope system, incorporated in the technique, observation times are short.

The construction of the cell and the preparation of the dispersions has already been discussed in Sections 3.1.6 and 3.2.1 respectively. The optical cell was mounted in a water-filled Perspex tank fitted to a vertical microscope stage. The water in the tank was maintained at 298.0 $\pm$ 0.1 K and room temperature at 298 $\pm$ 1 K to prevent distillation of the butanol from one part of the cell to another. A voltage stabilised power supply was used to provide a d.c. potential of 450 $\pm$ 1 V across the cell. The magnitude and reversibility of this potential were checked using a high impedance digital voltmeter connected in parallel with the cell.

The scattered light from the particles was observed under dark ground illumination conditions using a microscope, with a total magnification of 200 X. In one eyepiece was a squared graticule which had been calibrated with a standard stage micrometer. Using a digital stop clock (accurate to 0.02 s) the time taken for the particle to traverse a number of squares under the applied electric field was measured. In order to minimise operator timing error and Brownian motion error the number of squares was chosen such that the times were between 5 and 10 seconds. To prevent polarisation of the electrodes the potential gradient was reversed after each timing and it was subsequently verified that particle speed was independent of the sign of the applied field. Eight concordant particle times were obtained, at each of up to nine levels throughout the full

depth of the cell, the position of each level being predetermined such that the intervals between R^2/a^2 values were uniform.

The particle speeds, given by the reciprocal times (1/t) taken to cover one square, were averaged for each level and a plot of 1/t v. R^2/a^2 constructed. Using a least squares analysis, the slope and intercepts at R^2/a^2 equal to 0 and 0.375 were determined and the electrophoretic and electro-osmotic velocities calculated as shown earlier. From a knowledge of the magnitude of the applied field and the effective cell length, obtained conductimetrically, these velocities were converted to the corresponding mobilities. Zeta potentials were calculated using graphs of the type shown in Fig. 3.2.2.

3.3 Particle Counting

Flocculation is kinetically a second order reaction, the rate of disappearance of particles is given by

$$-\frac{dN}{dt} = k'N^2 \qquad (3.3.1)$$

where k' is the second order rate constant

N is the number of particles per unit volume.

Integration of equation (3.3.1) gives

$$\frac{1}{N} = \frac{1}{N_o} + k't \qquad (3.3.2)$$

A plot of $\frac{1}{N}$ against t is therefore linear with a slope equal to the rate constant, k'.

Dispersions were prepared and the cell mounted and thermostatted on the microscope in the same way as for electrophoresis. To minimise wall effects the focussing was adjusted so that the particles under observation were halfway through the cell. Particles in randomly chosen graticule squares, near the centre of the field of view, were counted as a function

of time (t). Usually about 8 counts were taken at approximately uniform time intervals and in each case the number of particles counted was in excess of 200. Using this method, the time taken in counting was constant, (ca. 2 minutes) so allowing t to be defined as the time at which counting commenced.

The value of k' was determined from a graph of the reciprocal of the average number of particles per square ($\frac{1}{N}$) against t. To determine the volume viewed it was necessary to determine the depth of focus. This was found from the mean of 30 readings of distance between the clear distinction and out of focus positions for a number of particles.

Experimental values of stability ratio, W, are defined as the ratio of the most rapid experimental rate constant to the reduced rate constant i.e.

$$W = k_o/k' \qquad (3.3.3)$$

Experimental values of W may then be compared to those predicted by equation (2.4.23).

Ultramicroscopy involves observation of the light scattered by particles. The light intensity is a function of the refractive index difference between the particles and the medium. Since the refractive indices of PTFE and butanol are similar (ca. 1.4), dispersions of latex in butanol cannot be seen clearly enough to allow direct particle counting. Modification of the medium refractive index may be achieved by the addition of a miscible liquid of substantially different refractive index, e.g. methyl salicylate (1.54).

Particle counting of systems involving PTFE latices was therefore carried out using a 1 mm spectrophotometer cell containing a mixture of 0.1 cm^3 of dispersion, removed from the cell with a syringe, and 0.1 cm^3 of methyl salicylate (2 X distilled BDH Laboratory Grade). To facilitate sampling, dry nitrogen was introduced into the cell from the vacuum frame and a "Suba-seal stopper" fitted to the neck of the cell.

3.4 Conductivity Measurements

Conductance measurements were used to check the electrolyte concentrations of dispersions. Conductivities were calculated from the measured potential difference across a 10,000Ω resistor connected in series with the cell when the potential drop across the whole system was 100 V.

From Ohm's Law

$$V_{cell} \cdot R_{10,000\Omega} = V_{10,000\Omega} \cdot R_{cell}$$

$$\text{Since } R_{cell} >> R_{10,000}, \; V_{cell} \simeq 100V$$

$$R_{cell} = \frac{100.10,000}{V_{10,000}} \quad \Omega$$

Although these measurements are very approximate, by comparing the values of resistance obtained for different dispersions, they may be used to detect impurities within a particular system.

CHAPTER FOUR

Results and Discussion

In a review[67] of colloidal stability of dispersions in non-aqueous media, Lyklema commented that the vast majority of stability investigations reported have been for aqueous systems. As a result, theory and practical work are well developed for aqueous systems but are less well understood for non-aqueous systems.

Vincent[91] has said that the major stabilising factor for dispersions in rigorously dry, low polarity media is steric stabilisation. It is only recently that a more complete understanding of the factors involved has been obtained. For some dispersions in low permittivity media, stability has been related to zeta potential[55] but, in view of the low ion concentration present in such systems, there is controversy[8] about the method used to calculate the repulsive interaction.

In the field of semi-polar media, such as alcohols, there is also a lack of reported work. Romo's results[52] for dispersions of alumina in alcohols undoubtedly demonstrate that dispersion stability is related to the zeta potential, which is itself affected by traces of water in the system. As yet, however, no direct comparison of experimental stability ratios with those predicted by DLVO theory has been published for dispersions in alcohols. This is not surprising in view of the experimental and theoretical complexities of these systems. For example, in Romo's work stability was also a function of water concentration at fixed zeta potential. Furthermore, one of the fundamental experimental tests of DLVO theory is the flocculation effect of an indifferent electrolyte on a colloidal dispersion. Even assuming adequate dissociation and the existence of a theoretical model to account for the presence of ion pairs in the double layer there is still the problem of demonstrating that the electrolyte is totally indifferent. Comparison of two solutions of different electrolytes is difficult, because of their differing solubilities and dissociation constants it is unlikely that both will exhibit similar behaviour.

Fowkes[68] has explained the effects of water on the zeta potential of oxides in alcohols as a proton exchange mechanism but this has not been investigated for other polar solids. If, indeed, it is the proton which is potential determining then HCl solutions in dry alcohol would provide a more controllable method of modifying pH. The pH scale in alcohols will naturally differ from that in water, the equilibria being different and, in the presence of traces of water, somewhat more complex. In conclusion, one of the major errors in both aqueous and non-aqueous stability work may be attempting to relate stability to the electrokinetic potential and not to the Stern potential.

The following section describes the characterisation of a number of materials dispersed in butanol. The effects of water, HCl and LiCl on electrophoretic mobility and stability have been determined and discussed. Subsequent sections deal with the quantitative comparisons between theoretical predictions of DLVO theory and experimental results for both homoflocculating and heteroflocculating systems.

4.1 Characterisation of a Number of Dispersions in Butanol

4.1.1 Effect of Water

Electrophoresis

Particle mobilities of Graphon, Polystyrene and Black Pearls as a function of water concentration are shown in Fig 4.1.1. The permittivity and conductivity of butanol (17.1; $9 \times 10^{-9}\ \Omega^{-1}\ cm^{-1}$ respectively) are large enough to allow reproducible electrophoretic mobilities to be determined in the absence of any backing electrolyte. Mobilities were observed to be independent of the time elapsing after water addition. The criteria for reliable electrophoresis, as given by van der Minne and Hermanie[46] are that particle mobility should be independent of the sign of the electrode polarity and that the distribution of mobilities should be

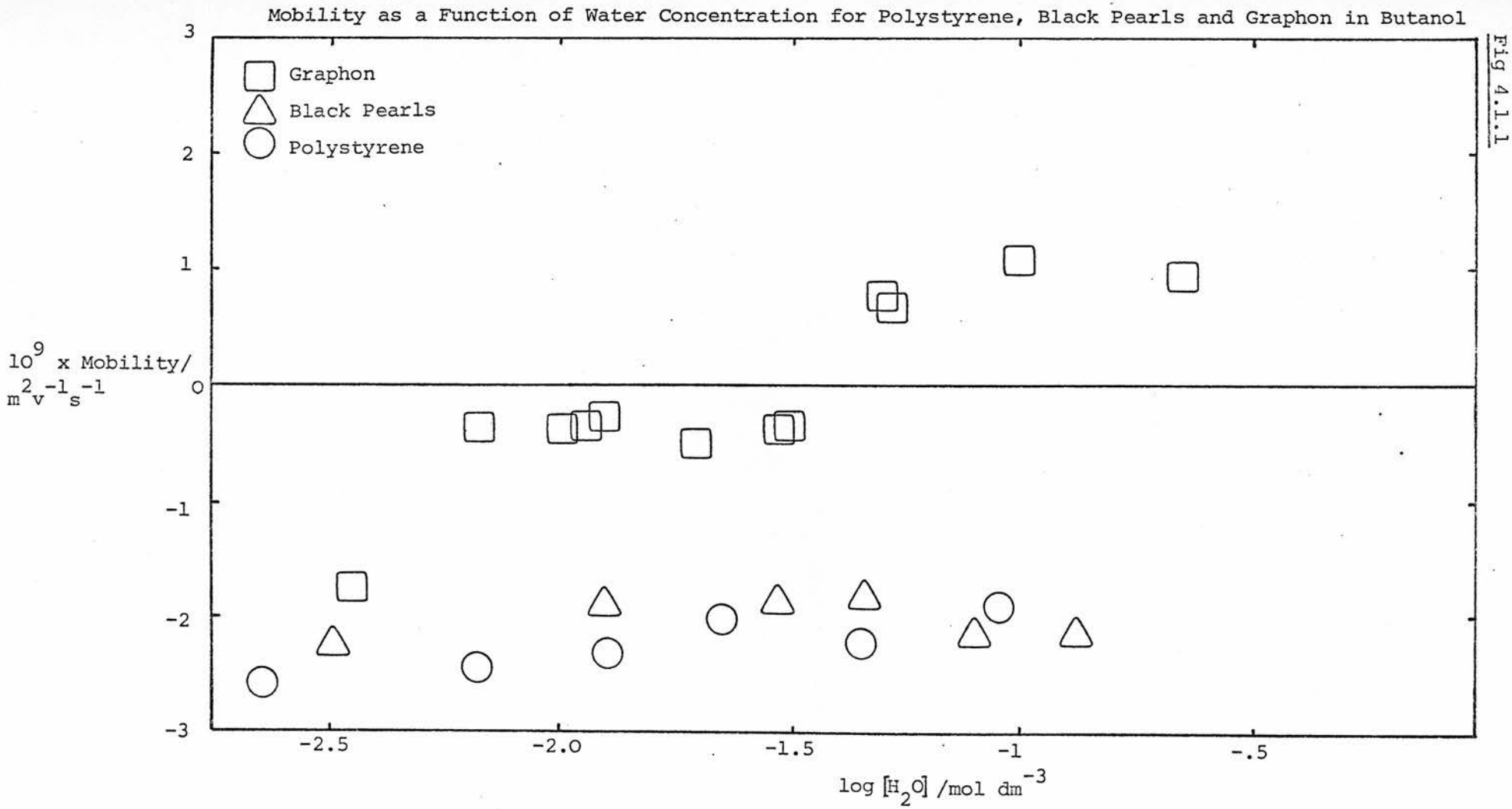
Mobility as a Function of Water Concentration for Polystyrene, Black Pearls and Graphon in Butanol
Graphon
Black Pearls
Polystyrene
10^9 x Mobility/ $m^2 v^{-1} s^{-1}$
3
2
1
0
-1
-2
-3
-2.5
-2.0
-1.5
-1
-.5
log $[H_2O]$ /mol dm^{-3}

Fig 4.1.1

symmetrical about the central plane. By determining mobilities throughout the full width of the cell and reversing the field direction between each particle timing, these requirements were satisfied. Particle velocities were also observed to be directly proportional to the magnitude of the applied field as anticipated theoretically. Polarisation effects were avoided by the frequent field reversal and the use of a relatively low electric field strength (< 50 V cm^{-1}).

A typical plot of 1/t v. $(R/a)^2$ is shown in Fig 4.1.2, the data for each side of the cell are colinear, indicating a symmetric parabolic flow pattern through the cell. Electrophoretic mobility may be determined directly from the intercept at $(R/a)^2 = 0.375$ or from the slope and intercept as described in Section 3.2.2. In view of the very low ion concentrations in these systems the zeta potential can be calculated approximately from the Hückel equation (3.2.10)

$$\zeta = (1.5.\ 0.00258/17.1.\ 8.85 \times 10^{-12})V_E$$

$$= 2.56 \times 10^{7}.\ V_E \qquad V$$

where V_E is the mobility.

Accurate determination of the depth at which particles are observed and the measurement of the water concentration constitute the major errors. For high water concentrations the latter is negligible and the technique of observing particles at a number of depths helps to reduce the former. The error in the mobility can only be estimated from the error in the calculated slope and intercept values (< 5%) which do not account for any systematic error in depth determination.

Owing to the nature of the type of groups on the surfaces of Black Pearls and Polystyrene it is not surprising that these particles are negatively charged in dry butanol. Water produces only a small reduction

Fig 4.1.2

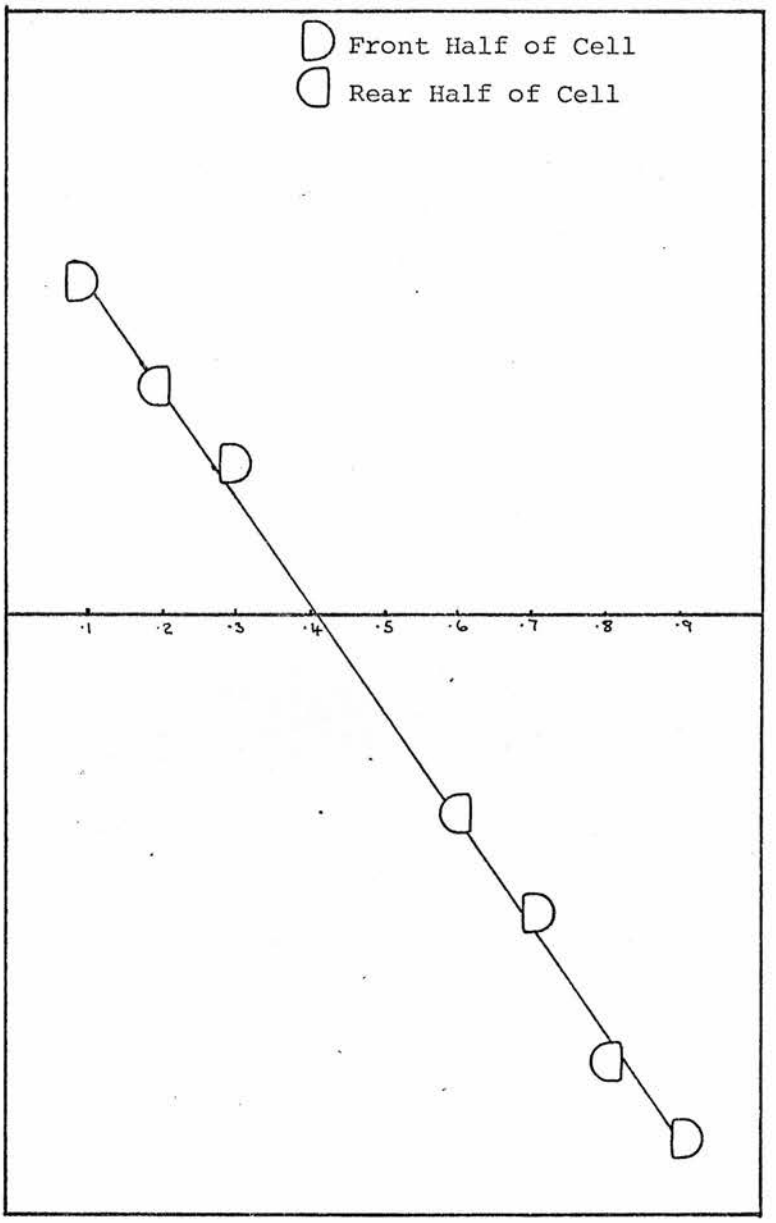

Mobility as a Function of $(R/a)^2$ for Graphon in Butanol (176 ppm H_2O)

in mobility in comparison to that observed for oxides.[52,65] Although this suggests that the water slightly reduces the basicity of the surface with respect to the solution, as in the model discussed by Fowkes[68], other possible effects of water must also be considered. Since the surfaces of Black Pearls and Polystyrene are hydrophilic it is anticipated that there is a positive surface excess of water which may lead to a reduction in mobility. It must be emphasised that even at very low water concentrations there is sufficient water for multi-layer coverage of the particles if it is assumed that the majority of the water is at the interface. For example, 1 p.p.m. by volume (5.5×10^{-5} mol dm^{-3}) of water corresponds to about 10^7 molecules of water per particle . As a result of any surface excess of water the permittivity and viscosity of the medium in the vicinity of the particle will not be the same as that in the bulk solution and it may not be valid to approximate these values to those of butanol. From the Hückel equation it is evident that an increase in viscosity (η) and/or a reduction in dielectric constant (ε) will lead to a reduction in mobility for the situation where the zeta potential remains constant. However, it would be anticipated that the effect of water would be to reduce η and increase ε in the region of the interface which, for a constant zeta potential, corresponds to an increase in mobility. Since mobility is observed to decrease with increasing water concentration, either the effects on ε and η are negligible or the actual reduction in zeta potential is greater than predicted by the Hückel equation alone. Note that both cases indicate that a reduction in zeta potential occurs.

As well as altering any structured region in the vicinity of the particle, water will also solvate the charged surface more efficiently than butanol. The combination of these effects on the position of the slipping plane is difficult to discuss in view of the limited information available. It is generally assumed that the Stern plane and the slipping

plane are close together and that the approximation that $\zeta \simeq \psi_\delta$ can be made. If the slipping plane is farther from the particle surface than the Stern plane then, as a result of the exponential potential decay in the diffuse double layer, ζ will be less than ψ_δ. The larger the distance between the two "planes" the greater will be the difference between ψ_δ and ζ. However, for the systems under discussion the ion concentrations are very low which means that the potential decays slowly as a function of distance. In order to produce a 25% reduction in zeta potential it would require the slipping plane to move out a distance of the order of $10^{-8} - 10^{-7}$m. It is unreasonable to assume that water could produce such an effect.

In conclusion, if it is assumed that the free ion concentration remains roughly constant, then the reduction in mobility produced by the addition of water corresponds to a reduction in ψ_δ. Such an effect can probably be best explained in terms of a proton exchange model as discussed by Fowkes.[68]

For Graphon, the variation of electrophoretic mobility with water concentration is much greater than for Black Pearls or Polystyrene. In accounting for this it is necessary to consider the source of particle charge. It is possible that the supposed apolar surface of Graphon contains some minor impurities. The presence of weakly acidic sites which are ionised in butanol but protonated on the addition of water would explain the observed mobilities. However, from a knowledge of the behaviour of butanol at the Graphon interface it is possible to postulate other models. According to Findenegg[98] the butanol molecules at the Graphon interface exist in a hydrogen bonded lattice as shown in Fig. 4.1.3. Since proton transfer is enhanced in this situation it may be possible for such a region to support a proton deficiency, producing a net negative charge on the particle. Addition of water increases the

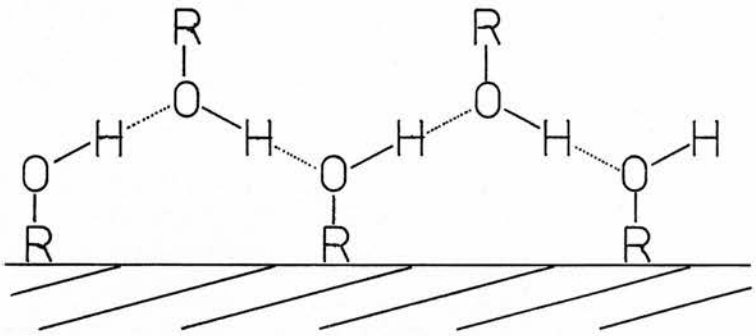

Fig 4.1.3. Alcohol Structuring at the Graphite Interface

concentration of the ROH_2^+ species with respect to that of RO^- and so renders the particles positive. The three equilibria which must be considered in this mechanism are,

$$2\ ROH \underset{}{\overset{K_1}{\rightleftharpoons}} RO^- + ROH_2^+$$

$$2\ H_2O \overset{K_2}{\rightleftharpoons} HO^- + H_3O^+$$

$$H_3O^+ + ROH \overset{K_3}{\rightleftharpoons} ROH_2^+ + H_2O$$

where K_1, K_2 and K_3 are the respective equilibrium constants.

Assuming electrical neutrality and activity coefficients of unity,

$$[OH^-] + [RO^-] = [H_3O^+] + [ROH_2^+]$$

the following relationship may be derived,

$$\frac{[RO^-]}{[ROH_2^+]} = \left(\frac{K_1}{K_3}\right)\left\{\frac{K_3 + X}{K_1 + K_2K_3X}\right\} \qquad (4.1.1)$$

where $X = [H_2O] \Big/ [ROH]$

The value of K_3 is known[144] (ca. 10^{-2}) and if K_1 and K_2 are estimated to be 10^{-20} and 10^{-14} respectively then equation (4.1.1) becomes,

$$\frac{[RO^-]}{[ROH_2^+]} = \frac{1 + 10^2X}{1 + 10^4X} \qquad (4.1.2)$$

From equation (4.1.2) it may be seen that increasing water concentration increases the proportion of ROH_2^+ with respect to RO^- and that at the isoelectric point $[RO^-]/[ROH_2^+] \simeq 0.35$. (See Fig. 4.1.1)

It seems unlikely that the RO^- concentration in the dry system would be large enough to give rise to such a high zeta potential. However, it must be remembered that, since the ion concentration is very low the particle surface charge density required would be very small.

Another possible explanation is in terms of a dipole orientation model. Since the surface is coated with layers of uniformly orientated dipoles the position of the slipping plane with respect to these dipoles will be important. The effect of the presence of adsorbed dipolar molecules on electrophoretic mobility has been discussed by Mackor[145] for the acetone/silver iodide system. However, if dipolar orientation is responsible, the effect of water is difficult to explain. Furthermore, evidence, which will be presented later, suggests that the charging mechanism for Graphon involves proton exchange. Either of the earlier two explanations therefore appear more valid.

Stability

Since the free ion concentration in these systems is unknown, and consequently the value of κ unobtainable, quantitative comparison of measured stabilities with those predicted theoretically is impossible. For this reason stabilities have been determined qualitatively, a stable dispersion being defined as one in which there was no discernable change

in particle number over several days. As would be expected from DLVO theory, Polystyrene and Black Pearls were stable at all water concentrations studied and Graphon was stable for all dispersions in which particle mobility exceeded $\pm$ 1.5 x 10^{-9} $m^2 s^{-1} v^{-1}$. Some of these stable dispersions were kept for very long periods without exhibiting any change in particle number. e.g. Samples of polystyrene concentrate were observed to be stable for periods exceeding two years.

Although other workers[95,96] have attributed instability in wet non-aqueous media to the overlap of "water clouds" around the particles, no such effect was observed for these sytems.

4.1.2 Effect of Hydrochloric Acid

Electrophoresis

Fig 4.1.4 illustrates the electrophoretic mobilities of Black Pearls, Polystyrene, PTFE and Graphon as a function of HCl concentration. No experimental data points have been shown for Polystyrene, the reason for this will be explained in the next section. No backing electrolyte is used, both in the interests of maximum stability and in order that any observed effects are entirely attributable to the presence of hydrochloric acid. This means that the free ion concentration varies, which, could itself produce a variation in electrophoretic mobility.

On addition of hydrochloric acid to butanol the reaction,

$$HCl + ROH \longrightarrow ROH_2^+ + Cl^-$$

probably goes virtually to completion and the concentration of ROH_2^+ (plus a small proportion of H_3O^+) may be taken as the stoichiometric concentration of HCl. This assumption is in accord with the results of catalytic studies by Brönsted and Vance,[146] who showed that HCl was practically completely dissociated in iso-amyl alcohol. Fig 4.1.4 is therefore analogous to a mobility/pH plot for an aqueous system.

Fig 4.1.4

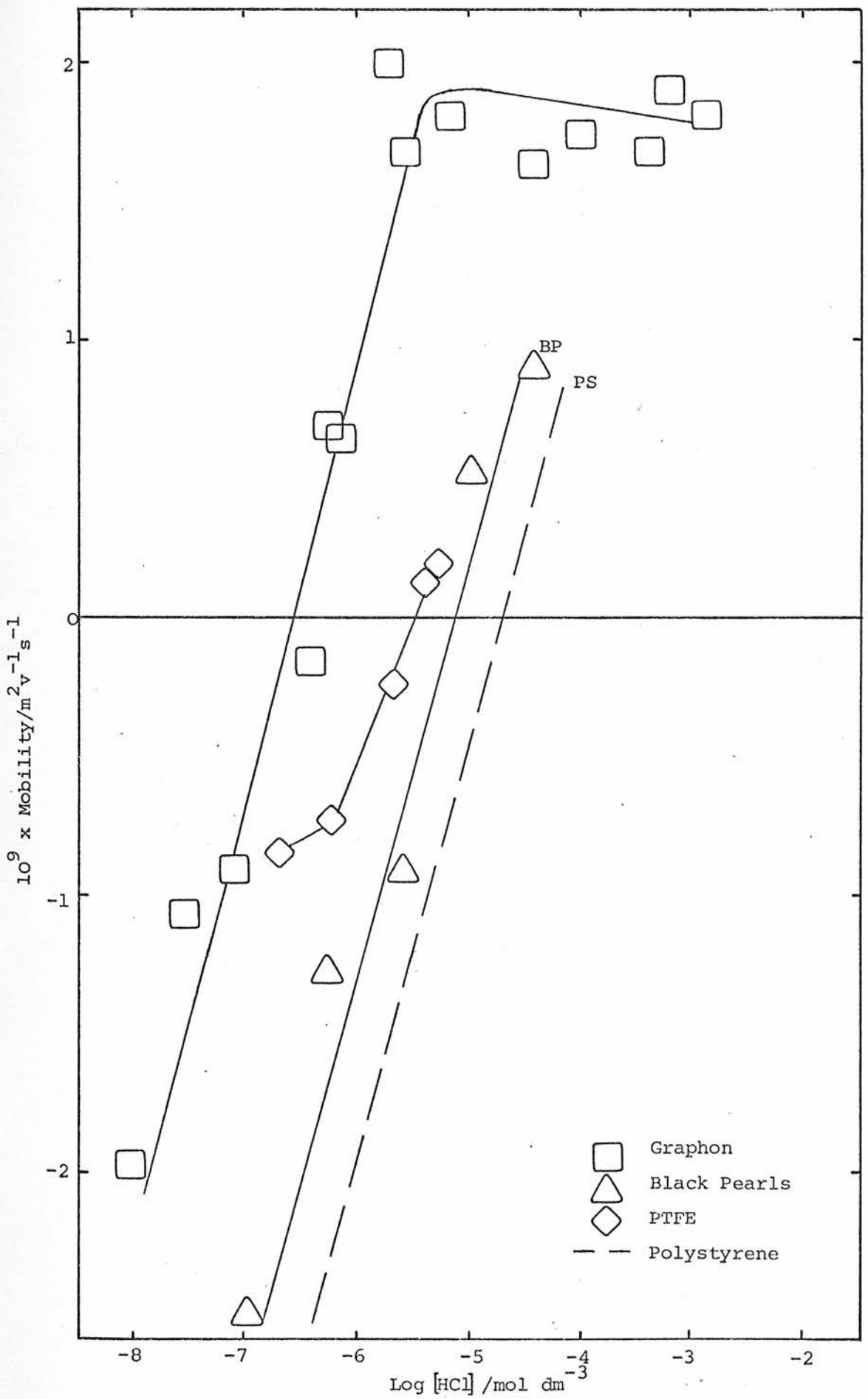

Mobility in Butanol as a Function of HCl Concentration

The gradients of the curves are all very similar, ca. 1.6 x 10^{-9} $m^2V^{-1}s^{-1}$ per $\log_{10}[HCl]$ unit, which, using the Hückel equation corresponds to ca.40 mV per 10 fold change in ROH_2^+ concentration. The similarity in the behaviour of the different systems suggests that the same reaction, almost certainly the adsorption of protons onto the particle surface, is occurring in each case. Protons are known to be the potential determining ions of the Black Pearls, Polystyrene and PTFE surfaces and since Graphon behaves in an almost identical manner to these particles it appears likely that the proton is also potential determining for the Graphon surface. The relative positions of the isoelectric points illustrate the differing acid strengths of the respective surface groups on each type of particle i.e. Polystyrene ($-SO_4H$) > Black Pearls (CO_2H) > PTFE ($CF_2(CH_2)_2CO_2H$ and CF_2CO_2H) >> Graphon in terms of acid strengths of surface groups.

Whatever the nature of the groups on the Graphon surface they are extremely weakly acidic in comparison with those on the other three surfaces.

Stability

Long term stability was observed for dispersions in which particle mobility was greater than $\pm$ 1.5 $\times 10^{-9}$ $m^2s^{-1}v^{-1}$. All the PTFE dispersions studied were unstable. Only Graphon dispersions exhibited large enough positive mobilities to produce stable dispersions.

Quantitatively determined stabilities for Graphon and Polystyrene dispersions at a number of acid concentrations are presented and discussed in Sections 4.2.1 and 2.

4.1.3 Polystyrene Dispersions in Butanol Solutions of HCl

Electrophoresis

Fig 4.1.5, showing the electrophoretic mobility of Polystyrene as a function of HCl concentration, illustrates the very large deviation in the results for this experiment. Since the error involved in measuring the mobility is comparatively small, this spread in results must be due to an inaccuracy in determining the HCl concentration, or, to be more precise, the ROH_2^+ concentration. Moreover, as is shown in Table 4.1.1 the conductivity does not rise uniformly with increasing calculated ROH_2^+ concentration. As for all the dispersions used, the acid concentration and thus the concentration of ROH_2^+ is calculated from a knowledge of the volume of standard HCl solution added to the system. However, it appears that in this case, for some as yet unspecified reason, it is invalid to equate the proton concentration with the concentration of HCl added.

Small variations in water concentration will alter the relative proportions of ROH_2^+ and H_3O^+ present in solution. Table 4.1.2 illustrates that although the effect of this is shown by increased conductivity, particle mobility is independent of large variations in water concentration at fixed HCl and particle concentration. (Particle concentration is fixed in order that the total number of surface groups remains approximately constant). This infers that the equilibrium between adsorbed and dissociated proton species is independent of the nature of the solvating species. Furthermore, although there is probably a positive surface excess of water at the particle surface this has no effect on mobility. This confirms the validity of the assumption that any variation in permittivity or viscosity in the region of the interface or any movement of the position of the slipping plane caused by water can be neglected. The large scatter of experimental points in Fig 4.1.5 is therefore not a result of subtle variations in small amounts of undetected water which may be present.

Fig 4.1.5

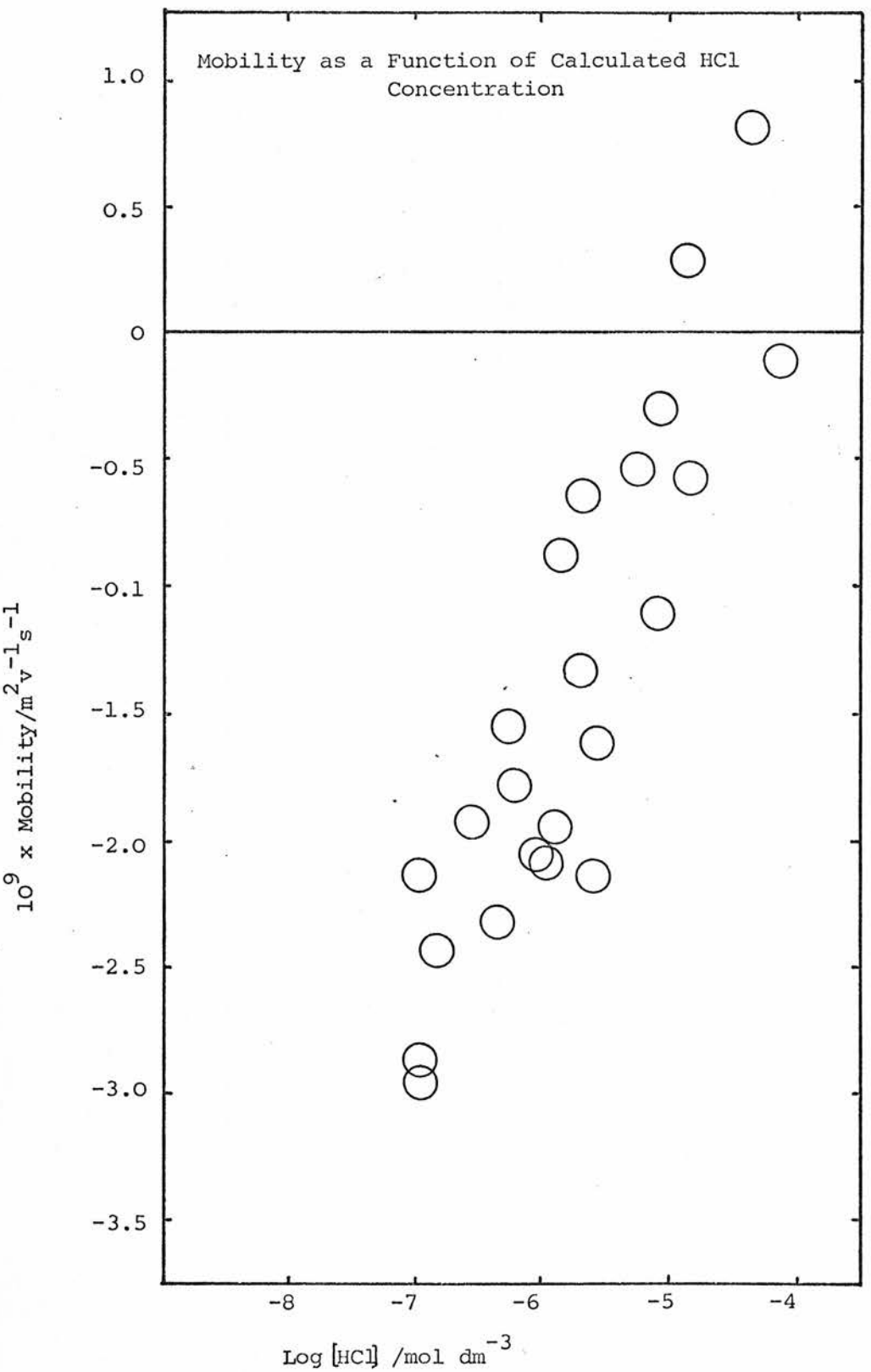
Mobility as a Function of Calculated HCl Concentration
1.0
0.5
0
-0.5
-0.1
-1.5
-2.0
-2.5
-3.0
-3.5
-8
-7
-6
-5
-4
10^9 x Mobility/$m^2 v^{-1} s^{-1}$
Log [HCl] /mol dm^{-3}

Log [HCl] calc.	10^9 x Mobility/ $m^2 s^{-1} v^{-1}$	10^8 x Conductivity/ mho	Log [HCl] app.
-7.0	-2.16	2.8	-6.1
-7.0	-2.96	1.3	-6.7
-6.85	-2.46	1.8	-6.4
-6.55	-1.92	4.1	-5.9
-6.4	-2.34	2.3	-6.2
-6.3	-1.56	6.8	-5.7
-6.2	-1.80	2.8	-6.1
-6.0	-2.10	2.8	-6.1
-6.0	-2.10	3.1	-6.07
-5.9	-0.89	10	-5.5
-5.8	-1.98	4.2	-5.9
-5.8	-0.66	7	-5.7
-5.7	-1.32	5.85	-5.8
-5.6	-1.62	6.2	-5.7
-5.6	-2.16	4.3	-5.9
-5.3	-0.56	16.8	-5.3
-5.1	-0.97	28	-5.1
-4.9	+0.27	34	-5.0
-4.8	-0.60	33	-4.9
-4.4	+0.75	153	-4.3
-4.2	-0.12	108	-4.4

Table 4.1.1. Mobility of Polystyrene in Butanol as a Function of the Calculated and Apparent HCl Concentrations

Water Concentration/ ppm	10^9 x Mobility/ $m^2 s^{-1} v^{-1}$	10^8 x Conductivity/ mho
0	-1.57	9.7
33	-1.53	9.9
81	-1.57	10.4
150	-1.53	10.6
350	-1.53	11.8
625	-1.53	13.2
1150	-1.57	14.7

Table 4.1.2. Mobility and Conductivity of Polystyrene in Butanol as a Function of Water Concentration at Fixed HCl ($\sim 5 \times 10^{-6}$ mol dm^{-3}) and Particle Number Concentration ($\sim 10^{14}$ m^{-3})

For any acid concentration, the only variable in the system is the volume fraction of Polystyrene concentrate present in each sample, an accurate measure of which can be obtained from particle number density. Using this method it is possible to investigate the effects of the presence of different volume fractions of Polystyrene concentrate in media for which the prepared HCl concentrations are constant.

Table 4.1.3 illustrates the dependence of mobility and conductivity on particle number at a fixed calculated concentration of 5×10^{-6} mol dm^{-3} HCl. It is immediately evident that the actual ionic concentration is not equivalent to the calculated value and that the deviation is a result of the volume of particle concentrate present. It is extremely unlikely that the effect is entirely due to the concentrate medium, since this would require that its ionic concentration was very large, so large in fact, that

10^{-14} x Particle Number/ m^{-3}	10^{9} x Mobility/ $m^{2}v^{-1}s^{-1}$	10^{8} x Conductivity/ mho
2.86	-1.85	10.5
1.42	-1.62	12.5
0.86	-1.38	13.9
0.57	-1.08	14.7

Table 4.1.3 Mobility and Conductivity of Polystyrene (Original Concentrate) in 5 x 10^{-6} mol dm^{-3} HCl Solution as a Function of Particle Number

flocculation of the concentrate would be expected. Furthermore, the concentrate has previously been extensively dialysed against distilled butanol.

It therefore appears that the surface groups on the particles are primarily responsible for altering the ionic concentration. The equilibrium between protons in solution and on the particle surface causes the bulk ROH_2^+ concentration to be displaced from 5 x 10^{-6} mol dm^{-3} HCl to a lower value. A reduction in particle number leads to a reduction in mobility which implies that the bulk ROH_2^+ concentration is moving closer to the desired value of 5 x 10^{-6} mol dm^{-3} HCl.

Tables 4.1.4-6 show mobility and conductivity as a function of particle number in media prepared to contain 5 x 10^{-6} mol dm^{-3} HCl, for concentrates which have been dialysed to 10^{-7}, 5 x 10^{-7} and 10^{-6} mol dm^{-3} HCl respectively. Having been dialysed to these concentrations means that the surface groups on the particles are in equilibrium with a medium of the dialysate concentration.

10^{-14} x Particle Number/ m^{-3}	10^{9} x Mobility/ $m^{2}v^{-1}s^{-1}$	10^{8} x Conductivity/ mho
2.86	-1.50	7.5
1.43	-1.26	8.7
0.80	-1.32	9.7
0.26	-1.08	10.5

Table 4.1.4 10^{-7} mol dm^{-3} HCl Polystyrene Concentrate

10^{-14} x Particle Number/ m^{-3}	10^{9} x Mobility/ $m^{2}v^{-1}s^{-1}$	10^{8} x Conductivity/ mho
2.60	-1.14	8.0
1.30	-0.90	9.0
0.63	-0.57	10.3
0.34	-0.36	11.0

Table 4.1.5 5 x 10^{-7} mol dm^{-3} HCl Polystyrene Concentrate

10^{-14} x Particle Number/ m^{-3}	10^{9} x Mobility/ $m^{2}v^{-1}s^{-1}$	10^{8} x Conductivity/ mho
2.69	-0.76	12.0
1.49	-0.26	12.6
.91	-0.19	12.6
.69	-0.01	12.8

Table 4.1.6 10^{-6} mol dm^{-3} HCl Polystyrene Concentrate

Tables of Mobility as a Function of Particle Number of Polystyrene, from Concentrates Dialysed to Different HCl Concentrations, in 5 x 10^{-6} mol dm^{-3} HCl

Attempting to increase the medium concentration by "diluting" with 5×10^{-6} mol dm^{-3} HCl would be expected to displace the equilibrium proton concentration to some intermediate value. The position of the equilibrium concentration would be expected to be closer to 5×10^{-6} mol dm^{-3} HCl for the dispersions in which the concentrate HCl concentration was larger. The mobility measurements, shown in Tables 4.1.4-6, demonstrate that this is the case. Thus, for Polystyrene dispersions the proton concentration cannot be determined from the volume of standard HCl solution added.

A 10^{-7} mol dm^{-3} HCl concentrate in a medium prepared at 10^{-6} mol dm^{-3} HCl again indicates (Table 4.1.7) a variation in the equilibrium concentration of ROH_2^+ with particle number.

10^{-14} x Particle Number/ m^{-3}	10^{9} x Mobility/ $m^2 v^{-1} s^{-1}$	10^{8} x Conductivity/mho
4.01	-2.28	2.5
2.29	-2.04	3.1
1.14	-1.74	3.6
0.63	-1.68	3.6

Table 4.1.7 Mobility as a Function of Particle Number of Polystyrene (10^{-7} mol dm^{-3} HCl Concentrate) in 10^{-6} mol dm^{-3} HCl.

However Table 4.1.8 illustrates that a 10^{-6} mol dm^{-3} HCl concentrate in a medium prepared to the same acid concentration has an equilibrium concentration of ROH_2^+ of that concentration. Therefore in order that the ROH_2^+ concentration of any dispersion may be known it is necessary to dialyse a sample of Polystyrene concentrate to the required concentration before use.

10^{-14} x Particle Number/m^{-3}	10^{9} x Mobility/ $m^{2}v^{-1}s^{-1}$	10^{8} x Conductivity/mho
6.85	-2.58	1.7
4.85	-2.70	1.8
3.42	-2.82	1.5
2.57	-2.70	1.4
1.83	-2.76	1.2
1.31	-2.52	1.4
0.90	-2.64	1.2
0.69	-2.52	1.3

Table 4.1.8 Mobility of Polystyrene (10^{-6} mol dm^{-3} HCl Concentrate) as a Function of Particle Number in 10^{-6} mol dm^{-3} HCl.

The dialysis of the above samples of Polystyrene was carried out by the following method. Approximately 2 cm^{3} of the original concentrate was dialysed primarily to $\sim 10^{-7}$ mol dm^{-3} HCl (2 x against 25 mls of 10^{-7} mol dm^{-3} HCl) then to $\sim 5 \times 10^{-7}$ mol dm^{-3} HCl (2 x against 25 mls of 5×10^{-7} mol dm^{-3} HCl) and then finally to 10^{-6} mol dm^{-3} HCl (5 x against 25 mls of 10^{-6} mol dm^{-3} HCl). Samples were removed from the dialysis tube at each stage and used for the work reported.

Increasing the equilibrium concentration of ROH_2^+ of the concentrate by dialysis has been shown to lead to a higher equilibrium concentration in the final dispersion. However, comparison of Tables 4.1.7 and 8 shows that the mobility of particles of the 10^{-6} mol dm^{-3} HCl concentrate in 10^{-6} mol dm^{-3} HCl is greater than that of particles of the 10^{-7} mol dm^{-3} HCl concentrate in 10^{-6} mol dm^{-3} HCl. This is not as expected, since the equilibrium concentration of ROH_2^+ is predicted to be less than

10^{-6} mol dm^{-3} in the latter case. However, inspection of Tables 4.1.3-6 shows that dialysis initially leads to a reduction in conductivity of a dispersion for any particle number density. This implies that not only is the dialysis increasing proton concentration but it is also reducing the bulk free ion concentration. The presence of other ions, probably sodium from the latex preparation, will affect particle mobility. Although their removal has little effect on solutions at high proton concentrations (5 x 10^{-6} mol dm^{-3} HCl), the effect on the 10^{-6} mol dm^{-3} HCl solutions is shown by increased mobility. Conductivities of the two concentrates in 10^{-6} mol dm^{-3} HCl corroborate this explanation.

In order to obtain electrophoretic mobility v. log [HCl] plots of the type shown earlier (Fig 4.1.4), it is necessary to use another method of calculating the concentration of HCl present. If it is assumed that the contribution to the conductivity of all ions in solution other than protons is constant then conductance can be used to estimate the proton concentration. Obviously this assumption is very approximate, since the concentration of Cl^- undoubtedly varies.

Fig 4.1.6 shows the conductance of butanol solutions of HCl in the absence of Polystyrene. From this graph the conductivities of the Polystyrene dispersions (Table 4.1.1) have been converted to "apparent HCl concentrations". Fig 4.1.7 shows electrophoretic mobility as a function of the apparent HCl concentration. This is the curve shown in Fig 4.1.4 for Polystyrene.

In conclusion, to avoid this particle concentration effect all dispersions involving Polystyrene are prepared from 10^{-6} mol dm^{-3} HCl concentrate in a 10^{-6} mol dm^{-3} HCl/butanol solution.

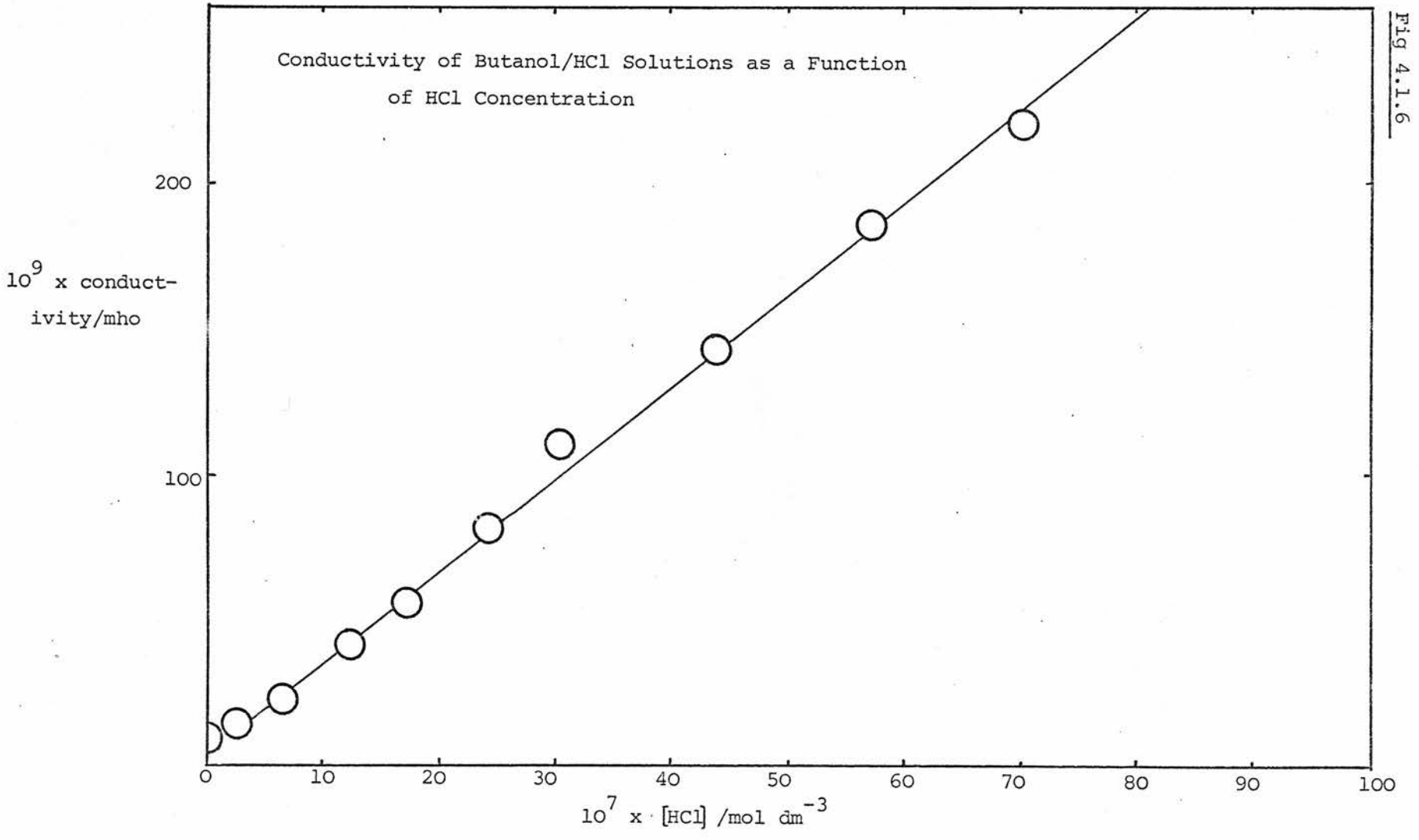
Conductivity of Butanol/HCl Solutions as a Function of HCl Concentration
200
100
10^9 x conductivity/mho
0
10
20
30
40
50
60
70
80
90
100
10^7 x [HCl] /mol dm^{-3}

Fig 4.1.6

Fig 4.1.7

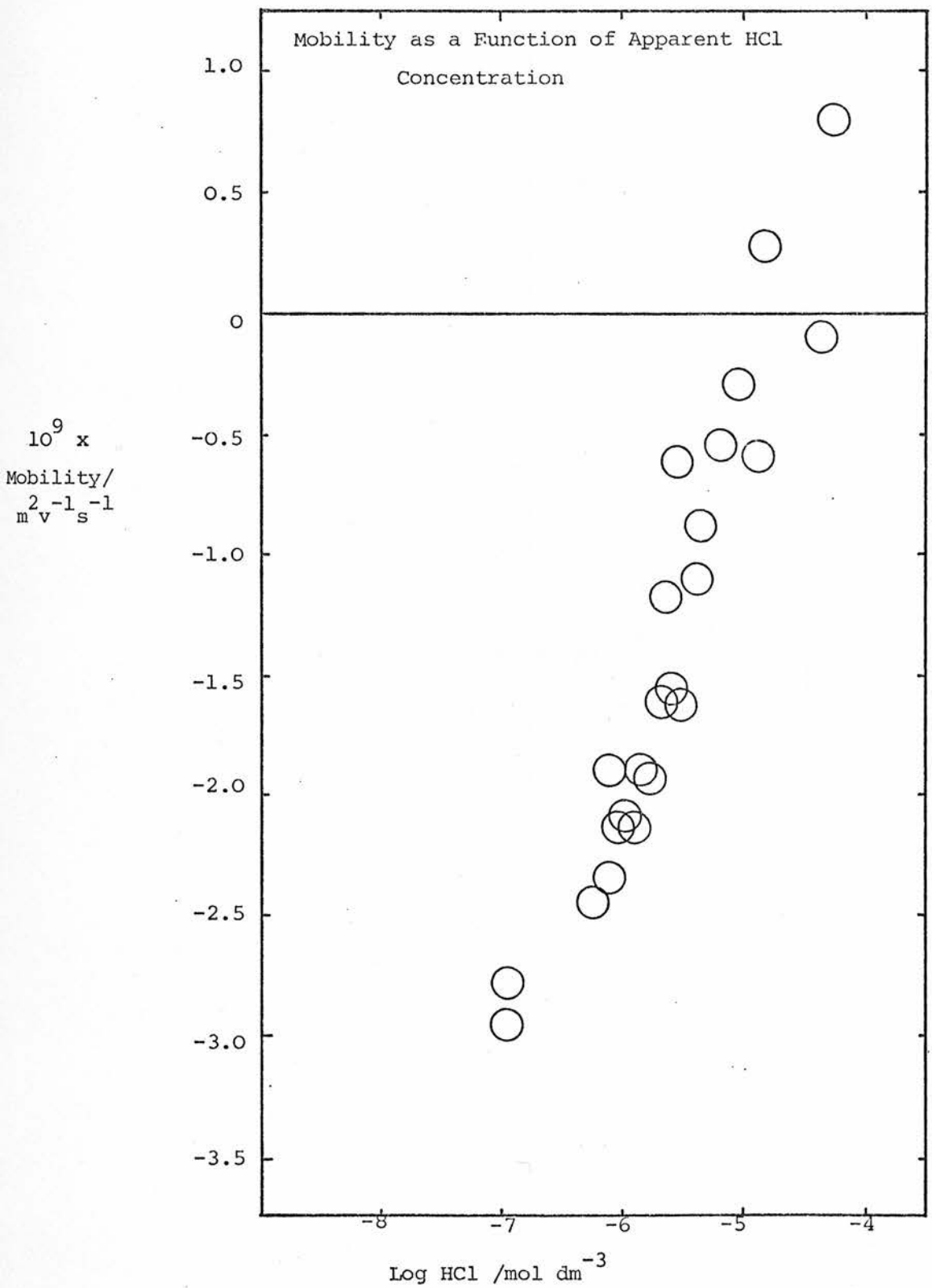
Mobility as a Function of Apparent HCl Concentration
1.0
0.5
0
-0.5
-1.0
-1.5
-2.0
-2.5
-3.0
-3.5
10^9 x Mobility/ $m^2 v^{-1} s^{-1}$
-8
-7
-6
-5
-4
Log HCl /mol dm^{-3}

4.1.4 Dispersions in Butanol Solutions of LiCl

Unlike hydrochloric acid, lithium chloride is not totally dissociated in butanol. Shkodin et al[147] have published tables of molar conductivity (Λ) as a function concentration of LiCl in a number of alcohols including butanol. Values of Λ_o, the molar conductance at infinite dilution, are also given and as a first approximation the ratio Λ/Λ_o can be used[148] to estimate the degree of dissociation (α), i.e.

$$\alpha = \Lambda/\Lambda_o \qquad (4.1.3)$$

However this expression neglects the effect of the ionic environment on the mobility of the ions and should be modified to

$$\alpha = \Lambda/\Lambda_i \qquad (4.1.4)$$

where Λ_i is the hypothetical molar conductance that the electrolyte would have if it was completely dissociated at a concentration $c_i = \alpha c$.
From an equation of the form

$$\Lambda + Sc_i^{\frac{1}{2}} = \Lambda_o - 1/K \left(\frac{\Lambda^2 c(1O^{-2Ac_i^{\frac{1}{2}}})}{\Lambda_o - Sc^{\frac{1}{2}}}\right) \qquad (4.1.5)$$

where S is the limiting slope of the Onsager conductance equation

$$(\Lambda_i = \Lambda_o - Sc_i^{\frac{1}{2}}),$$

A is the Debye-Hückel constant,

K is the Association constant,

by using a series of approximations,[149] values of K and c_i are calculated. A computer program[150] has been used to do this and the values of c_i obtained are compared with those predicted using equation 4.1.3 in fig 4.1.8.

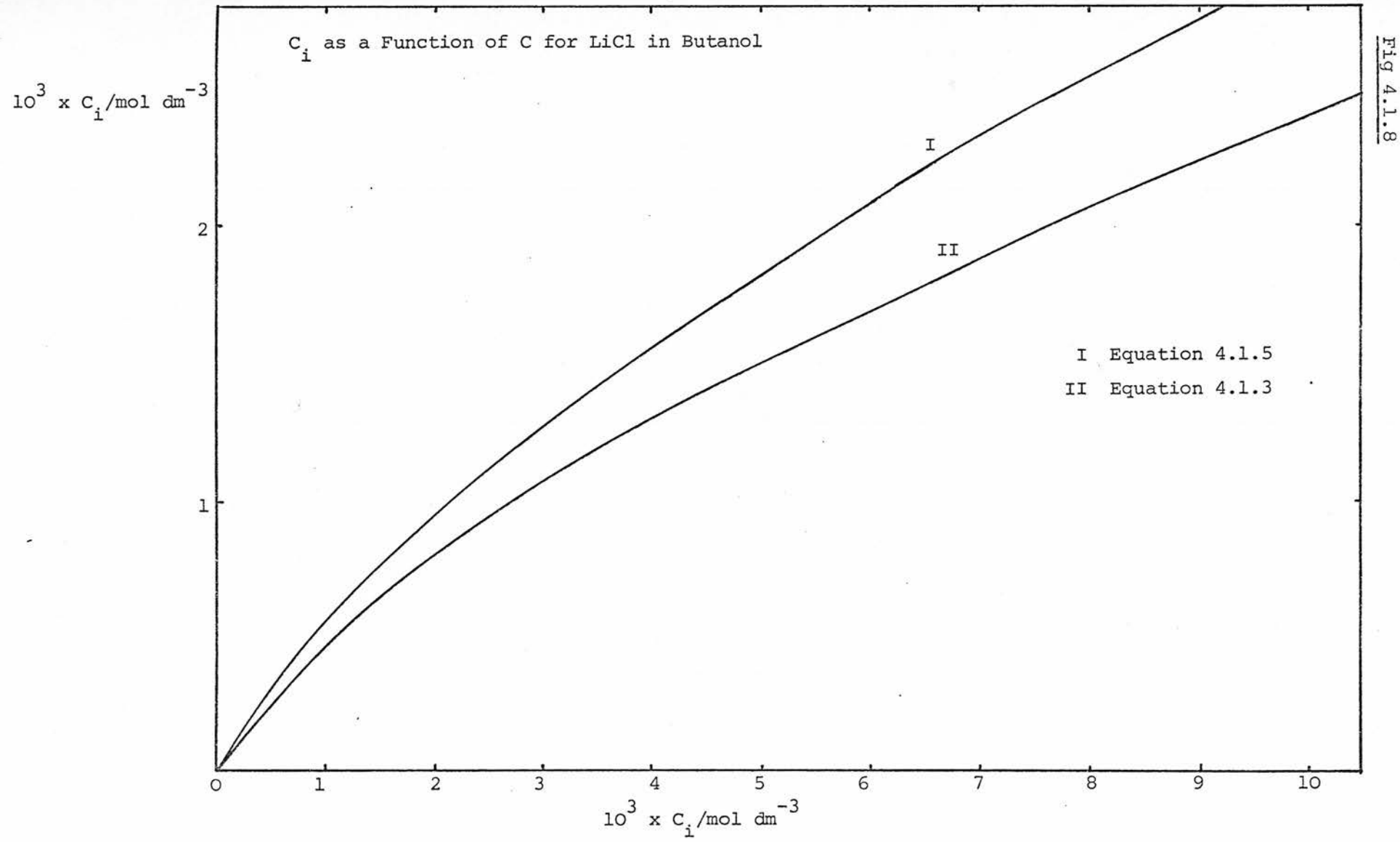
C_i as a Function of C for LiCl in Butanol
$10^3 \times C_i$/mol dm^{-3}
I
II
I Equation 4.1.5
II Equation 4.1.3
0
1
2
3
4
5
6
7
8
9
10
$10^3 \times C_i$/mol dm^{-3}

Fig 4.1.8

Throughout this Thesis the free ion concentrations of LiCl solutions have been calculated from equation 4.1.5.

Fig 4.1.9 shows the effect of LiCl concentration on the zeta potentials of dispersions of Graphon (2×10^{-5} mol dm^{-3} HCl) and Polystyrene (10^{-6} mol dm^{-3} HCl). Zeta potentials were calculated from mobilities using the Wiersema, Loeb and Overbeek[140] approach, described in Section 3.2.2, employing graphs of the type shown in Fig 3.2.2. For both Graphon and Polystyrene the limiting concentration of LiCl studied was approximately that at which total instability occurred.

Within the region studied the zeta potential of Graphon is almost independent of LiCl concentration. At similar concentrations the same is true for Polystyrene but at higher LiCl concentrations the zeta potential is markedly reduced. Aqueous dispersions typically exhibit similar behaviour,[151,152] the zeta potential being relatively insensitive to electrolyte at low concentrations but falling approximately linearly with $\log_{10}c$ of electrolyte at higher concentrations. There are a number of possible explanations of this observed relationship between electrolyte concentration and zeta potential.

a) Specific adsorption of counter-ions increases the charge density in the Stern layer (σ_1) and therefore reduces ψ_δ and hence also the zeta potential.

b) Increasing electrolyte concentration increases the charge in the diffuse layer (σ_2) which increases σ (the surface charge density) if σ_1 remains constant because

$$\sigma = \sigma_1 + \sigma_2$$

Since

$$\sigma = K(\psi_o - \psi_\delta)$$

where K is the capacitance of the Stern layer, if ψ_o remains constant ψ_δ

Fig 4.1.9

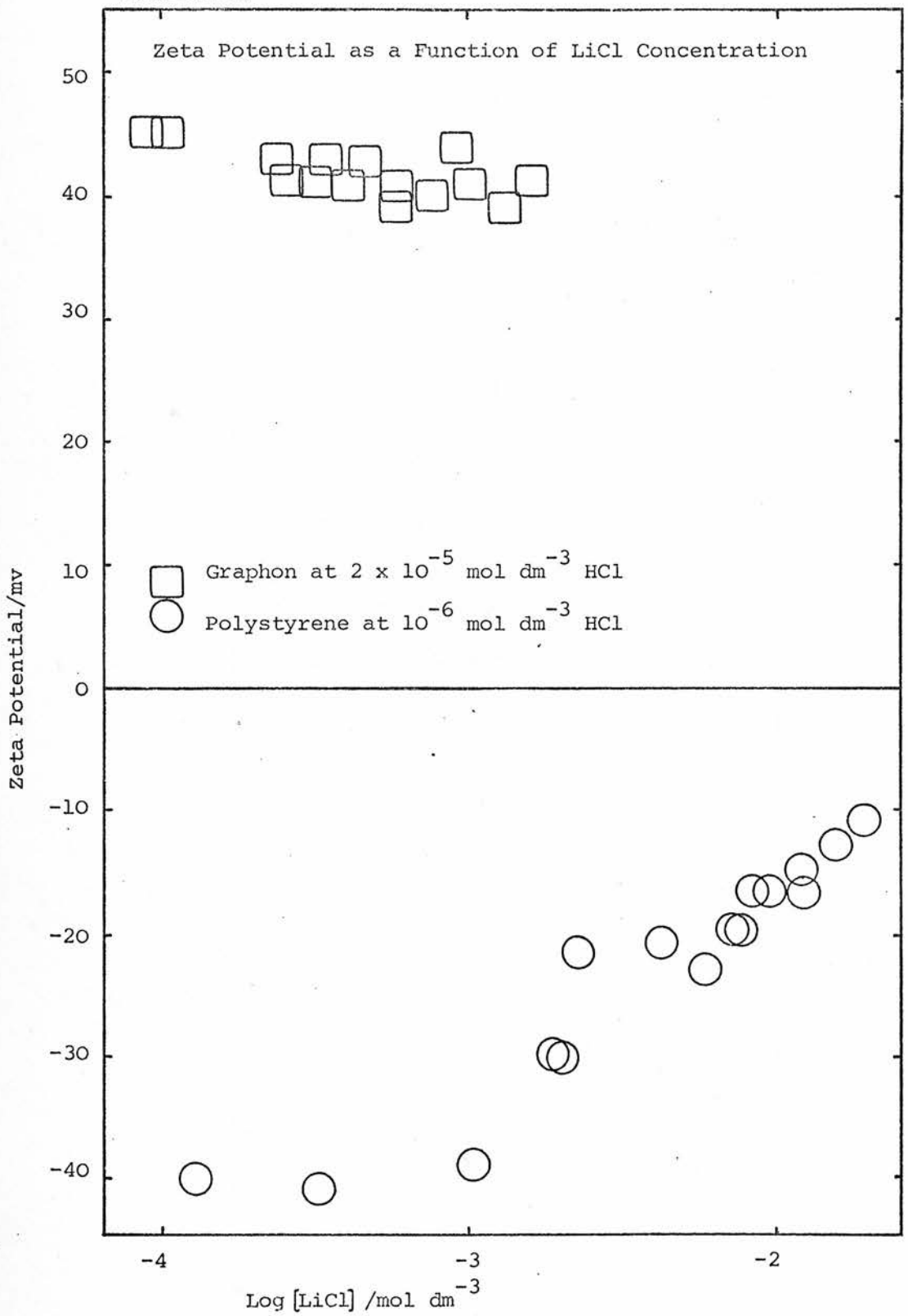
Zeta Potential as a Function of LiCl Concentration
50
40
30
20
10
0
-10
-20
-30
-40
Zeta Potential/mv
Graphon at 2 x 10^-5 mol dm^-3 HCl
Polystyrene at 10^-6 mol dm^-3 HCl
-4
-3
-2
Log [LiCl] /mol dm^-3

decreases. If σ remains constant, then $\sigma_1 + \sigma_2$ is constant, and since both of these are directly related to electrolyte concentration and to ψ_δ, increasing electrolyte concentration reduces ψ_δ.

c) Increasing electrolyte concentration increases the rate of potential decay in the diffuse double layer. If the shear plane is at some finite distance further from the surface than the Stern plane then the difference between ζ and ψ_δ will be accentuated by a steeper potential gradient, i.e. a higher electrolyte concentration.

d) Movement of the position of the plane of shear, relative to the position of the Stern plane, can increase or reduce the magnitude of the effect produced by (c).

From the available information it is not possible to decide which of these explanations, or combination of them, is responsible.

A comparison of the theoretical stability ratios, calculated using these values of zeta potential, with those observed experimentally is given in Sections 4.2.3 and 4.

4.2 Homoflocculation

Particle counting techniques as described in Section 3.3 have been used to obtain flocculation rates of a number of dispersions. The stability ratio, W, of any dispersion is defined as the factor by which the measured rate is reduced from the rapid rate for that dispersion, i.e. in terms of rate constants

$$W = k_o/k' \qquad (3.3.3)$$

where k_o is the rapid rate constant,

k' is the reduced rate constant.

Rapid rate flocculation is observed when V_R is negligible and the only interactions considered are van der Waals attraction and viscous effects. The stability ratio is therefore a measure of the effect of a V_R term on the flocculation rate. It is defined in this manner regardless of whether V_R is a repulsive or an attractive term. When the electrostatic interaction, V_R, is attractive, the flocculation rate is greater than the Smoluchowski diffusion controlled rapid rate and W is fractional. For a homoflocculating system V_R will always be repulsive and W will always be greater than, or equal to 1.

The dependence of the Hamaker function on κ leads to a slight variation in van der Waals interaction (V_A) at different electrolyte concentrations. As a result of this the above definition of W is not strictly accurate. However, the variation in V_A is generally very small and the error produced in the value of W is negligible in comparison to the experimental errors in the counting technique. Even so, just sufficient electrolyte to produce rapid rate flocculation is used in the measurement of the experimental rapid rates.

Tables 4.2.1 a, b, c and d show the experimentally measured rapid rate constants for Graphon, Black Pearls, Polystyrene and PTFE respectively. Unless otherwise stated, the mean values of the rapid rate constants given are those used to derive the experimental stability ratios presented in this work.

The Smoluchowski equation for diffusion controlled flocculation (2.4.11) predicts a value of 2.13×10^{-18} $m^3 s^{-1}$ for the rapid rate constant of flocculation for dispersions in butanol. This expression neglects the effect of long range van der Waals attraction and of the repulsive viscous interaction. Since these two terms tend to counterbalance one another the value predicted by equation (2.4.11) is often similar to the experimental rapid rate constant, as in the case of the two latex dispersions.

Tables 4.2.1 a,b,c and d. Rapid Rate Constants for Dispersions in Butanol

4.2.1a Graphon in 10^{-6} mol dm^{-3} HCl/butanol

Concentration of LiCl/mol m^{-3}	10^{18} x Rate Constant/$m^3 s^{-1}$
1.5	3.03
2.0	2.39
2.6	2.74
3.0	3.21
Mean Value 2.8 $\pm$ .4 x 10^{-18} $m^3 s^{-1}$	

4.2.1b Black Pearls in 10^{-6} mol dm^{-3} HCl/butanol

Concentration of LiCl/mol m^{-3}	10^{18} x Rate Constant/$m^3 s^{-1}$
0.02	3.00
0.02	2.83
Mean Value 2.9 $\pm$ .1 x 10^{-18} $m^3 s^{-1}$	

4.2.1c Polystyrene in 10^{-6} mol dm^{-3} HCl/butanol

Concentration of LiCl/mol m^{-3}	10^{18} x Rate Constant/$m^3 s^{-1}$
20.4	2.23
19.2	2.01
19.2	2.39
15.4	2.27
Mean Value 2.2 $\pm$ .2 x 10^{-18} $m^3 s^{-1}$	

4.2.1d PTFE in 10^{-6} mol dm^{-3} HCl/butanol

Concentration of LiCl/mol m^{-3}	10^{18} x Rate Constant/$m^3 s^{-1}$
0.02	3.18
0.02	2.04
0.10	1.75
0.10	1.89
Mean Value 2.2 $\pm$ .7 x 10^{-18} $m^3 s^{-1}$	

For the carbon dispersions the attractive interaction is much larger than for the latex dispersions and, as a result, the experimental rapid rate constant is greater.

4.2.1 Stability of Graphon Dispersions in Butanol Solutions of HCl

A comparison of experimental and theoretical stability ratios of Graphon dispersed in HCl/butanol solutions is given in Table 4.2.2.

Log [HCl]	Zeta Potential/mV	κa	Water Concentration/ ppm	Log W_{exp}	Log W_{theory}
-6.2	+16	∿1	0.7	.7	1.2
-5.6	+43	∿1	2.5	>2.5	12.1
-5.2	+49	2.4	7	>2.5	13.1
-4.5	+38	5	35	>2.5	4.2
-4.0	+39	9	104	1.5	1.7
-3.6	+33	15	276	1.3	.34
-3.2	+38	21	630	1.2	.1
-2.9	+37	33	1431	.2	0

Table 4.2.2 Stability of Graphon Dispersions in Butanol Solutions of HCl

The theoretical value of W is obtained (computer program WHAMSP) from equation (2.4.23) where V_R is calculated using the linearised Derjaguin expression (equation 2.1.29) and V_A is calculated using the Hamaker function for Graphite (Fig 2.2.8) in equation (2.2.5). From the values of κa given it may be seen that the Derjaguin expression is only strictly valid for the dispersions with the larger concentrations of HCl. However, since all but one of the other dispersions are of particles with high zeta potentials, changing the equation used to calculate V_R will only slightly alter the absolute value of W, which will, in any case, be very large.

When dispersions are very stable it becomes difficult to define a value of W accurately. When no change in particle number was observed over a period of 24 hours the logarithm of the stability ratio has been assigned the value of >2.5.

As predicted theoretically, dispersion stability is dependent on ψ_δ (equated here to ζ) and on double layer thickness. The experimental and theoretical values of log W exhibit similar trends and are of the same order of magnitude, although there is some deviation between the absolute values. If it is not merely an experimental error, this non-agreement is probably related to the high concentration of water present in these dispersions. The water concentration increases linearly with the concentration of HCl as a result of the inherent "wetness" of the standard solution. Even if the possible effects that water may have on the determination of the zeta potential may be disregarded it may still affect the relative magnitudes of the repulsive and attractive particle-particle interactions.

4.2.2 Stability of Polystyrene Dispersions in Butanol Solutions of HCl.

Table 4.2.3 shows the stability ratios of Polystyrene dispersions in butanol as a function of apparent HCl concentration.

Log HCl_{app}	Zeta Potential/mV	κa	Water Concentration/ppm	Log W_{exp}
-5.4	-41	2.2	3	> 3
-5.5	-25	-	3	2.45
-5.1	-23	-	9	0.74
-4.7	-16	4.8	20	0.25

Table 4.2.3 Stability of Polystyrene Dispersions in Butanol Solutions of HCl

If it is assumed that the proton concentration may be equated to the apparent HCl concentration and that κ may be calculated purely from a consideration of the proton concentration then it may be shown that κ

is small and changes by a factor of about 2 ($1.4 - 3 \times 10^{7} m^{-1}$) over the range of concentrations studied. However, it is not strictly valid to make these assumptions since the proton and chloride ion concentrations are not equivalent in this system and consequently the actual values of κ are difficult to define. Using an estimated value of $\kappa = 2 \times 10^{7} m^{-1}$ the theoretical ζ v. log W curves shown in Fig 4.2.1 have been constructed. The stability ratios were calculated as described in Section 4.2.1 using the Hamaker function shown in Fig 2.1.12; for curve (a) equation 2.1.29 was used to calculate V_R whereas for curves (b) and (c) equation 2.1.34, with $\beta = 1$ and 0.6 respectively, was used. For any interaction, β varies between 0.6 and 1 as a function of interparticle separation. Therefore curves (b) and (c) represent the extremes of stability ratios which may be expected from the use of equation (2.1.34) to calculate V_R. Using a variable value of β will produce a curve lying somewhere between them but since the experimental points do not lie within this region the calculation is not merited.

From the experimental data it appears that the double layer is thinner than calculated. The value of κ was calculated using the approximate expression,

$$\kappa = (2e^2 n z^2 / \varepsilon k T)^{\frac{1}{2}} \qquad (2.1.10)$$

where n and z are taken as the concentration and charge number of the counter-ion respectively. Normally, for a symmetrical electrolyte, this is valid, however, for an unsymmetrical electrolyte or for this situation in which there are unequal concentrations of counter-ions and co-ions, the following expression should be used.

$$\kappa = (e^2 \sum_i n_i z_i^2 / \varepsilon k T)^{\frac{1}{2}} \qquad (4.2.1)$$

where n_i is the bulk concentration of each ion,

z_i is the valency of each ion.

Fig 4.2.1

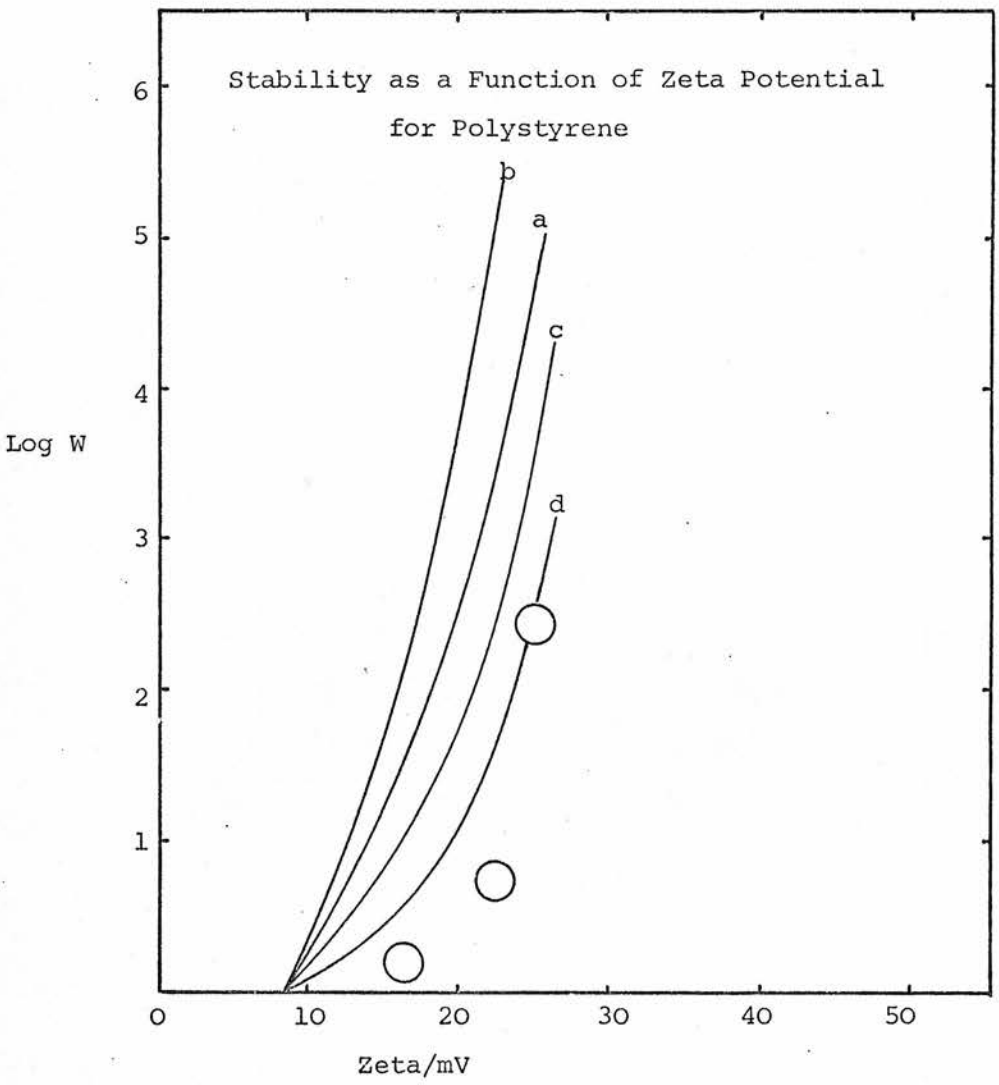
Stability as a Function of Zeta Potential
for Polystyrene
Log W
6
5
4
3
2
1
0
10
20
30
40
50
Zeta/mV
b
a
c
d

Since protons have been adsorbed onto the surface the proton and chloride ion concentrations are non-equivalent. This immediately invalidates the assumption that conductivity can be taken as a measure of the proton concentration. Since chloride ions will now contribute significantly to the conductivity and as the transport number of the chloride ion is much less than that of the proton, the ionic strength may be much larger than anticipated. As a result, the use of equation (4.2.1) will produce a value of κ which is larger than was previously calculated. Curve (d) of Fig 4.2.1 is calculated using a value of κ of $7 \times 10^{7} m^{-1}$ in the linear Derjaguin expression (equation 2.1.29) for V_R. This corresponds to an ionic strength of 10x that calculated and still theory and experiment are not in agreement. It would seem unlikely that the ionic strength would be so different from that estimated conductimetrically.

4.2.3 Stability of Graphon Dispersions in Butanol as a Function of LiCl Concentration

Experimentally determined values of log W as a function of LiCl concentration are compared with a theoretically predicted curve in Fig 4.2.2. The curve is calculated as before using the Hamaker function shown in Fig 2.2.8 and using an average value of the zeta potential of +42 mV in equation (2.1.29) to calculate V_R. (According to Fig 4.1.9 the zeta potential within the range of concentrations studied lies between +41 and +43 mV). The HCl concentration is fixed at 2×10^{-5} mol dm^{-3} in which, in the absence of LiCl, the dispersions are very stable, no change in particle number being observed over a period of several days.

The quantitative agreement between the theoretical curve and the experimental points is excellent. This implies that it is acceptable to use the graphite dispersion data to calculate the Hamaker function of

Fig 4.2.2.

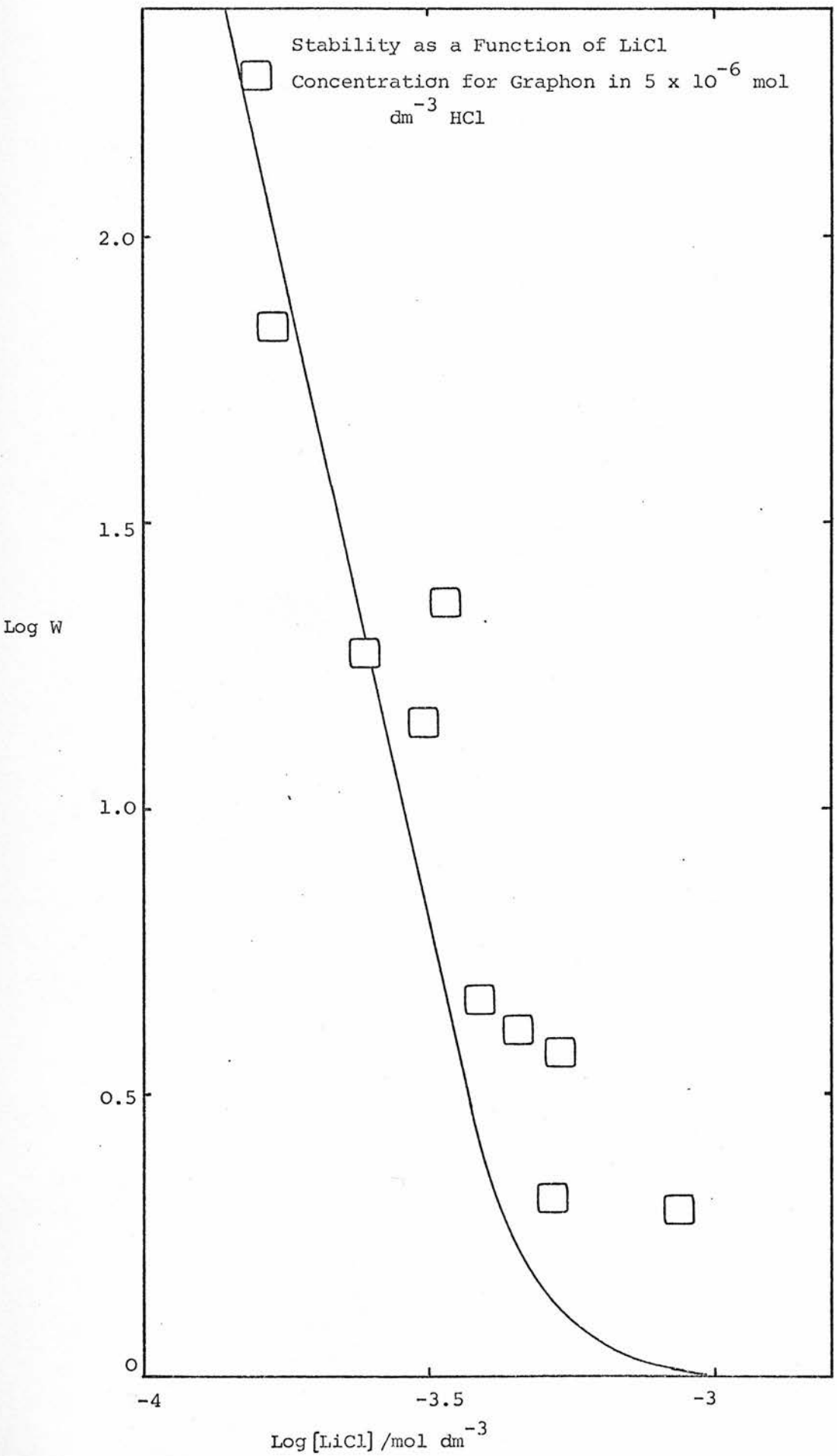
Stability as a Function of LiCl Concentration for Graphon in 5 x 10^-6 mol dm^-3 HCl
2.0
1.5
1.0
0.5
0
Log W
-4
-3.5
-3
Log [LiCl] /mol dm^-3

Graphon. If this is so, then using the same data to calculate the Hamaker function of Graphon in water produces a value of 12.5 x 10^{-20} J at 1 x 10^{-9} m.

4.2.4 Stability of Polystyrene Dispersions in Butanol as a Function of LiCl Concentration.

Fig 4.2.3 shows experimentally determined values of log W as a function of LiCl concentration for Polystyrene dispersed in butanol at fixed HCl concentration (10^{-6} mol dm^{-3}). Over the range of concentrations studied the zeta potential varies from -21 mV to -15 mV (Fig 4.1.9). Curve (a) of Fig 4.2.3 is calculated using a constant value for the zeta potential of -21 mV and the "salt corrected" Hamaker function shown in Fig 2.2.13. It indicates that all these dispersions are more stable than is theoretically predicted. It must be concluded that either DLVO theory is inapplicable to this system or that at least one of the parameters used in the calculation is incorrect.

DLVO theory would not be expected to be applicable if the Polystyrene was sterically stabilised. It is possible that Polystyrene particles in butanol do not exist as smooth spheres as intimated by the electron micrographs but instead have a rough, steric stabiliser coated surface. The steric stabiliser would be loops and tails of Polystyrene chains which, although attached to the particle would not be fully incorporated into it. Whether these loops and tails project into solution or lie on the particle surface may be a factor controlled by the electrolyte concentration and thus stability would be related to the concentration of LiCl present. For this argument to hold, a similar dependence of the chain environment on proton concentration would have to be postulated to explain the results discussed in Section 4.2.2 and the apparent dependence of stability on zeta potential would have to be discounted. It is this last point which makes the steric stabilisation idea difficult to accept.

Fig 4.2.3

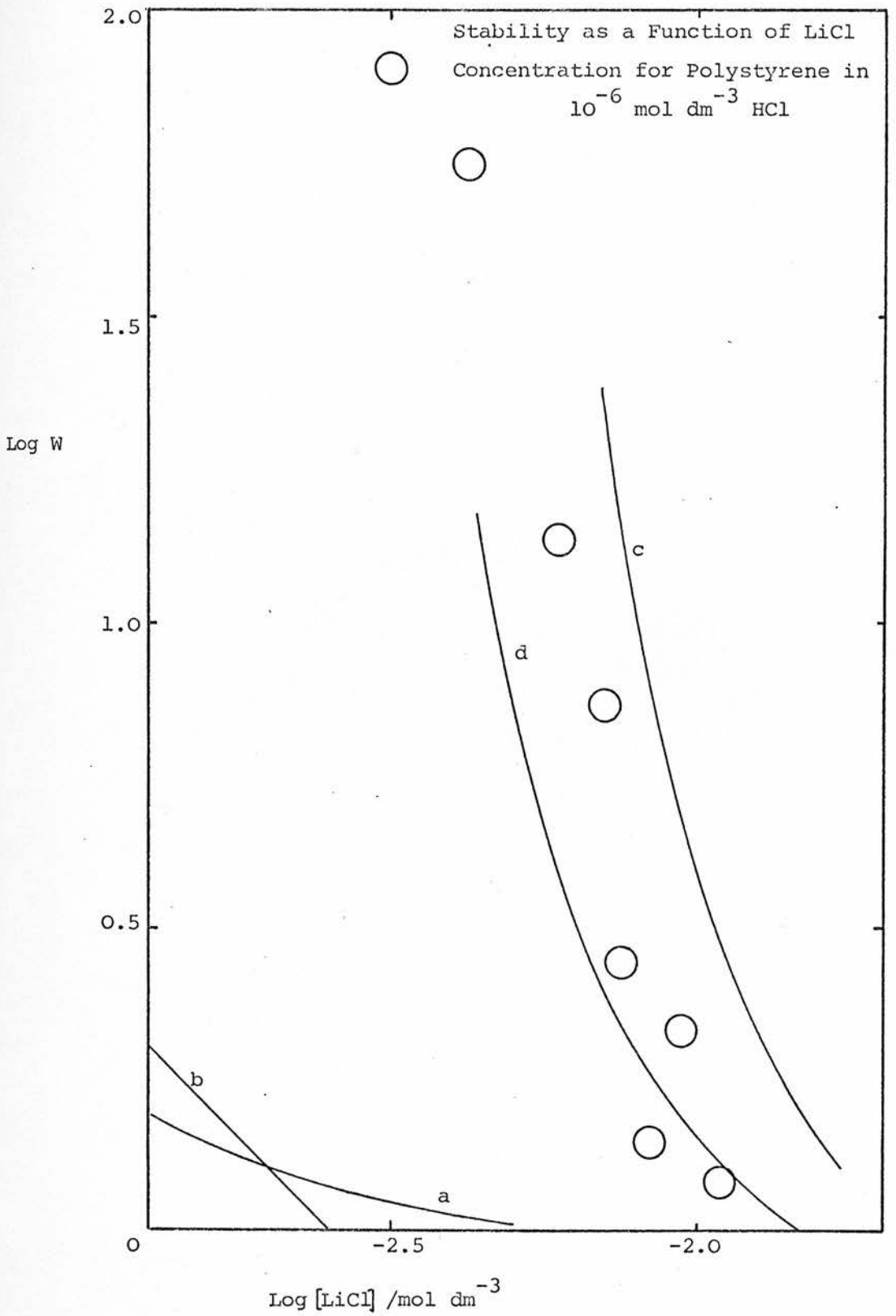
Stability as a Function of LiCl
Concentration for Polystyrene in
10^{-6} mol dm^{-3} HCl
2.0
1.5
1.0
0.5
0
Log W
a
b
c
d
-2.5
-2.0
Log [LiCl] /mol dm^{-3}

With regard to an error in the parameters used in the calculation, a number of possibilities are discussed here.

i) Particle Size: It is not unreasonable to suppose that some swelling of the Polystyrene particles occurs in butanol. Consequently it may be inappropriate to use the average particle size obtained from electron micrographs of dry particles. Curve (b) (Fig 4.2.3) was calculated as before except that a value of 3.2×10^{-7} m was substituted in place of 1.6×10^{-7} m for the particle radius. Doubling the particle radius corresponds to a volume increase of 8x and is probably the maximum conceivable swelling before the particle would be considered to dissolve. It is therefore apparent that the discrepancy between theory and experiment cannot be interpreted in terms of an error in the particle size.

ii) Interparticle Separation: It is possible that the charged groups on the Polystyrene are situated some distance from the particle surface attached to the "free" end of a polymer chain. This would result in a larger repulsive term for any given intersurface separation (the parameter from which V_A is evaluated) and so lead to greater stability. Again, as in the case of the steric stabilisation model this idea is not concordant with the earlier work (Section 4.2.2) in which dispersions were observed to be less stable than calculated. For this model to apply, it would require that the "stand-off" distance of the charged groups was a function of LiCl and/or HCl concentrations.

iii) Hamaker Function: Increasing electrolyte concentration induces a more rapid decay of the Hamaker function with distance. This has been accounted for in the calculations, the "salt corrected" Hamaker function (Fig 2.2.13) for the interaction having been used. Curve (c)(Fig 4.2.3) has been constructed using an arbitrarily chosen fixed value for the Hamaker function of 10^{-21} J and ignoring any retardation. This value is very much less than is calculated by the Lifshitz approach and is 3x less than that predicted by the London-Hamaker approach.

iv) Zeta Potential: Curve (d) (Fig 4.2.3) has been calculated using a fixed value for the zeta potential (equated to ψ_δ in the calculation) of -33 mV. Its close proximity to the experimental points suggests a re-examination of the assumption that ζ and ψ_δ may be equated. At low electrolyte concentration it may be valid to make this assumption since the potential decay with distance within the diffuse double layer is small. Consequently, if the slipping plane is a little further out from the particle surface than the Stern plane, the difference between ψ_δ and ζ is small. However, for high electrolyte concentrations the potential decay is large and the difference between the two potentials may be large. It must also be borne in mind that the position of the slipping plane may change with changing electrolyte concentration.

Webb, Bhatnagar and Williams[153] have investigated the relationship between ζ and ψ_δ for aqueous dispersions of anatase (TiO_2) at different electrolyte concentrations. It was shown that for any given electrolyte concentration ζ tended to a finite maximum value which was independent of increasing ψ_δ. Increasing electrolyte concentration reduced the maximum possible value of the zeta potential. These results agree qualitatively with the theoretical predictions of the Lyklema and Overbeek[141] concept of a "variable slipping plane".

It may therefore be the case that in the Polystyrene/butanol system at high electrolyte concentration ζ is not equivalent to ψ_δ and that the variation in ζ with increasing electrolyte concentration does not reflect a similar change in ψ_δ.

In the above discussion it has been attempted to establish which one parameter is most likely to be in error. This is probably an over-simplification of the problem since it is most likely that the discrepancies between the theoretical and experimental stabilities arise from a combination

of factors. For example, if the particle is considered to take in solvent and swell, its bulk dielectric properties will alter and the Hamaker function will change. Also, such a "fluid particle" would tend to deform during the interaction, the magnitude and the nature of the deformation being a function of the forces involved. Similarly, the distribution of the charged groups and their position in relation to the particle surface (if it is indeed valid to consider a surface) is unknown. Finally the relationship between ζ and ψ_δ is unknown, particularly at high electrolyte concentrations.

It is interesting to note that Polystyrene dispersions, despite their supposed ideality, exhibit stabilities which do not agree with those predicted theoretically. Conversely, Graphon dispersions are neither monodisperse nor do they contain spherical particles and yet the correlation between experimental and theoretical stability is good.

4.3 Heteroflocculation

Heteroflocculation is a general term describing the flocculation between dissimilar particles but does not indicate the nature of the dissimilarity. A more specific expression, describing the flocculation between two oppositely charged particles, is mutual flocculation. Mutually flocculating systems are capable of exhibiting flocculation rates, known as super-fast rates, which are greatly in excess of the diffusion controlled rate. Hogg, Healy and Fuerstenau[33] have calculated that super-fast flocculation is greatest when $\kappa a < 1$ and that for κa values larger than this the flocculation rate tends to the diffusion controlled rate. Enüstun and Turkevich[36] found that the most rapid flocculation rate was obtained when the particles have large equal and opposite charges. Theoretically no such relationship is expected. In the light of experimental results and theoretical calculations these ideas have been discussed in this section.

Many of the calculations of W given here must be regarded as approximations owing to the use of equation (2.2.29) to calculate V_R. This equation is only strictly valid when $\kappa a > 10$ but, in the absence of a more suitable equation, it has been necessary to use it to describe systems for which κa values are much less than 10.

Heteroflocculation results were obtained from particle counting techniques of dispersions prepared as described in Section 3.2.1c. From a knowledge of W_{11}, W_{22} and W_T a value of W_{12} is calculated using equation (2.4.24). Although W_{11} and W_{22} may be easily defined, the definition of W_T and consequently W_{12} is more difficult. The difficulty arises from an inability to determine accurately a diffusion controlled flocculation rate for the overall system. It is therefore necessary to define two values of W_T, one with respect to the 1-1 rapid rate and the other with respect to the 2-2 rapid rate. Thus, two extreme values of W_{12} are obtained, the true value lying somewhere between them.

4.3.1 Effect of Charge

Theoretical values of W_{12} for a mutually flocculating Graphon/Polystyrene system are compared with those observed experimentally in Table 4.3.1. The range of values of zeta potential was obtained by using slightly differing concentrations of HCl, about a mean value of 10^{-6} mol dm^{-3}. Increasing HCl concentration is indicated by an increasing value of the Graphon zeta potential and a corresponding reduction in that of the Polystyrene. Although these values of zeta potential are correct for the individual systems they will vary slightly on mixing, due to the effects of the Polystyrene surface groups, which may be regarded as buffering the bulk HCl concentration towards 10^{-6} mol dm^{-3}. As a result the HCl concentrations will be different, that of the Graphon dispersion will be as prepared but that of the Polystyrene dispersion will be closer

N Fraction of Graphon	GRAPHON ζ/mV	W_{11}	POLYSTYRENE ζ/mV	W_{22}	W_{12} w.r.t. Graphon	W_{12} w.r.t. Polystyrene	W_{12} theory
0.36	+ 8	1	-102	>100	1.1	0.79	0.25
0.56	+28	>50	-58	>100	0.59	0.46	0.25
0.57	+36	>100	-59	>100	0.47	0.37	0.25
0.84	+38	>100	-56	>100	0.38	0.30	0.25
0.15	+47	>100	-49	>100	0.45	0.36	0.25
0.84	+71	>100	-40	>100	0.43	0.34	0.25

Table 4.3.1 Heteroflocculation of Graphon and Polystyrene in Approximately 10^{-6} mol dm^{-3} HCl/Butanol

to 10^{-6} mol dm^{-3}. Consequently, for dispersions in which the prepared HCl concentration is less than 10^{-6} mol dm^{-3} mixing will slightly increase the absolute values of both zeta potentials whereas for dispersions in which the HCl concentration is in excess of 10^{-6} mol dm^{-3} the converse is true. In spite of this slight variation in zeta potential the general trend of the results presented remains unchanged. The first two values of W_{12} in Table 4.3.1 still correspond to a mutually flocculating system for which the absolute values of the zeta potentials of the two particles are dissimilar.

Theoretically, W_{12} is independent of the respective particle charges, but experimentally the maximum rate is observed when the charges on the particles are approximately equal and opposite. As proposed by Enüstun *et al*,[36] slower flocculation occurs when the zeta potential of one particle is much lower than that of the other.

The use of the linearised Derjaguin expression (equation 2.4.29) for these systems ($\kappa a \sim 1$) is not strictly valid and leads to an overestimation of V_R (the electrostatic attraction) which may explain why the theoretical W_{12} is less than that observed experimentally.

4.3.2 Effect of Double Layer Thickness

The above results describe mutual flocculation for a system in which the double layer is thick ($\kappa a \sim 1$) and as a result the electrostatic attractive interaction is long range. Table 4.3.2 shows the experimental and theoretical value of W_{12} for the mutual flocculation of Polystyrene and Graphon in 10^{-6} mol dm^{-3} HCl and 2×10^{-3} mol dm^{-3} LiCl. For these dispersions the van der Waals and viscous interactions are similar to those of the systems discussed in Section 4.3.1, but the electrostatic attractive interaction is now of much shorter range, ($\kappa a \sim 40$). Consequently, the flocculation rate approaches that of the diffusion controlled rate and W_{12} tends to 1, a result which is in accordance with the value predicted theoretically.

Since Graphon is unstable at this electrolyte concentration the range of values of N, the fraction of Graphon present, is restricted to <0.6. For values of N greater than this the probability of a Graphon-Graphon interaction approaches that of a Graphon-Polystyrene interaction and the error in $W_{12\ exp}$ is greatly increased. For the range of values of N studied $W_{12\ exp}$ is independent of N and agrees with the value predicted theoretically.

N Fraction of Graphon	GRAPHON ζ/mV	GRAPHON W_{11}	POLYSTYRENE ζ/mV	POLYSTYRENE W_{22}	W_{12} w.r.t. Graphon	W_{12} w.r.t. Polystyrene	W_{12} theory
0.35	+42	1	-	-	0.94	0.71	0.96
0.52	-	1	-30	$>10^2$	1.16	0.81	0.96
0.58	-	1	-30	$>10^2$	0.92	0.64	0.96
0.18	+36	1	-	-	1.03	0.81	0.96

Table 4.3.2 Heteroflocculation of Graphon and Polystyrene in 10^{-6} mol dm^3 HCl/2×10^{-3} mol dm^3 LiCl/Butanol

4.3.3 Effect of Particle Size

Princen and de Vena-Peplinski[38] have found an experimental dependence of mutual flocculation rate on the ratio of the particle sizes. To investigate this, mutual flocculation between Graphon (radius = 1.25×10^{-7} m) and Black Pearls (radius = 1.4×10^{-8} m) has been studied. In order that the results of the heteroflocculation may be directly comparible with the systems discussed in Section 4.3.1 it is necessary, ideally, that all parameters, excluding size, are the same for both systems. However, due to the different acid strengths of the surface groups involved (Black Pearls v. Polystyrene), this is impossible. Furthermore, if the electrolyte concentration is such that κa for Graphon is ~ 1, then κa for Black Pearls is ~ 0.1.

An electrolyte concentration of 2×10^{-5} mol dm^{-3} LiCl in approximately 10^{-6} mol dm^{-3} HCl, resulting in κa (Graphon) ~ 4 and κa (Black Pearls) ~ 0.4 was used. The absolute HCl concentration is unimportant since it is identical for both dispersions.

In spite of this 10 fold difference in κa values, $W_{12\ exp}$ is very similar (Table 4.3.3) to that obtained for the Graphon/Polystyrene interaction when $\kappa a \sim 1$. Experimentally therefore, the variation in size appears to have little effect.

Although a more detailed comparison is perhaps invalid it is interesting to note two apparent anomalies.

1) Theoretically W_{12} for the Black Pearls/Graphon interaction is twice that of the Polystyrene/Graphon interaction and yet experimentally both exhibit similar stability ratios.

2) Although the zeta potentials of Graphon and Black Pearls are not equal and opposite the value of W_{12} is similar to that for Graphon/Polystyrene heteroflocculation when the zeta potentials are equal and opposite.

N Fraction of Graphon	BLACK PEARLS ζ/mV	W	GRAPHON ζ/mV	W	W_{12} w.r.t. Graphon	W_{12} Theory
0.80	-17	1	+67	$>10^2$	0.42	0.56
0.47	-15	1	+63	$>10^2$	0.45	0.58
0.66	-17	1	+56	$>10^2$	0.41	0.58

Table 4.3.3 Heteroflocculation of Graphon and Black Pearls in 10^{-6} mol dm^{-3} HCl/2 x 10^{-5} mol dm^{-3} LiCl/Butanol

Although, from the limited information available, it is difficult to explain the discrepancies in the results, the following general conclusions may be made.

1) Super rapid rates are observed for mutually flocculating dispersions in butanol.
2) DLVO theory predicts values of W_{12} which are in qualitative agreement with those observed experimentally.
3) W_{12} is independent of the relative concentrations of the two heteroflocculating components.
4) Experimentally, the rate of mutual flocculation is observed to be dependent on the respective zeta potentials, equal and oppositely charged particles flocculating most rapidly. This is not predicted theoretically.
5) Both theoretically and experimentally, κ is found to be the dominant factor controlling mutual flocculation rates. (This is as anticipated since κ dictates the range of the electrostatic interaction).
6) There is no marked dependence on size variation beyond that anticipated from the simultaneous effect on κa.

4.3.4 Repulsive van der Waals Forces

For all the systems discussed above, the van der Waals potential energy of the hetero-interaction was one of attraction. The presence of an electrostatic attraction caused an increase in the flocculation rate and so produced a fractional value of W_{12}. In the absence of an electrostatic term (V_R) interparticle collisions occur at approximately the diffusion controlled rate and the flocculation rate is dependent on the electrodynamic interaction (V_A). Generally V_A is attractive and each encounter leads to flocculation into a deep primary minimum. However, if V_A is repulsive, as in the case of the Graphon/PTFE interaction in butanol, flocculation does not occur and the stability is infinite. Conventional expressions, of the form of equation 2.4.23, cannot be used to describe this situation. It is no longer valid to consider the size of an energy barrier as a criterion of stability. This is immediately evident if the situation in which V_A is zero is envisaged, where, in the absence of an electrostatic term (V_R), the total energy of interaction (V_T) is also zero. As a result there is neither a primary maximum or primary minimum but W is infinite. Theoretically the predicted value of W is 1.

Consideration of the more realistic situation, where V_A is repulsive and V_R is attractive, leads to V_T curves of the type shown in Fig. 4.3.1 and 2. The presence of a long range electrostatic attraction produces a shallow potential minimum into which flocculation may occur. For separations greater than $\sim 5 \times 10^{-9}$ m these curves are not unlike those for systems in which V_A is attractive and V_R is negligible. It is therefore anticipated that W_{12} for the PTFE/Graphon interaction will be about 1, corresponding approximately to the diffusion controlled rate. However, the major difference is that for this interaction the minimum is very shallow and redispersion will probably occur easily.

Table 4.3.4 shows the experimentally obtained values of W_{12} for the heteroflocculation of PTFE and Graphon in 2 x 10^{-5} mol dm^{-3} LiCl and 10^{-4} mol dm^{-3} LiCl solutions in 10^{-6} mol dm^{-3} HCl/butanol. Increasing the electrolyte concentration reduces the range over which the electrostatic interactions are effective and also produces a shallower potential minimum. (Fig. 4.3.1 and 2)

Concentration of LiCl/ mol dm^{-3}	N Fraction of Graphon	GRAPHON ζ/mV	GRAPHON W_{11}	PTFE ζ/mV	PTFE W_{22}	W_{12} w.r.t. Smoluchowski
2 x 10^{-5}	0.88	+47	$>10^2$	-	1	1.45
2 x 10^{-5}	0.57	-	$>10^2$	-13	1	1.60
2 x 10^{-5}	0.82	+47	$>10^2$	-	1	0.93
10^{-4}	.75	-	$>10^2$	-9	1	7.9
10^{-4}	.62	+46	$>10^2$	-	1	1.9
10^{-4}	.74	-	$>10^2$	-9	1	2.0

Table 4.3.4 Heteroflocculation of Graphon and PTFE in 10^{-6} mol dm^{-3} HCl/ Butanol Solutions at Different LiCl Concentrations.

This is reflected experimentally by a slightly larger W_{12} at the higher electrolyte concentration.

These values of W_{12} have been calculated with respect to a Smoluchowski diffusion controlled rate (k_o = 2.13 x 10^{-18} m^{-3} s^{-1}) for the Graphon/PTFE rapid rate. W_{12} is therefore a measure of the apparent rate of flocculation with respect to a diffusion controlled rate. Since redispersion undoubtedly occurs, the rate of change of particle number does not indicate the number of encounters which lead to flocculation.

Fig 4.3.1

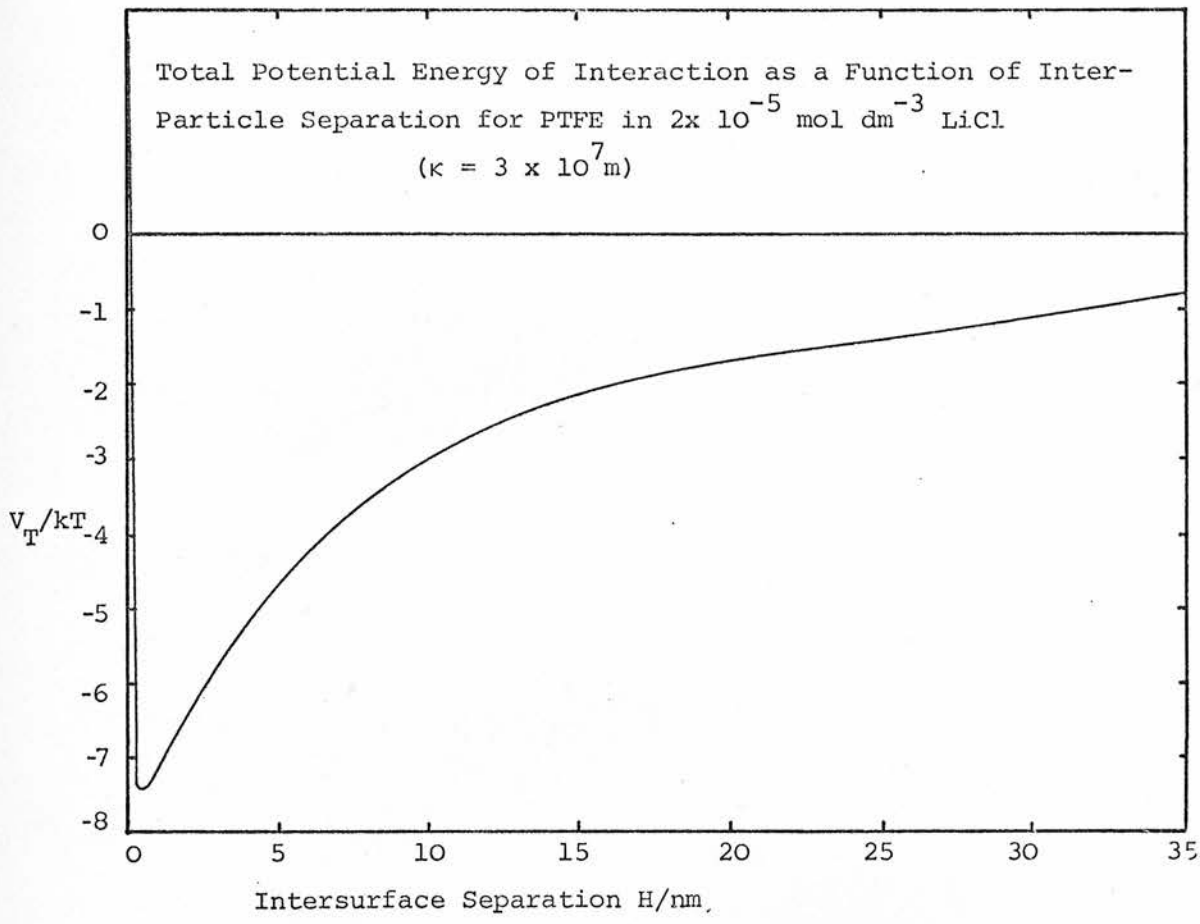

Fig 4.3.2

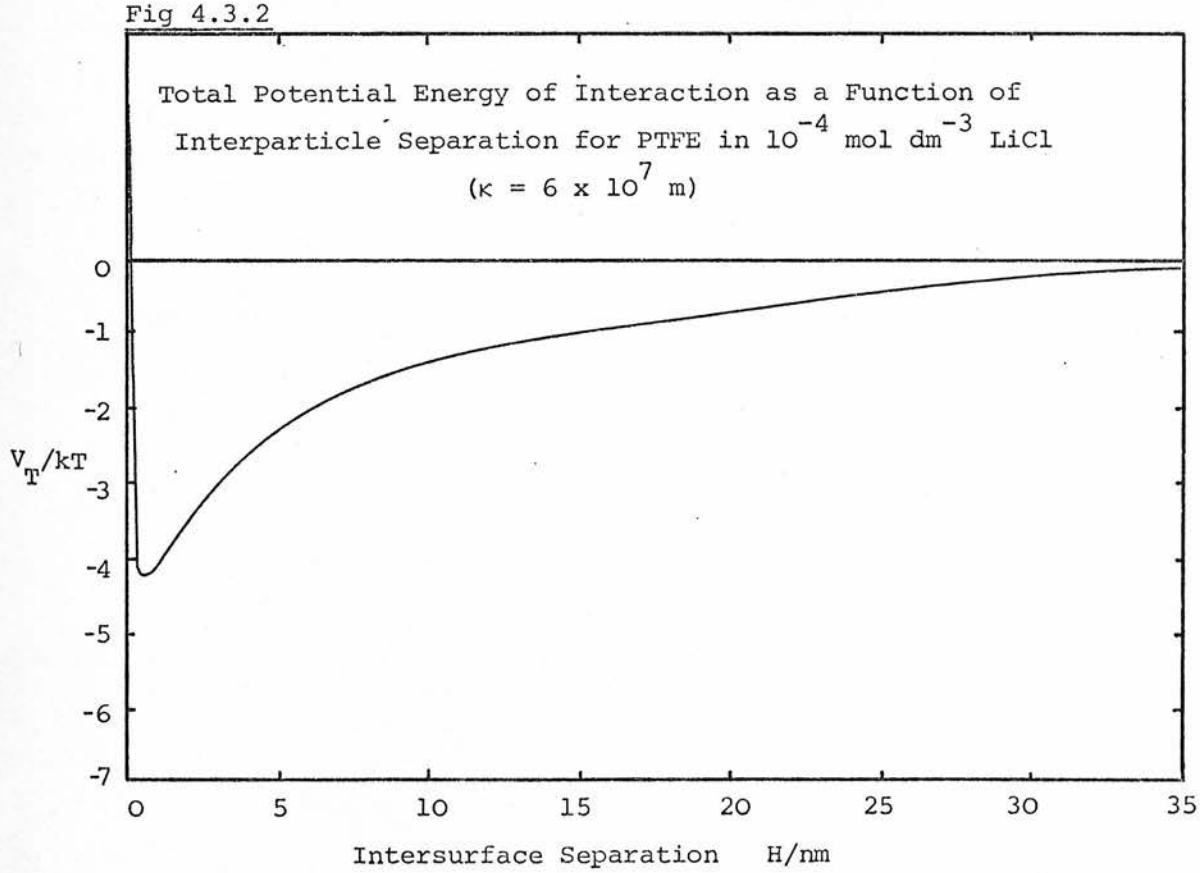

After some time an equilibrium situation between dispersed and flocculated particles will be achieved. The position of this equilibrium with respect to the relative numbers of dispersed and flocculated particles will be a particle number density dependent function but this has not yet been investigated experimentally.

It must be remembered that the experimental technique used to obtain these results would aid deflocculation. Withdrawal of samples through a hypodermic needle would undoubtedly produce large shear forces on the dispersion. Although this technique was not found to have flocculant or dispersant action on homoflocculating PTFE or Graphon systems this will certainly not be the case for the heterosystem and some redispersion is inevitable.

The absolute depth of the potential energy minimum is difficult to define due to the lack of dispersion data for Graphon. Figs. 4.3.1 and 2 were constructed using "salt corrected" Hamaker functions (Fig 2.2.9) for the Graphon/PTFE interaction, calculated using ε_o (Graphon) = 100. This value is almost certainly not an overestimate and therefore any correction required in it will serve to increase V_A and so reduce the depth of the minimum.

Despite the difficulties in interpretation, these results indicate very strongly the presence of a repulsive van der Waals force. Ideally it would be preferable to eliminate the V_R term completely in order that the observed W_{12} value could be explained entirely in terms of the effects of V_A. This may be achieved by using a proton concentration corresponding to the zero point of charge of one particle or by using a very high electrolyte concentration. The former of these is experimentally difficult while the latter is undesirable since high electrolyte concentrations lead to a reduction in the Hamaker function and also cause rapid rate homoflocculation of both dispersions.

To unequivocably demonstrate a repulsive van der Waals interaction requires that total dispersion stability be obtained in the absence of any electrostatic or steric interaction. However, this is impossible, since under such conditions homoflocculation must occur. Other possible methods by which a repulsive van der Waals interaction may be demonstrated will be discussed in Section 4.5.

4.4 Summarising Remarks

1) A combined electrophoresis/particle counting cell was developed in order to allow the preparation and observation of butanol dispersions in absolute isolation from atmospheric contamination.

2) The lack of information relating to dispersions in semi-polar media necessitated wide ranging investigation of the colloidal systems involved.

3) Electrophoresis results indicated that proton transfer was the fundamental charging mechanism of the dispersions studied. Water has been shown to have no major effects on the systems other than those resulting from its relative acidity with respect to butanol.

4) Stability has been related to the magnitude of the zeta potential and to the electrolyte concentration. Theoretically predicted stabilities using DLVO theory agreed with those observed experimentally for Graphon dispersions but differed significantly from those for dispersions of Polystyrene.

5) Mutual flocculation was studied and similar qualitative trends to those found for aqueous systems were observed.

6) Results indicating that the electrodynamic interaction between PTFE and Graphon is one of repulsion have been presented.

4.5 Suggestions for Future Work

Remarkably few investigations of the properties of dispersions in semi-polar media have been reported in the literature. A survey of the characteristics of dispersion stability in one alcohol, butanol, has been conducted. The work reported here may be regarded both as a source of ideas and as a framework on which future work may be based.

Ideas for future investigations which have been generated by this work fall into four broad categories.

a) Colloidal studies in butanol.

b) Colloidal studies in alcohols.

c) Mutual flocculation.

d) Van der Waals interactions between carbon and PTFE.

a) A vast number of properties of dispersions in butanol still require investigation. Perhaps of most interest and relevance to the work reported in this Thesis would be a study of the charging mechanism of the Graphon/butanol interface. If the charge were attributable to the formation of a structured alcohol layer then the magnitude of the electrical potential would be temperature dependent since increasing temperature would increase the degree of disorder in the interfacial region.

The use of a number of samples from different batches of Graphon would indicate whether the particle charge results from impurities on the carbon surface.

b) According to Findenegg[97-99] the degree of hydrogen bonded structuring at the carbon interface at any temperature is, to a first approximation, a function of the chain length of the alcohol. Study of a range of alcohols would not only provide information on the charging mechanism of Graphon but would also provide an insight to the effects of permittivity and viscosity changes on dispersion properties.

c) The major controlling factor in mutual flocculation is almost certainly the "thickness" of the double layer. However the significance of variations in particle size and electrical potential are not clearly understood. Extensive investigations of these factors are essential if a grasp of the principles involved in this very important colloidal phenomenon is to be attained. In order to simplify the experimental technique it is probably advisable that these investigations are, at least in the preliminary stages, confined to aqueous systems.

d) Theoretically the van der Waals interaction of PTFE with materials of high permittivity, such as carbon, is repulsive in certain media. Experimentally this has not yet been conclusively demonstrated.

The work in this Thesis describes an attempt to use a heteroflocculating colloidal system to illustrate this phenomenon. The fundamental disadvantage inherent in the colloidal technique is the unavailability of PTFE particles which are both large enough to be detectable using an ultramicroscope but small enough to remain in suspension. Research into the preparation of PTFE dispersions is therefore an important aspect in the extension of this work.

The rotating disk method has been successfully applied to studies of the heterocoagulation process.[154-156] The examination of disks exhibiting either Graphon or PTFE faces, which have been rotated in butanol dispersions of the other material may yield information on the sign and magnitude of the van der Waals interaction.

By monitoring the degree of removal of carbon particles from a cellophane film on the inner of two rotating concentric cylinders, Visser[157] has measured the forces of adhesion between carbon blacks and cellophane in an aqueous solution. Substitution of the medium for butanol and the cellophane for PTFE would enable this technique to be used to measure the forces of adhesion between PTFE and Graphon in butanol.

The most conclusive evidence of the nature of the van der Waals interaction between PTFE and carbon would be obtained by direct measurement. Such measurements have been made by Tabor and Winterton[158,159] to evaluate the force of attraction between two molecularly smooth mica plates. The extension of their technique for a PTFE/butanol/carbon system, although theoretically desirable would be experimentally very difficult.

REFERENCES

1) G. Gouy, J.Phys., 1910, 9, 457.

2) D.L. Chapman, Phil.Mag., 1913, 25, 475.

3) I. Langmuir, J.Chem.Phys., 1938, 6, 873.

4) S. Levine, Proc.Roy.Soc., 1935, A170, 145, 165
J. Chem.Phys., 1939, 7, 831.

5) S. Levine and G.P. Dube, Trans. Faraday Soc., 1939, 35, 1125, 1141.

6) B.V. Derjaguin and L.D. Landau, Acta Physicochim, U.R.S.S., 1941, 14, 633.

7) E.J.W. Verwey and J.Th.G. Overbeek, Theory of the Stability of Lyophobic Colloids, (Elsevier, Amsterdam, 1948).

8) D.W.J. Osmond, Disc. Faraday Soc., 1966, 42, 247.

9) D. Gingell and V.A. Parsegian, J.Theor.Biol, 1972, 36, 41.

10) B.W. Ninham and V.A. Parsegian, Biophys. J., 1970, 10, p.646.

11) P. Richmond and B.W. Ninham, J.Colloid Interface Sci, 1972, 40, 406.

12) I.M. Lifshitz, Sov.Phys, J.E.T.P.2, 1956, 73.

13) M. Faraday, Phil.Trans., 1857, 147, 145.

14) T. Graham, Phil.Trans., 1861, 151, 183.

15) G. Quincke, Poggendorf's Ann, 1861, 113, 513.

16) H. Helmholtz, Ann.Physik, 1879, 7, 337.

17) H. Siedentopf and R. Zsigmondy, Ann.Physik, 1903, 10, 1.

18) Wo. Ostwald, Kolloid-Z, 1907, 1, 291.

19) W.B. Hardy, Z.physik Chem, 1900, 33, 385.

20) F. Powis, Z.physik Chem., 1915, 89, 186.

21) H. Freundlich, Kapillarchemie (Akademische Verlagsgesellschaft, Leipzig, 3rd ed., 1923), p.580; English translation, Colloid and Capillary Chemistry (Dutton, New York, 1926).

22) H. Freundlich, K. Joachimsohn and G. Ettisch, Z. Physik Chem., 1929, A141,249

23) Wo. Ostwald, J.Phys.Chem., 1938, 42, 981.

24) H.C. Hamaker, Physica, 1937, 4, 1058.

25) B.V. Derjaguin, Disc.Faraday Soc., 1966, 42, 319.

26) A. Watillon and A.M. Joseph-Petit, Disc. Faraday Soc., 1966, 42, 143.

27) J.H. Schenkel and J.A. Kitchener, Trans. Faraday Soc., 1960, 56, 161.

28) R.H. Ottewill and J.N. Shaw, Disc. Faraday Soc., 1966, 42, 154.

29) A. Kotera, K. Furusawa and K. Kudo, Kolloid-Z., 1970, 240, 837.

30) G.R. Wiese and T.W. Healy, Trans. Faraday Soc., 1970, 66, 490.

31) B.V. Derjaguin, Disc. Faraday Soc., 1954, 18, 85.

32) O.F. Devereux and P.L. de Bruyn, Interaction of Plane Parallel Double Layers (M.I.T. Press, Cambridge, Mass., 1963).

33) R. Hogg, T.W. Healy and D.W. Fuerstenau, Trans. Faraday Soc., 1966, 62, 1638.

34) A. Kitahara and H. Ushiyama, J. Colloid Interface Sci., 1973, 43, 73.

35) W.D. Cooper, P. Fearon and G.D. Parfitt, 1973, 69, 1261.

36) B.V. Enustun and J. Turkevich, J.Amer.Chem.Soc., 1963, 85, 3317.

37) A. Lottermoser and K. May, Kolloid-Z., 1932, 58, 61.

38) L.H. Princen and M. Devena-Peplinski, J. Colloid Interface Sci. 1964, 19, 786.

39) E. Buckingham, Trans.Am.Electrochem.Soc., 1906, 9, 265.

40) B.C. Soyenkoff, J.Phys.Chem., 1931, 35, 2993.

41) V.R. Damerell and R. Mattson, J.Phys.Chem., 1944, 48, 134.

42) V.R. Damerell and K. Gayer and H. Laudenschlager, J.Phys.Chem., 1945, 49, 436.

43) J.L. van der Minne, Rec.Trav.Chim., 1946, 65, 549.

44) W.J. Moore, Physical Chemistry (Longmans-4th Edition) 358.

45) A. Gemant, J.Phys.Chem., 1939, 43, 743.

46) J.L. van der Minne and P.H.J. Hermanie, J.Colloid Sci., 1952, 7, 600.

47) V.K. La Mer and H.C. Downes, J.Amer.Chem.Soc., 1931, 53, 888.
1933, 55, 1840.

48) R.M. Fuoss, Chem.Revs., 1935, 17, 27.

49) L.E. Strong and C.A. Kraus, J.Amer.Chem.Soc., 1950, 72, 166.

50) J.L. van der Minne and P.H.J. Hermanie, J.Colloid Sci, 1953, 8, 38.

51) L.A. Romo, J.Phys.Chem., 1963, 67, 386.

52) L.A. Romo, Discuss.Faraday Soc., 1966, 42, 232.

53) D.N.L. McGown, G.D. Parfitt and E. Willis, J.Colloid Sci., 1965, 20, 650.

54) K.E. Lewis and G.D. Parfitt, Trans Faraday Soc., 1966, 62, 1652.

55) D.N.L. McGown and G.D. Parfitt, Discuss. Faraday Soc., 1966, 42, 225.

56) F.M. Fowkes, Discuss.Faraday Soc., 1966, 42, 243.

57) F.W. Meadus, I.E. Puddington, A.F. Sirianni and B.D.Sparks, J.Colloid Interface Sci., 1969, 30, 46.

58) B.V. Derjaguin, Discuss.Faraday Soc., 1966, 42, 318.

59) A. Sanfeld, C. Devillez and P.J. Terlinck, J.Colloid Interface Sci., 1970, 32, 33.

60) A. Sanfeld, C. Devillez and S. Wahrmann, J.Colloid Interface Sci., 1971, 36, 359.

60) W.D. Cooper and P. Wright, J. Colloid Interface Sci., 1976, 54, 28.

61) A. Kitahara, S. Karasawa and H. Yamada, J.Colloid Interface Sci., 1967, 25, 490.

62) G.D. Parfitt, J.A. Wood, and R.T. Ball, J.C.S. Faraday Trans. I, 1973, 69, 1908.

63) J.C. Maxwell, A. Treatise on Electricity and Magnetism, 1873 (Macmillan, London) Vol 1, 247.

64) O. Griot, Trans Faraday Soc., 1966, 62, 2904.

65) F.J. Micale, Y.K. Lui and A.C. Zettlemoyer, Discuss Faraday Soc., 1966, 42, 238.

66) S. Yoshizawa, N. Watanabe, I. Tari, Denki Kagaku Oyobi Kogyo Butsuri Kataku 1969, 37, 575.

67) J. Lyklema, Adv. Colloid Interface Sci., 1968, 2, 65.

68) F.M. Fowkes, Discuss Faraday Soc., 1966, 42, 246.

69) E.J.W. Verwey, Rec.Trav.Chim., 1941, 60, 625.

70) P. Jackson and G.D. Parfitt, Kolloid-Z, 1971, 244, 240.

71) V.R. Damerell and A. Urbanic, J.Phys.Chem., 1944, 48, 125.

72) M. van der Waarden, J.Colloid Sci., 1950, 5, 317.

73) E.L. Mackor, J.Colloid Sci., 1951, 6, 492.

74) E.L. Mackor and J.H. van der Waals, J.Colloid Sci., 1952, 7, 535.

75) M.J. Vold, J.Colloid Sci., 1961, 16, 1.

76) E.J. Clayfield and E.C. Lumb, J.Colloid Interface Sci., 1966, 22, 269, 285.

77) E.W. Fischer, Kolloid-Z., 1958, 160, 120.

78) D.J. Meier, J.Phys.Chem., 1967, 71, 1861.

79) F.Th.Hesselink, J.Phys.Chem., 1969, 73, 3488.

80) F.Th.Hesselink, J.Phys.Chem., 1971, 75, 65.

81) F.Th.Hesselink, A. Vrij and J.Th.G. Overbeek, J.Phys.Chem., 1971, 75, 2094.

82) R.H. Ottewill and T. Walker, Kolloid-Z, 1968, 227, 108.

83) D.M. Andrews, E.D. Manev, and D.A. Haydon, Special Discuss.Faraday Soc., 1970, 1, 46.

84) D.H. Napper, Trans.Faraday Soc., 1968, 64, 1701.

85) R. Evans and D.H.Napper, Kolloid-Z., 1973, 251, 409.

86) D.H. Napper, J.Colloid Interface Sci., 1970, 32, 106.

87) D.H. Napper, J.Colloid Interface Sci., 1970, 33, 384.

88) D.H. Napper and A. Netschey, J.Colloid Interface Sci., 1971, 37, 528.

89) V.K. Dunn and R.D. Vold, J.Colloid Interface Sci, 1976, 54, 22.

90) A. Kitahara, M. Hoshino, T. Fujii, N. Yoshino and T. Yoshino, Kogyo Kaguku Zasshi, 1970, 73, 2081.

91) B. Vincent, Colloid Science, Volume 1, Specialist Periodical Report, (Chemical Society, London, 1973).

92) G.D. Parfitt and E. Willis, J.Colloid Interface Sci., 1966, 22, 100.

93) P. Bagchi and R.D. Vold, J.Colloid Interface Sci., 1970, 33, 405.

94) S.G. Lawrence and G.D. Parfitt, J.Colloid Interface Sci., 1971, 35, 675.

95) H.M. Smith and I.E. Puddington, Canadian J.Chem., 1960, 38, 1911.

96) H.R. Kruyt and F.G. van Selms, Rec.Trav.Chim., 1943, 62, 407, 415.

97) G.H. Findenegg, J.Colloid Interface Sci. (1971), 35, 249.

98) G.H. Findenegg, J.Chem.Soc.Faraday Trans I, 1972, 68, 1799.

99) G.H. Findenegg, J.Chem.Soc.Faraday Trans.I., 1973, 69, 1069.

100) E.M. Breshchenko, Khim.Tech.Topl.Masel. 1957, 9, 32.

101) A.J. Groszek, Proc.Roy.Soc.A. 1970, 314, 73.

102) R.H. Ottewill and B. Vincent, J.Chem.Soc.Faraday Trans. 1, 1972, 68, 1533.

103) O. Stern, Z. Electrochem., 1924, 30, 508.

104) D.C. Grahame, Chem. Revs., 1947, 41, 441.

105) G.M. Bell, S. Levine and L.N. McCartney, Jour.Colloid Interface Sci., 1970, 33, 335.

106) A. Bierman, J.Colloid Sci., 1955, 10, 231.

107) J.N. Israelachvili and D. Tabor, Prog.Surf.Memb.Sci., 1973, 7, 1.

108) J. Gregory, Adv.Colloid Interface Sci., 1969, 2, 396.

109) J. Visser, Adv. Colloid Interface Sci., 1972, 3, 331.

110) V.A. Parsegian, Physical Chemistry: Enriching Topics from Colloid and Surface Sci., 1975, Ed. H. van Olphen and K.J. Mysels, Theorex, California.

111) P. Richmond, Colloid Science, Vol 2, (Chemical Society publication) 130. 1975

112) J.D. van der Waals, 1873, Ph.D. Thesis, University of Leiden.

113) P. Debye, Phys-Z, 1920, 21, 178.

114) W.H. Keesom, Phys-Z, 1921, 22, 129.

115) S.C. Wang, Phys-Z, 1927, 28, 663.

116) F. London, Z.Phys., 1930, 63, 245.

117) R. Eisenschitz and F. London, Z.Phys., 1930, 60, 491.

118) J.C. Slater and J.G. Kirkwood, Phys.Rev., 1931, 37, 682.

119) E.A. Moelwyn-Hughes, Physical Chemistry 2nd Edn., 393.

120) H. Voellmy, Z. Phys. Chem., 1927, 127, 305.

121) H.B.G. Casimir and D. Polder, Phys.Rev., 1948, 73, 360.

122) G.C. Peterson, Personal communication.

123) D. Gingell and V.A. Parsegian, J.Colloid Interface Sci., 1973, 44, 456.

124) M. von Smoluchowski, Physik Z., 1916, 17, 557, 585.
Z. Phys.Chem., 1917, 92, 129.

125) N. Fuchs, Z.Physik, 1934, 89, 736.

126) D.N.L. McGown and G.D. Parfitt, J.Phys.Chem., 1967, 71, 449.

127) L.A. Spielman, J.Colloid Interface Sci., 1970, 33, 562.

128) M. Stimson and G.B. Jeffery, Proc.Roy.Soc., 1926, A111, 110.

129) J. Happel and H. Brenner, Low Reynolds Number Hydrodynamics (Prentice Hall, Englewood Cliffs, New Jersey, 1965).

130) H.V. Venkatassetty and G.H. Brown, J.Phys.Chem., 1962, 66, 2075.

131) P.A. Hiltner, Y.S. Papir and I.M. Krieger, J.Phys.Chem., 1971, 75, 1881.

132) K. Fischer, Angew.Chem., 1935, 48, 384.

133) D. Rivin, Paper presented at the Fourth Rubber Technology Conference, London, 1962 - Carbon Black Surface Chemistry.

134) S. Komagata, J.Electrochem Soc. Japan, 1933, 1, 97.

135) M. von Smoluchowski, Handbuch der Elektrizitatat und des Magnetismus, vol 2, page 366, Leipzig, Germany (1914).

136) E. Huckel, Phys.Z, 1924, 25, 204.

137) D.C. Henry, Proc.Roy.Soc., 1931, A133, 106.

138) J.Th.G. Overbeek, Adv. in Colloid Sci., 1950, 3, 97.
Kolloid Chem.Beih., 1943, 54, 287.

139) F. Booth, Nature, Lond., 1948, 161, 83.
Proc. Roy.Soc., 1950, A203, 514.

140) P.H. Wiersema, A.L. Loeb and J.Th.G. Overbeek, J.Colloid Interface Sci., 1966, 22, 78.

141) J. Lyklema and J.Th.G. Overbeek, J.Colloid Sci., 1961, 16, 501.

142) R.J. Hunter, J.Colloid Interface Sci., 1966, 22, 231.

143) D. Stigter, J.Phys.Chem., 1964, 68, 3600.

144) L.S. Levitt and B.W. Levitt, J.Phys.Chem., 1970, 74, 1812.

145) E.L. Mackor, Rec.Trav.Chim., 1951, 70, 747, 763.

146) J.N. Brönsted and J.E. Vance, Z.Phys.Chem., 1932, AbtA, 163, 240.

147) A.M. Shkodin, L.P. Sadovnichaya and V.A. Podolyanko, Elektrokhimiya, 1968, 4, 718.

148) S. Arrhenius, Z.Phys.Chem., 1887, 1, 631.

149) The International Encyclopedia of Physical Chemistry, 4/15, King 32-34.

150) Program borrowed from Dr. B.M. Lowe, Chemistry Dept., University of Edinburgh, West Mains Road, Edinburgh.

151) J.Th.G. Overbeek, Colloid Science 1 (H.R. Kruyt, Elsevier Publishing Company), 226.

152) R.J. Hunter and H.J.L. Wright, J.Colloid Interface Sci., 1971, 37, 564.

153) J.T. Webb, P.D.Bhatnagar and D.G. Williams, J.Colloid Interface Sci., 1974, 49, 346.

154) J.K. Marshall and J.A. Kitchener, J.Colloid Interface Sci., 1966, 22, 342.

155) M. Hull and J.A. Kitchener, Trans.Faraday Soc.,1969, 65, 3093.

156) G.E. Clint, J.H. Clint, J.M. Corkill and T. Walker, J.Colloid Interface Sci., 1973, 44, 121.

157) J. Visser, J.Colloid Interface Sci., 1970, 34, 26.

158) D. Tabor and R.H.S. Winterton, Nature, 1968, 219, 1120.

159) D. Tabor and R.H.S. Winterton, Proc.Roy.Soc., 1969, A132, 435.

Appendix 1

The Debye-Lorentz expression to calculate $\varepsilon(i\xi)$ is

$$\varepsilon(i\xi) = 1 + \sum_{mw} \frac{c_{mw}}{1 + \xi/\omega_{mw}} + \sum_{i} \frac{c_j}{1 + (\xi/\omega_j)^2}$$

The frequencies ω_{mw} and ω_j are the relaxation frequencies associated with dipolar rotation and electronic and molecular vibrations, and the coefficients c_{mw} and c_j are the associated oscillator strengths.

Garg and Smyth [a] have measured values of the dielectric constant and dielectric loss (ε' and ε'') of butanol as a function of frequency at 293 K. Analysis of the data indicates that butanol undergoes three different relaxations within the microwave region. The frequencies (ω_{mw}) of these are given as

$$\omega_{mw}(1) = 1.49 \times 10^{9} \text{ rad } s^{-1}$$
$$\omega_{mw}(2) = 3.7 \times 10^{10} \text{ rad } s^{-1}$$
$$\omega_{mw}(3) = 4.2 \times 10^{11} \text{ rad } s^{-1}$$

Cole's method of linear plotting in which $\varepsilon''X$ and ε''/X are plotted against ε' was used to calculate the limits of the three dispersion regions. The parameter X is defined as λ_c/λ where λ_c is the characteristic wave length given by $\lambda_c = 2\pi c/\omega_{mw}$ and c is the speed of light. From the intercepts with the abscissa the values of ε' when ε'' is zero are obtained. These correspond to the limits of each relaxation and for butanol are given by

$$\varepsilon_1 = 17.7; \quad \varepsilon_2 = 4.75; \quad \varepsilon_3 = 3.06; \quad \varepsilon_4 = 2.32$$

From these the values of the oscillator strengths may be calculated as

$$c_{mw}(1) = \varepsilon_1 - \varepsilon_2 = 12.95$$
$$c_{mw}(2) = \varepsilon_2 - \varepsilon_3 = 1.69$$
$$c_{mw}(3) = \varepsilon_3 - \varepsilon_4 = 0.74$$

As there was some uncertainty in the exact values of the intercepts it was necessary to check the calculated values of c_{mw}. For Debye relaxation

$$\varepsilon(\omega) = \varepsilon'(\omega) - i\varepsilon''(\omega) = 1 + \sum_{mw} \frac{c_{mw}}{1 - i\omega/\omega_{mw}}$$

Multiply by $\dfrac{(1 + i\omega/\omega_{mw})}{(1 + i\omega/\omega_{mw})}$

$$= 1 + \sum_{mw} \frac{c_{mw}(1 + i\omega/\omega_{mw})}{1 + \omega^2/\omega^2_{mw}}$$

$$= 1 + \sum_{mw} \frac{c_{mw}}{(1 + \omega^2/\omega^2_{mw})} + \sum_{mw} \frac{c_{mw}(i\omega/\omega_{mw})}{1 + \omega^2/\omega^2_{mw}}$$

$\therefore$ $$\varepsilon' = 1 + \sum_{mw} \frac{c_{mw}}{(1 + \omega^2/\omega^2_{mw})}$$

$$\varepsilon'' = 1 + \sum_{mw} \frac{c_{mw}(\omega/\omega_{mw})}{(1 + \omega^2/\omega^2_{mw})}$$

It was therefore possible to compare the experimental results of Garg and Smyth with those predicted from these expressions using the calculated parameters. Deviations between experimental and theoretical values of ε' and ε'' were minimised by modification of the parameters, c_{mw} and ω_{mw}. It was found that the best agreement was obtained using the following values.

$c_{mw}(1) = 12.95$; $\omega_{mw}(1) = 1.49 \times 10^{9}$ rad s^{-1}

$c_{mw}(2) = 1.69$; $\omega_{mw}(2) = 4.05 \times 10^{10}$ rad s^{-1}

$c_{mw}(3) = 0.79$; $\omega_{mw}(3) = 4.2 \times 10^{11}$ rad s^{-1}

The oscillator strength for the I.R. regions was calculated from

$$C_{IR} = \varepsilon'_4 - n_o^2 = 2.27 - (1.399)^2 = 0.31$$

where ε'_4 is the modified limit of the third dispersion region in the microwave and n_o is the refractive index in the visible region. Butanol has four main absorptions in the IR region at (6.1, 5.5, 2.7 and 2.1) x 10^{14} rad s^{-1}. These have been averaged to give $\omega_{IR} = 4.1 \times 10^{14}$ rad s^{-1}. Ninham and Parsegian [b] have demonstrated that the calculation is relatively insensitive to this averaging technique for a water/hydrocarbon system. Similarly, in this case, particularly since the value of c_{IR} is so small, the use of an average value of ω_{IR} will have little effect.

The oscillator strength for the UV region is given by $C_{UV} = n_D^2 - 1 = 0.96$.

It is common to approximate ω_{UV} to the first ionisation potential, which, for butanol is $\sim$ 10 eV. This corresponds to a value of

$$\omega_{UV} = 1.6 \times 10^{-6} \text{ rad } s^{-1}$$

References

a) S.K. Garg and C.P. Smyth, J.Phys.Chem., 1965, 69, 1294.

b) B.W. Ninham and V.A. Parsegian, Biophysical Journal, 1970, 10, 646.

Appendix 2

A computer program (POLYFIT) has been used to fit the calculated Hamaker functions to a curve described by a series of polynomials of the form,

$$A = a + bl + cl^2 + dl^3 + el^4 + fl^5 + gl^6$$

where A is the Hamaker function,

l is the interparticle separation

a,b,c etc. are the polynomial coefficients.

The coefficients for the various functions used as given below.

Fig 2.2.7 Graphon/Butanol/Polystyrene

ε_o (Graphon) = 100

$0 - 1 \times 10^{-9}$ m, $A = 3.08 \times 10^{-20}$ J

Range	1×10^{-9}m-1×10^{-8}m	1×10^{-8}m-1×10^{-7}m	1×10^{-7}m-1×10^{-6}m
a	$+0.316 \times 10^{-19}$	$+0.322 \times 10^{-19}$	$+0.955 \times 10^{-20}$
b	-0.245×10^{-12}	-0.155×10^{-11}	-0.101×10^{-12}
c	-0.708×10^{-3}	$+0.406 \times 10^{-4}$	$+0.496 \times 10^{-6}$
d	$+0.242 \times 10^{6}$	-0.592×10^{3}	-0.129×10^{1}
e	-0.427×10^{14}	$+0.439 \times 10^{10}$	$+0.182 \times 10^{7}$
f	$+0.372 \times 10^{22}$	-0.128×10^{17}	-0.130×10^{13}
g	-0.125×10^{30}	0	$+0.366 \times 10^{18}$

Fig 2.2.8 Graphon/Butanol/Graphon

Fig 2.2.11 Graphon/Butanol/Graphon in 10^{-3} mol dm^{-3} LiCl

ε_o (Graphon) = 100

0 - 1 x 10^{-9} m, A = 12 x 10^{-20} J

	$1x10^{-9}m-1x10^{-8}m$	$1x10^{-8}m-1x10^{-7}m$	$1x10^{-7}-5x10^{-7}m$
a	$+0.124 \times 10^{-18}$	$+0.125 \times 10^{-18}$	$+0.637 \times 10^{-19}$
b	-0.357×10^{-11}	-0.444×10^{-11}	-0.669×10^{-12}
c	$+0.189 \times 10^{-4}$	$+0.111 \times 10^{-3}$	$+0.385 \times 10^{-5}$
d	0	-0.168×10^{4}	-0.120×10^{2}
e	0	$+0.132 \times 10^{11}$	$+0.187 \times 10^{8}$
f	0	-0.414×10^{17}	-0.114×10^{14}
g	0	0	0

Fig 2.2.9 Graphon/Butanol/PTFE in 2 x 10^{-5} mol dm^{-3} LiCl

ε_o (Graphon) = 100

0 - 1 x 10^{-9} m A = -0.75×10^{-21} J

	$1x10^{-9}m-6.5x10^{-8}m$	$6.5x10^{-8}m-5x10^{-7}m$
a	-0.937×10^{-21}	-0.222×10^{-21}
b	$+0.191 \times 10^{-13}$	$+0.156 \times 10^{-13}$
c	-0.935×10^{-7}	-0.325×10^{-6}
d	0	$+0.237 \times 10$
e	0	-0.758×10^{7}
f	0	$+0.105 \times 10^{14}$
g	0	-0.501×10^{19}

Graphon/Butanol/PTFE in 10^{-4} mol dm^{-3} LiCl

	$1x10^{-9}m$-$2x10^{-8}m$	$2\ x10^{-8}m$-$6.5x10^{-8}m$	$6.5x10^{-8}$-$5x10^{-7}m$
a	-0.969×10^{-21}	-0.439×10^{-20}	-0.222×10^{-21}
b	$+0.271 \times 10^{-12}$	$+0.569 \times 10^{-12}$	$+0.156 \times 10^{-13}$
c	-0.763×10^{-4}	-0.309×10^{-4}	-0.325×10^{-6}
d	$+0.112 \times 10^{5}$	$+0.900 \times 10^{3}$	$+0.237 \times 10$
e	-0.816×10^{12}	-0.144×10^{11}	-0.758×10^{7}
f	$+0.283 \times 10^{20}$	$+0.120 \times 10^{18}$	$+0.105 \times 10^{14}$
g	-0.375×10^{27}	-0.398×10^{24}	-0.501×10^{19}

Fig 2.2.10 Graphon/Butanol/Polystyrene in 2×10^{-3} LiCl

ε_o (Graphon) = 100

$0 - 1 \times 10^{-9}$ m $A = 3.2 \times 10^{-20}$ J

	$1x10^{-9}m$-$1x10^{-8}m$	$1x10^{-8}m$-$1x10^{-7}m$	$1x10^{-7}m$-$1x10^{-6}m$
a	$+0.328 \times 10^{-19}$	$+0.334 \times 10^{-19}$	$+0.945 \times 10^{-20}$
b	-0.245×10^{-12}	-0.155×10^{-11}	-0.101×10^{-12}
c	-0.708×10^{-3}	$+0.406 \times 10^{-4}$	$+0.496 \times 10^{-6}$
d	$+0.242 \times 10^{6}$	-0.592×10^{3}	-0.129×10
e	-0.427×10^{14}	$+0.439 \times 10^{10}$	$+0.182 \times 10^{7}$
f	$+0.372 \times 10^{22}$	-0.128×10^{17}	-0.130×10^{-3}
g	-0.124×10^{30}	0	$+0.366 \times 10^{18}$

Fig 2.2.12 Polystyrene/Butanol/Polystyrene

$o - 1 \times 10^{-9}$ m $A = 12.4 \times 10^{-21}$ J

	$1x10^{-9}$m - $3x10^{-8}$m	$2.5x10^{-8}$m-$1x10^{-7}$m	$1x10^{-7}$m-$5x10^{-7}$m
a	$+0.131 \times 10^{-19}$	$+0.106 \times 10^{-19}$	$+0.256 \times 10^{-20}$
b	-0.537×10^{-12}	-0.359×10^{-12}	-0.130×10^{-14}
c	$+0.835 \times 10^{-5}$	$+0.667 \times 10^{-5}$	o
d	o	-0.579×10^{2}	o
e	o	$+0.189 \times 10^{9}$	o
f	o	o	o
g	o	o	o

Fig 2.2.13 Polystyrene/Butanol/Polystyrene in 10^{-2} mol dm^{-3}LiCl

$o - 1 \times 10^{-9}$ m $A = 12.4 \times 10^{-21}$ J

	$1x10^{-9}$m-$1x10^{-8}$m	$1x10^{-8}$m-$7.5x10^{-8}$m
a	$+0.127 \times 10^{-19}$	$+0.130 \times 10^{-19}$
b	$+0.111 \times 10^{-12}$	-0.998×10^{-12}
c	-0.524×10^{-3}	$+0.450 \times 10^{-4}$
d	$+0.117 \times 10^{6}$	-0.121×10^{4}
e	-0.112×10^{14}	$+0.184 \times 10^{11}$
f	$+0.397 \times 10^{21}$	-0.144×10^{18}
g	o	$+0.445 \times 10^{24}$

Appendix 3

Computer Programs

SALTHAM 1 is one of three similar programs to calculate Hamaker functions, differing from each other in the method used to evaluate $(i\xi)$; viz., the Debye-Lorentz method for both particles, the Kramers-Kronig method for both particles or the Debye-Lorentz method for one particle and the Kramers-Kronig method for the other. In the program given here the third approach is used.

POLYFIT. A small program which utilises a NAG(AØ2ABF) subroutine to fit Hamaker functions to curves described by simple polynomials.

WHAMSP. This program calculates stability ratios and potential energy curves for the interaction of two spherical colloidal particles. It incorporates the Spielman Hydrodynamic correction (obtained as a subroutine from Dr. G.C. Peterson; Unilever Ltd.). Hamaker functions are calculated from the polynomial data generated by POLYFIT.

(WHAMSP)

```
C      CALCULATION OF P.E. CURVES AND STABILITY RATIO FOR COLLOIDAL
C            DISPERSIONS USING A LIFSHITZ HAMAKER FUNCTION
C            AND THE SPIELMAN DIFFUSION CORRECTION SUBRUTINE
       DIMENSION P(7),PP(7),PPP(7)
       INTEGER I,J,M,K,IT,TI
       DOUBLE PRECISION E1,L1,L2,A1,A2,A21,KA,X,Y,Z,A,B,C,S1,S2
      1,EE,KT,PS3,PS4,PS1,PS2,EC,APM,E,G,SUM,SUM1,VR1,AA,AB,AC,VA,VR,E3,
      9VB(5),VS(5),VU(5),HA(5),W,WW,E2,AD,AE,AF,STEP,STEP1,VRPS,VRSIG,
      4BB,YO,EP,SA,SB,XD,APMIN
       JJJ=1
       JJ=1
       WRITE(6,176)
  176  FORMAT(' ','DO YOU WANT VA VR VT DATA Y=1 N=2 ')
       READ,IT
       IF(IT.EQ.1.0)GOTO 1822
       WRITE(6,183)
  183  FORMAT(' ','DO YOU WANT A AS FUNC OF DIST Y=1,N=2 ')
       READ,TI
  1822 TI=2
        GOTO 182
  182   WRITE(6,177)
   177 FORMAT(' ','DIELECTRIC CONST.,EPS,.001 ')
       READ,E,EP
       WRITE(6,184)
   184 FORMAT(' ','SPLT1,SPLT2,UPPER LIMIT,APMAX,APMIN ')
       READ,SPLT1,SPLT2,UPPER,APMAX,APMIN
       WRITE(6,178)
   178 FORMAT(' ','7 POLYNOMIAL COEFS TO DESCRIBE HAM FUNC ')
       READ,P
       WRITE(6,178)
       READ,PP
       WRITE(6,178)
       READ,PPP
       WRITE(6,179)
   179 FORMAT(' ','RADIUS OF PARTICLE 2 ')
    10 READ,A2
       JJJ=JJJ+1
       IF(A2.GT.9999.)GOTO 29
       WRITE(6,180)
   180 FORMAT(' ','RATIO A2 TO A1,KAPPA ')
       READ,A21,KA
       I=0
       J=0
       H=0
       A1=A2/A21
       WRITE(6,200)A1,A2
       G=0.25*(A1+A2)
   200 FORMAT('-','PTCLE RAD 1= ',E9.2,'M,PTCLE RAD 2= ',E9.2,'M ')
       WRITE(6,203)APMAX,E,KA
   203 FORMAT(' ','A= ',E7.1,'J,D= ',F4.1,'KA= ',E9.1)
       WRITE(6,181)
   181 FORMAT(' ','CONST. POT.=1,CONST. CHARGE=2,WAIT,2POTS ')
       READ,M
       GOTO (1,2,3,4),M
     1 WRITE(6,300)
   300 FORMAT('0','CONSTANT POTENTIAL ON A1 AND A2 ')
```

WHAMSP CONTINUED

```
      GOTO 5
    2 WRITE(6,301)
  301 FORMAT('0','CONSTANT CHARGE ON A1 AND A2')
      GOTO 5
    3 WRITE(6,302)
  302 FORMAT('0','CONSTANT POTENTIAL ON A1 AND CHARGE ON A2')
      GOTO 5
    4 WRITE(6,303)
  303 FORMAT('0','CONSTANT CHARGE ON A1 AND POTENTIAL ON A2')
    5 GOTO (128,128,130,131),M
  128 READ,PS1,PS2
      WRITE(6,600)PS1,PS2
  600 FORMAT('0','PS1= ',E15.3,'PS2= ',E15.3)
      GOTO 132
  130 READ,PS1,S2
      WRITE(6,601)PS1,S2
  601 FORMAT('0','PS1= ',E15.3,'S2= ',E15.3)
      GOTO 132
  131 READ,PS2,S1
      WRITE(6,602)PS2,S1
  602 FORMAT('0','PS2= ',E15.3,'S1= ',E15.3)
  132 KT=4.114E-21
      EE=E*1.112D-10
      EC=1.602D-19
      SUM=1./6.
      SUM1=1./6.
      IF(IT.GT.1)GOTO 193
      WRITE(6,201)
  201 FORMAT('0','     VA        VR        VT        H        VA
     1        VR        VT        H        VA        VR        VT
     1     H')
  193  CONTINUE
      GOTO 501
  502 PS1=PS1/(1.D3)
      PS2=PS2/(1.D3)
  501 IF(H-G)11,12,12
   11 H=H+G/500.
      IF(H.GT.37./KA)GOTO 400
      GOTO 150
   12 H=H+G/25.
      IF(H.GT.37./KA)GOTO 400
  150 A=DEXP(2.*KA*H)
      GOTO 401
  400 A=EXP(74.)
  401 B=1./A
      C=1./(A-B)
      X=88./(7.*EE*KA)
      Y=A+B
      Z=A-B
      GOTO (116,116,117,118),M
  116 PS1=PS1/(1.D3)
      PS2=PS2/(1.D3)
      GOTO 503
  119 PS1=X*(2.*S2/Z+S1*Y/Z)
      PS2=X*(2.*S1/Z+S2*Y/Z)
      GOTO 503
  117 PS2=(Z*S2*X+2.*PS1)/Y
```

WHAMSP CONTINUED

```
      PS1=PS1/(1.D3)
      PS2=PS2/(1.D3)
      GOTO 503
  118 PS1=(Z*S1*X+2.*PS2)/Y
      PS1=PS1/(1.D3)
      PS2=PS2/(1.D3)
  503 PS3=PS1*PS1+PS2*PS2
      PS4=2.*PS1*PS2
      VR1=EE*A1*A2*PS3/(4.*(A1+A2))
      AA=2.*A1*A2
      AB=(2.*(A1+A2)+H)*H
      AC=AA+AA+AB
C       CALC OF HAMAKER FUNCTION
      IF(H.GT.1E-8)GOTO 778
      IF(JJ.LT.10)GOTO 777
      JJ=1
  777 CONTINUE
      GOTO 779
  778 IF(JJ.LT.100)GOTO 779
      JJ=1
  779  IF(H.LT.1E-9)GOTO 656
      IF(H.LT.UPPER)GOTO 659
      APM=APMIN
      GOTO 658
  659 IF(H.LT.SPLT1)GOTO 654
      IF(H.LT.SPLT2)GOTO 660
      GOTO 661
  654 APM=P(1)+P(2)*H+P(3)*H**2+P(4)*H**3+P(5)*H**4+P(6)*H**5
     1       +P(7)*H**6
      GOTO 658
  660 APM=PP(1)+PP(2)*H+PP(3)*H**2+PP(4)*H**3
     1  +PP(5)*H**4+PP(6)*H**5+PP(7)*H**6
      GOTO 658
  661 APM=PPP(1)+PPP(2)*H+PPP(3)*H**2+PPP(4)*H**3+PPP(5)*H**4
     1  +PPP(6)*H**5+PPP(7)*H**7
      GOTO 658
  656 APM=APMAX
  658 IF(TI.EQ.1)GOTO 657
      GOTO 655
  657  IF(JJ.GT.I)GOTO 655
      IF(JJJ.GT.2)GOTO 655
      WRITE(6,186)H,APM
  186 FORMAT(' ',2E14.6)
  655 CONTINUE
      JJ=JJ+1
      APM=-APM/6.0
      VA=APM*(AA/AB+AA/AC+DLOG(AB/AC))
      IF(H-150./KA)14,15,15
   14 E1=1./DEXP(KA*H)
      GOTO 16
   15 E1=1.E-65
   16 L1=DLOG(1.+E1)
      L2=DLOG(1.-E1)
      GOTO(504,505,504,504),M
  504 VRPS=VR1*((PS4/PS3)*(L1-L2)+L1+L2)
      VR=VRPS/KT
```

WHAMSP CONTINUED

```
      GOTO 506
  505 YO=EC*PS1/KT
      BB=DSQRT(1.+YO*YO/((DSINH(KA*H/2.))**2))
      VRSIG=(KA*EE*(KT/(EC))**2)*(2.*YO*DLOG(BB+YO*DCOSH(KA*H/2.DO)
     8/DSINH(KA*H/2.DO))/(1.+YO))-DLOG(YO*YO+DCOSH(KA*H)+BB*DSINH(KA*H)
     9+KA*H)
      VR=VRSIG/KT
  506 VA=VA/KT
      VT=VA+VR
      IF(ABS(VT)-90.)17,18,18
   17 E2=EXP(VT)
      GOTO 19
   18 E2=1.E-25
   19 IF(DABS(VA)-9.0D1)20,21,21
   20 E3=DEXP(VA)
      GOTO 22
   21 E3=1.E-25
   22 IF(H-G)23,24,24
   23 AD=G/500.
      GOTO 25
   24 AD=G/25.
   25 AE=A1+A2+H
      SA=H/A1
      SB=1.00+A21+SA
      XD=DSPIEL(SB,A21,EP)
      AF=AD*(A1+A2)*XD/(2.*AE*AE)
C     CALCULATION OF STABILITY RATIO
      STEP=AF*E2
      STEP1=AF*E3
      SUM=SUM+STEP
      SUM1=SUM1+STEP1
      IF(I-5)30,31,31
   31 IF(H-500.D-10)32,26,26
   32 IF(DABS(VR)-1000.)33,34,34
   34 IF(VR.GT.0.0)GOTO 50
      VR=-1000.
      GOTO 33
   50 VR=1000.
   33 IF(DABS(VA)-1.0D3)35,36,36
   36 VA=-1000.
   35 IF(ABS(VT)-1000.)37,38,38
   38 VT=1000.
   37 J=J+1
      H=H*1.D10
      VB(J)=VA
      VS(J)=VR
      VU(J)=VT
      HA(J)=H
      IF(J-4)39,40,40
   40   IF(IT.GT.1)GOTO 333
      WRITE(6,202)(VB(JA),VS(JA),VU(JA),HA(JA),JA=1,J)
  202 FORMAT(' ',4(3F8.1,F6.1))
  333 CONTINUE
      J=0
      GOTO 39
   39 I=0
```

WHAMSP CONTINUED

```
      H=H*1.D-10
   30 I=I+1
   26 PS1=PS1*1.D3
      PS2=PS2*1.D3
      IF(H-(A1+A2))501,28,28
   28 W=SUM/SUM1
      APM=-APM*6.
      WW=DLOG10(W)
      WRITE(6,204)W,WW
  204 FORMAT(' ','W= ',E17.9,'WW= ',E15.3)
      GOTO 10
   29 CONTINUE
      STOP
      END
      REAL FUNCTION DSPIEL*8(S,A21,EPS)
C  THE DOUBLE PRECISION FUNCTION DSPIEL CALCULATES THE RATIO OF THE
C RELATIVE DIFFUSION COEFFICIENTS AT INFINITE AND FINITE SEPARATIONS
C FOR TWO DISSIMILAR SPHERES
C  S=R/A1  WHERE R=CENTRE TO CENTRE DISTANCE
C  A21=A2/A1 WHERE A1 AND A2 ARE THE RADII OF SPHERES,A2>A1.
C  I.E.  DSPIEL=D12(INFINITY)/D12(S) - L.A.SPIELMAN,
C  J.COLL.INT.SCI.,33,P562,(1970)
C  EPS IS A CONVERGENCE PARAMETER
      DOUBLE PRECISION S,A21,EPS,AD,BD,A,B,AMB,APB,KS1,KS2,LS1,LS2,N2,N,
     1KN,RT2,AN,BN,CN,DN,AND,BND,CND,DND,DLTA,SAMB,SAPB,CAPB,EAMB,EBMA,
     2E1AMB,S1AMB,S1APB,C1APB,S2AMB,S2APB,C2APB,S3AMB,S3APB,C3APB,X1,X2
     3X3,Y1,Y2,Y3,KNUD,KH1,KH2,LH1,LH2,SA,F,FH
       IF(S.LT.(5.D0+A21)) GOTO 70
      DSPIEL=1.D0
      RETURN
   70 IF(S-(1.11D0+A21))40,50,50
   40 DSPIEL=1.D0/((1.D0+1.D0/A21)*(S-1.D0-A21))
      GOTO 60
   50 AD=(S*S-A21*A21+1.D0)/(2.D0*S)
      AD=AD+DSQRT(AD*AD-1.D0)
      A=DLOG(AD)
      BD=(S*S+A21*A21-1.D0)/(2.D0*A21*S)
      BD=BD-DSQRT(BD*BD-1.D0)
      B=DLOG(BD)
      AMB=A-B
      APB=A+B
      KS1=0.D0
      KS2=0.D0
      LS1=0.D0
      LS2=0.D0
      RT2=1.414213562373095
      SAMB=DSINH(AMB)
      SAPB=DSINH(APB)
      CAPB=DCOSH(APB)
      EAMB=DEXP(AMB)
      EBMA=1.D0/EAMB
C  THE FOLLOWING LOOP CALCULATES THE TERMS OF THE SERIES FOR KS1,KS2,
C   LS1 AND LS2
      N1=0
   10 N1=N1+1
      N=DFLOAT(N1)
```

WHAMSP CONTINUED

```
      M=N1+N1
      N2=DFLOAT(M)
      KN=N*(N+1.D0)/((N2-1.D0)*(N2+1.D0)*(N2+3.D0)*RT2     )
      X1=(N-0.5D0)*AMB
      Y1=(N-0.5D0)*APB
      X2=X1+AMB
      Y2=Y1+APB
      X3=X2+AMB
      Y3=Y2+APB
      S1AMB=DSINH(X1)
      S1APB=DSINH(Y1)
      C1APB=DCOSH(Y1)
      S2AMB=DSINH(X2)
      S2APB=DSINH(Y2)
      C2APB=DCOSH(Y2)
      S3AMB=DSINH(X3)
      S3APB=DSINH(Y3)
      C3APB=DCOSH(Y3)
      E1AMB=DEXP(-X2)
      DLTA=4.D0*S2AMB*S2AMB-((2.D0*N+1.D0)*SAMB)**2
      KNUD=KN/DLTA
      AN=(N2+3.D0)*(4.D0*E1AMB*S2AMB+(N2+1.D0)**2*EAMB*SAMB+
     1   2.D0*(N2-1.D0)*S2AMB*C2APB -2.D0*(N2+1.D0)*S3AMB*C1APB-
     2     (N2+1.D0)*(N2-1.D0)*SAMB*CAPB)*KNUD
      BN=-(N2+3.D0)*(2.D0*(N2-1.D0)*S2AMB*S2APB-
     1   2.D0*(N2+1.D0)*S3AMB*S1APB+(N2+1.D0)*(N2-1.D0)*SAMB*SAPB)*
     2     KNUD
      CN=-(N2-1.D0)*(4.D0*E1AMB*S2AMB-(N2+1.D0)**2*EBMA*SAMB+
     1   2.D0*(N2+1.D0)*S1AMB*C3APB-2.D0*(N2+3.D0)*S2AMB*C2APB+
     2    (N2+1.D0)*(N2+3.D0)*SAMB*CAPB)*KNUD
      DN=(N2-1.D0)*(2.D0*(N2+1.D0)*S1AMB*S3APB-
     1   2.D0*(N2+3.D0)*S2AMB*S2APB+(N2+1.D0)*(N2+3.D0)*SAMB*SAPB)*
     2     KNUD
      AND=(N2+3.D0)*(2.D0*(N2-1.D0)*S2AMB*S2APB-
     1     2.D0*(N2+1.D0)*S3AMB*S1APB-(N2+1.D0)*(N2-1.D0)*SAMB*SAPB)*
     2 KNUD
      BND=-(N2+3.D0)*(-4.D0*E1AMB*S2AMB-(N2+1.D0)**2*EAMB*SAMB+
     1 2.D0*(N2-1.D0)*S2AMB*C2APB-2.D0*(N2+1.D0)*S3AMB*C1APB+
     2     (N2-1.D0)*(N2+1.D0)*SAMB*CAPB)*KNUD
      CND=-(N2-1.D0)*(2.D0*(N2+1.D0)*S1AMB*S3APB-
     1     2.D0*(N2+3.D0)*S2AMB*S2APB-(N2+1.D0)*(N2+3.D0)*SAMB*SAPB)*
     2     KNUD
      DND=(N2-1.D0)*(-4.D0*E1AMB*S2AMB+(N2+1.D0)**2*EBMA*SAMB+
     1   2.D0*(N2+1.D0)*S1AMB*C3APB-2.D0*(N2+3.D0)*S2AMB*C2APB-
     2     (N2+1.D0)*(N2+3.D0)*SAMB*CAPB)*KNUD
      X1=(N2+1.D0)*(-AN+AND-BN+BND-CN+CND-DN+DND)
      X2=(N2+1.D0)*(-AN-AND+BN+BND-CN-CND+DN+DND)
      Y1=(N2+1.D0)*(+AN+AND+BN+BND+CN+CND+DN+DND)
      Y2=(N2+1.D0)*(+AN-AND-BN+BND+CN-CND-DN+DND)
      KS1=KS1+X1
      KS2=KS2+X2
      LS1=LS1+Y1
      LS2=LS2+Y2
      F=(KS1*KS2-LS1*LS2)/(KS1+KS2-LS1-LS2)
      IF(N1.GT.1)GOTO 30
   20 FH=F
```

WHAMSP CONTINUED

```
      GOTO 10
   30 IF(DABS((F-FH)/FH).GT.EPS) GOTO 20
      SA=DSINH(A)
      DSPIEL=RT2*(1.D0+1.D0/A21)*SA*F/6.D0
   60 CONTINUE
      RETURN
      END
```

(POLYFIT)

```
      IMPLICIT REAL*8(A-H,O-Z)
      DIMENSION X(20),F(20),W(20),P(7),SI(7)
      LOGICAL L
      L=.FALSE.
      READ,M
      K1=7
      DO 1 I=1,M
      READ,X(I),F(I),W(I)
    1 CONTINUE
      CALL E02ADF(M,X,F,W,K1,N,SI,P,L)
      WRITE(6,100)
  100 FORMAT('0','LEAST SQUARES FIT OF POLYNOMIAL')
      WRITE(6,200)
  200 FORMAT(' ','POLYNOM COEF'10X'FIT,ZIGMA**2')
      DO 2 I=1,K1
    2 WRITE(6,300) P(I),SI(I)
  300 FORMAT(' ',E14.6,5X,E14.6)
      WRITE(6,400)N
  400 FORMAT(' ','DEGREE OF BEST POLY IS',I4)
    4 READ,AB
      IF(AB.GT.1E10)GOTO 5
      ORD=P(1)+P(2)*AB+P(3)*AB**2+P(4)*AB**3+P(5)*AB**4+P(6)*AB**5
     1                +P(7)*AB**6
      WRITE(6,500)ORD,AB
  500 FORMAT(' ','Y=',E14.6,'AT X=',E14.6)
      GOTO 4
    5 STOP
      END
```

(SALTHAM1)

```
C          PROGRAM TO CALCULATE HAMAKER FUNCTIONS USING
C      THE LIFSHITZ APPROACH INCORPORATING THE ZERO FREQUENCY
C                        SALT CORRECTION.
      INTEGER N,J
       REAL L,PI,K,T,H,C,E1,E2,E3,O,E,SUM,DB,D,Z,TOT,U,BIT
      REAL INT,EX,L1,G,C11,C12,C13,W11,W12,W13,C21,C22,C23
      REAL W21,W22,W23,P,DP,A,Y1,Y2,VA1,VA2,AIMAJ
      REAL C21A,C21B,W21A,W21B,KRAM,KON,DIE
      DIMENSION OM(20),DIE(20)
      REAL KAP,GG,INTEG,RPP,PART1,PART2,PART3
      REAL PART,DIV,DPP,PP,LIMIT,C14,W14
      REAL S1,S3,C31,C32,C33,DB1,DB3,D1,D3,W31,W32,W33
      PI=3.141593
      K=1.380622E-23
      H=1.054592E-34
      C=2.99793E8
      READ,T,DP,U,AIMAJ
      WRITE(6,150)
 150  FORMAT(' ','GIVE ME THE 1ST PARTICLE DATA IN CM1 FORM')
      READ,C11,C12,C13,C14,W11,W12,W13,W14
      WRITE(6,151)
 151  FORMAT(' ','GIVE ME THE MEDIUM DATA IN SAME FORM PLEASE')
      READ,C21,C21A,C21B,C22,C23,W21,W21A,W21B,W22,W23
      WRITE(6,152)
 152  FORMAT(' ','GIVE ME 20 FREQ IN ERGS FOR 2ND PARTICLE')
      READ,OM
      WRITE(6,153)
 153  FORMAT(' ','NOW 20 CORRESPONDING E!! VALUES')
      READ,DIE
      WRITE(6,100)
  21  READ,L,E1,E2,E3
       IF(L.EQ.0.0)GOTO 23
      TOT=0.0
      N=0
      SUM=0.0
      J=1
      READ,KAP
      IF(KAP.EQ.0.0)GOTO 3
      LIMIT=100.0/(KAP*L)
      DPP=LIMIT/10000.0
      PP=1.0
      SUM=0.0
      GG=K*T*KAP**2/(4*PI)
32    RPP=SQRT(PP**2-1.0)
      PART1=(E1*RPP-E2*PP)/(E1*RPP+E2*PP)
      PART2=(E3*RPP-E2*PP)/(E3*RPP+E2*PP)
      PART3=EXP(-2*PP*KAP*L)
      PART=ALOG(1-PART1*PART2*PART3)
      INTEG=PP*DPP*PART
      SUM=SUM+INTEG
      IF(ABS(INTEG).GT.0.0)GOTO 33
      INTEG=1E-20
33    DIV=SUM/INTEG
      IF(ABS(DIV).GT.1E20)GOTO 31
      PP=PP+DPP
      IF(PP.GT.LIMIT)GOTO 31
```

SALTHAM1 CONTINUED

```
      GOTO 32
   31 SUM=-2*SUM*GG*12.0*PI*L**2/(1.5*K*T)
      WRITE(6,1234)PP,GG,SUM,PART1,PART2,PART3,PART
1234  FORMAT(' ',6E12.5)
      GOTO  4
3     Q=((E2-E1)/(E2+E1))*((E2-E3)/(E2+E3))
      Q=Q**J
      Q=Q/(J**3)
      SUM=SUM+Q
      J=J+1
      IF(ABS(Q).GT.ABS(SUM/10000.0))GOTO 3
      GOTO 4
    9 IF(ABS(INT).LT.ABS(TOT*1.0E-7))GOTO 8
    5 SUM=0.0
      E=2.0*PI*N*K*T/H
      IF(N.EQ.0)GOTO 1
      E1=1.0+(C11/(1.0+(E/W11)**2))+(C12/(1.0+(E/W12)**2))
     1  +(C13/(1.0+(E/W13)**2))+(C14/(1.0+(E/W14)**2))
      E2=1.0+(C21/(1.0+(E/W21)))+(C22/(1.0+(E/W22)**2))
     1           +(C23/(1.0+(E/W23)**2))
     1   +(C21A/(1.+(E/W21A)))+(C21B/(1.+(E/W21B)))
     ,KON=0.0
      DO37 I=1,19
      KRAM=DIE(I)*DM(I)*1.5193E15/
     1  (E**2+(DM(I)*1.5193E15)**2)
      KRAM=KRAM*(DM(I+1)-DM(I))*1.5193E15
      KON=KON+KRAM
   37 CONTINUE
      E3=1.0+(2*KON/PI)
    1 P=1
      GOTO 2
   10 IF(N.GT.100)GOTO 18
      GOTO 19
   18  IF(P.GT.40.0)GOTO 11
   17       IF(ABS(Q).LT.ABS(SUM*1.E-6))GOTO 11
      GOTO 2
19       IF(ABS(Q).LT.ABS(SUM/10000.0))GOTO 11
 2       S1=SQRT(E1/E2-1.0+P*P)
      S3=SQRT(E3/E2-1.0+P*P)
      DB1=(S1-P)/(S1+P)
      D1=(S1*E2-P*E1)/(S1*E2+P*E1)
      DB3=(S3-P)/(S3+P)
         D3=(S3*E2-P*E3)/(S3*E2+P*E3)
      Z=2.0*E*L*(E2**0.5)/C
      EX=EXP(-P*Z)
      L1=(1.0-DB1*DB3*EX)*(1.0-D1*D3*EX)
      Y1=P*ALOG(L1)
      IF(P.EQ.1.0)GOTO 39
      Q=(Y1+Y2)/2.0
      Q=Q*DP
39    Y2=Y1
      P=P+DP
      IF(P.EQ.(1.0+DP))GOTO 2
      SUM=SUM+Q
      IF(Q.EQ.0.0)GOTO 11
      IF(N-10)17,17,10
```

SALTHAM1 CONTINUED

```
   11 CONTINUE
4     IF(N.GT.0)GOTO 7
      INT=-SUM/2.0
      GOTO 6
   7  INT=Z*Z*SUM
   6  TOT=TOT+INT
100       FORMAT(' ','N',10X,'TOT')
  200 FORMAT(' ',I3,7X,E15.4)
  300 FORMAT(' ','THE VALUE OF A IS',2E15.4)
      N=N+1
      IF(N.LE.100)GOTO 9
    8 CONTINUE
      WRITE(6,200)N,TOT
      A=1.5*K*T*TOT
      WRITE(6,300)A,L
      BIT=((2.*U*U)/((2.*U+L)**2-(4.*U*U))
     1   +(2.*U*U)/(2.*U+L)**2
     1   +ALOG((2.*U+L)**2.-4.*U*U)/(2.*U+L)**2.))
       VA1=A*BIT
       VA2=AIMAJ*BIT
       WRITE(6,700)VA1,VA2
  700  FORMAT(' ','VA1=',E15.4,'VA2=',E15.4)


      GOTO 21

   23  CONTINUE
      STOP
      END
```